

Prediction of Mosquito Abundance in Temperate Regions, Using Ecological, Hydrological and
Remote Sensing Models

by

Yun Jian

Department of Environment
Duke University

Date: _____

Approved:

Marco Marani, Supervisor

William Pan, Co- supervisor

Sonia Silvestri

Song S. Qian

Gabriel Katul

Dissertation submitted in partial fulfillment of
the requirements for the degree of Doctor
of Philosophy in the Department of
Environment in the Graduate School
of Duke University

2014

ABSTRACT

Prediction of Mosquito Abundance in Temperate Regions, Using Ecological,
Hydrological and Remote Sensing Models

by

Yun Jian

Department of Environment
Duke University

Date: _____

Approved:

Marco Marani, Supervisor

William Pan, Co- supervisor

Sonia Silvestri

Song S. Qian

Gabriel Katul

An abstract of a dissertation submitted in partial
fulfillment of the requirements for the degree
of Doctor of Philosophy in the Department of
Environment in the Graduate School of
Duke University

2014

Copyright by
Yun Jian
2014

Abstract

New and old mosquito-borne diseases have emerged and re-emerged in temperate regions over the recent past, but an understanding of mosquito population dynamics, a fundamental step toward disease control, remains elusive. In particular, we are still lacking reliable predictive models of mosquito abundance in temperate areas due to the subtle links between the fluctuation of mosquito population and highly heterogeneous environmental drivers. Hence, this doctoral dissertation presents an interdisciplinary approach towards an improved understanding and prediction of the fluctuations in mosquito abundance in temperate regions. In the first part of this dissertation a hierarchical Gompertz-based model is used to assess the relative importance of endogenous (density dependence) and exogenous (environmental forcings) controls and their interactions in regulating the dynamics of a West Nile Virus vector (*Culex pipiens*) in the Po River delta in Italy. The results clearly detect the effects of density-dependence in the observed population dynamics for the mosquito species analyzed and highlight the controls exerted by environmental forcings and habitat conditions. Subsequently, the characteristic scales of temporal variability in mosquito populations, and the representativeness of observations at different sampling resolutions, are investigated using a 10 year daily mosquito sample from Brunswick County, North Carolina. The species present in the sample (among which *Aedes vexans* and *Culiseta melanura* are addressed in greater detail, as vectors of East Equine Encephalitis and West Nile Virus)

are investigated using a combination of time series analysis, individual based simulations, and density-dependent modeling approaches. Significant population fluctuations with characteristic periodicity between 2 days and several years are found in response to different regulation mechanisms. In particular, the observed fast fluctuations are importantly determined by a varying mosquito activity, rather than by reproduction/mortality processes, driven by rapid changes in meteorological conditions. Finally, in the third part of this study, a state space reconstruction (SSR) approach is used to understand how the predictability of mosquito abundance varies with aggregation time scale and with the prediction horizon, and how much can the prediction of mosquito abundance be improved by using daily observations compared to the commonly used once-per-week samples. The results show that the predictability of mosquito abundance decreases as the time scale of the models increases from one week to one month, while the predictability of per capita growth rate increases together with the modeling scale. It is also shown that the prediction of mosquito per capita growth rate can be improved using daily abundance observations. Furthermore, many mosquito models compare the observed and predicted abundance as a measure of model performance. However, my results suggest that short term forecasts of mosquito abundance may appear to have a significant capability due to the positive autocorrelation between abundance in subsequent time steps, even when the model's

ability to predict the abundance change is low. Model capability should thus be evaluated comparing observed and modelled per capita rates of change.

Contents

Abstract.....	iv
Contents.....	vii
List of Tables.....	x
List of Figures.....	xii
Acknowledgements	xvi
1. Introduction.....	1
1.1 Mosquito – borne diseases in temperate regions: an emerging challenge	1
1.2 An overview of our current understanding of mosquito population dynamics	3
1.3 Density dependence in mosquito population dynamics	8
1.4 Hydrologic controls in mosquito population dynamics	11
1.5 The representativeness of adult mosquito observations.....	13
1.6 Dissertation Objectives and Organization	16
2. Environmental Forcing and Density-dependent controls of <i>Culex pipiens</i> Abundance in a Temperate Climate (Northeastern Italy)	21
2.1 Introduction.....	21
2.2 Materials and methods	24
2.1.1 Study area and data collection	24
2.1.2 Modeling Approach.....	27
2.1.2.1 Soil moisture dynamics	28
2.1.2.2 Mosquito population modeling	29
2.2 Results.....	37
2.3 Discussion and conclusions.....	45

3. The Temporal Spectrum of Adult Mosquito Population Fluctuations: Conceptual and Modeling Implications.....	52
3.1 Introduction.....	52
3.2 Materials and methods	54
3.2.1 Study area and data	54
3.2.2 Data analysis.....	57
3.2.3 Fourier analysis	58
3.2.4 Autocorrelation, partial correlation, and data splitting	59
3.2.5 Models.....	60
3.2.5.1 Individual-Based life cycle simulation model	60
3.2.5.2 Density dependent population models	65
3.3 Results.....	67
3.4 Discussion and conclusions.....	77
4. Predicting Mosquito Abundance across Temporal Scales	82
4.1 Introduction.....	82
4.2 Methods	84
4.2.1 Study area and data	84
4.2.2 State space reconstruction (SSR) and Simplex Projection (SP)	84
4.3 Results.....	94
4.4 Discussion and conclusions.....	106
5. Dissertation conclusions	111
5.1 Overview of the results	111
5.2 Major contributions.....	115

Appendix A	118
A1. Conditional plots for per capita growth rate, log of abundance and temperature	118
A2. Relationship between rainfall and soil moisture	118
A3. WinBUGS model script	119
A4. Model evaluation	120
Appendix B.....	121
B1. IBS model formulation, developmental stages, and processes.	121
B2. Power spectrum of observed weather data	122
B3. Detailed functions and parameter values used in the IBS models	123
B4. Empirical relations between activity factor and rainfall.....	126
B5 ACF and PACF of Gompertz models for <i>Ae.vexans</i> with different density dependence (results for the Ricker model, not shown, are analogous).....	127
B6. ACF for observations and for models with different density dependence.	128
B7. Estimated coefficients for density dependent models	129
Appendix C	132
C1. Change of correlation between the predicted and observed values for prediction horizon.....	132
C2. Correlation between the predicted and observed values for co-prediction	134
C3. SP results of 7-day-ahead prediction using the once-per-week samples.....	137
C4. SP results of 7-day-ahead prediction using the daily samples	138
References.....	139
Biography	153

List of Tables

Table 1: Model performance when soil moisture or rainfall was used as predictors. 41

Table 2: Mean and standard deviation of multiplicative coefficients of exogenous factors in eq. (4). Soil water content, radiation, hours and wind speed were calculated as the average values one week before mosquito samplings. NDVI was calculated for a 75m x 75m window around each sampling site. (levels of significance are: * $p < 0.1$, ** $p < 0.05$, and *** $p < 0.01$)..... 43

Table 3: Density-dependent models (showing lag 0 as examples), where t is index of sample date; N is adult mosquito abundance; r_m is the maximum per capital growth rate; K is the carrying capacity 67

Table 4: The correlations and RMSE for the best models at three time scales for *Cs.melanura* and *Ae.vexans* 94

Table 5: The variables selected for the best models at three time scales for *Cs.melanura* and *Ae.vexans*..... 100

Table 6: The correlations and RMSE for the random walk models at three time scales. 106

Table 7: Estimated coefficients for density dependent models for mosquito abundance in the Brunswick County NC 129

Table 8: Correlation between the predicted and observed per capital growth rate changes for prediction horizon 132

Table 9: Correlation between the predicted and observed abundance changes for prediction horizon 133

Table 10: Correlation for co-prediction at weekly scale. Index for species: 1, *Ae.vexans*; 2, *Cs.melanura*; 3, *Cx.salinarius*; 4, *Cx.restuans*; 5, *Ps.columbiae*; 6, *Ps.ferox*; 7, *An.crucians*; 8, *Oc.atlanticus*; 9, *Oc.fulvus.pallens*; 10, *Cx.nigripalpus*; 11, *Cx.erraticus*; 12, *Cx.pipiens*; 13, *Ps.ciliata*; 14, *An.quadrimaculatus*; 15, *Ps.howardii*; 16, *Oc.canadensis* 134

Table 11: Correlation for co-prediction at biweekly scale. Index for species: 1, *Ae.vexans*; 2, *Cs.melanura*; 3, *Cx.salinarius*; 4, *Cx.restuans*; 5, *Ps.columbiae*; 6, *Ps.ferox*; 7, *An.crucians*; 8, *Oc.atlanticus*; 9, *Oc.fulvus.pallens*; 10, *Cx.nigripalpus*; 11, *Cx.erraticus*; 12, *Cx.pipiens*; 13, *Ps.ciliata*; 14, *An.quadrimaculatus*; 15, *Ps.howardii*; 16, *Oc.canadensis* 135

Table 12: Correlation for co-prediction at monthly scale. Index for species: 1, <i>Ae.vexans</i> ; 2, <i>Cs.melanura</i> ; 3, <i>Cx.salinarius</i> ; 4, <i>Cx.restuans</i> ; 5, <i>Ps.columbiae</i> ; 6, <i>Ps.ferox</i> ; 7, <i>An.crucians</i> ; 8, <i>Oc.atlanticus</i> ; 9, <i>Oc.fulvus.pallens</i> ; 10, <i>Cx.nigripalpus</i> ; 11, <i>Cx.erraticus</i> ; 12, <i>Cx.pipiens</i> ; 13, <i>Ps.ciliata</i> ; 14, <i>An.quadrimaculatus</i> ; 15, <i>Ps.howardii</i> ; 16, <i>Oc.canadensis</i>	136
Table 13: SP results of 7-day-ahead prediction using the once-per-week samples for <i>Cs.melanura</i>	137
Table 14: SP results of 7-day-ahead prediction using the once-per-week samples for <i>Ae.vexans</i>	137
Table 15: SP results of 7-day-ahead prediction using the daily samples for <i>Cs.melanura</i>	138
Table 16: SP results of 7-day-ahead prediction using the daily samples for <i>Ae.vexans</i> ..	138

List of Figures

Figure 1: Study area, spatial distribution of mosquito trap sites, and weather stations in the Po River delta area Italy.	25
Figure 2: (a) Autocorrelation function (ACF) and (b) partial rate correlation function (PRCF) for site 8 (Taglio di Po). The blue dashed lines represent 95% confidence intervals for the ACF and PRCF. The remaining sites, not shown here for brevity, display similar patterns.....	31
Figure 3: Box-plot of observed <i>Culex pipiens</i> abundance as a function of time. Horizontal segments represent the median across observation sites. Box edges indicate the 25% and 75% quantiles. Whiskers represent 1.5 times the interquartile ranges.....	37
Figure 4: Predicted vs observed values of <i>Culex pipiens</i> abundance and per-capita growth rates under different model formulations. a) and c) include rainfall as a predictor, while b) and d) refer to the inclusion of estimated soil moisture. Colors in a) and b) encode the density of points in the graph. Yellow indicates that a large amount of modelled vs observed points fall in that specific area of the graph. Grey points indicate that no other point lies in the immediate neighborhood. Solid lines indicate 1:1 correspondence.....	39
Figure 5: Time series of predicted and observed abundance. The first 3 rows are for 2010 and the last 4 rows are for 2011. Black dots are the observed values. The red lines are the mean predicted values and the blue lines are the 95% credible intervals of the predicted values based on the MCMC samples.....	40
Figure 6: α_1 for different sites. α_1 is the coefficient for mosquito abundance one week before present, i.e. it represents the magnitude of density dependence. The black dots are the mean values and the segments are the 95% credible intervals based on the MCMC samples. α_1 values for the sites with the black segments are significantly larger than 0 while α_1 values for the ones with grey segments are not. The left panel shows the result for 2010 and the right panel shows that for 2011.	42
Figure 7: Land use land cover effects on <i>Culex pipiens</i> abundance. Panel a) shows α_0 increases with NDVI. Panel b) shows α_1 decreases with distance to the nearest rice field.	45
Figure 8: Study area, sampling sites and weather stations in the Brunswick County North Carolina, U.S.	56

Figure 9: Main biological parameters as assumed in the IBS model. (a) Transition time from egg to larva as a function of temperature. (b) Transition time from larva to adult as a function of temperature. (c) Length of gonotrophic cycle for *Cs.melanura* as a function of temperature. (d) Marginal distribution of the number of eggs laid per batch. (e) Larval survival rate as a function of temperature for *Ae.vexans*. (f) Adult survival rate as a function of temperature for both *Cs.melanura* and *Ae.vexans*..... 61

Figure 10: Observed abundance for the 4 dominant species at the Chicken Trap site in the period 2004 – 2012. The subpanels show details of the abundance fluctuations for two specific periods identified by the grey windows in (a) and (b). 68

Figure 11: Power spectra for the 4 dominant species. The text marks the approximate locations of major peaks. 70

Figure 12: ACF for daily observations ((a) and (c)) and for subsampled weekly data ((b) and (d)). The dashed blue lines represent the 95% confidence intervals for the ACF. Significant peaks around 1 and 3-4 weeks, marked magenta in (c), are partly lost in the subsampled weekly data. 71

Figure 13: The mean abundance from 20 runs of IBS model driven by observed weather forcings for *Ae.vexans* and *Cs.melanura*: simulations without ((a) and (c)) and with ((b) and (d)) activity component. The grey lines represent the range (minimum and maximum) of 20 simulated values..... 73

Figure 14: PACF of observed abundances for *Ae.vexans* and *Cs.melanura*, ((a) and (f)), for IBS model realizations including activity ((b) and (g)), IBS model realizations without activity ((c) and (h)); Gompertz model realizations with density dependence at lag=0 days ((d) and (i)), and Ricker model realizations with density dependence at lag=0 days (Heptonstall (England : Parish) and Horsfall) and (j)) 75

Figure 15: Power spectrum of IBS model outputs with ((a), (b), and (c)) and without ((d), (e), and (f)) activity component. Panel (a) and (d): IBS model with constant temperature (18oC) and no rainfall effect; panel (b) and (e); IBS model with observed temperature, and no rainfall effect; panel (c) and (f) IBS model with observed temperature, and with rainfall effect on death rate, oviposition, and egg hatching driven by observed rainfall. 77

Figure 16: A conceptual spectrum highlighting the ecological/environmental processes driving mosquito dynamics at different time scales. 79

Figure 17: SSR from a single time series $\{x_t\}$ in the 2 dimensional case. 88

Figure 18: Time series of the 16 most dominant mosquito species in the Chicken site trap for the period 2004-2013.	93
Figure 19: Predictions of the growth rate from the best SP models at weekly, biweekly and monthly for <i>Cs.melanura</i> and <i>Ae.vexans</i> . The colors indicate the density of the points available for the evaluation.	95
Figure 20: The predictions of abundance from the best SP models at weekly, biweekly and monthly for <i>Cs.melanura</i> and <i>Ae.vexans</i>	96
Figure 21: The time series of predicted and observed growth rates at different time scales.	97
Figure 22 : The time series of predicted and observed abundance at different time scales.	98
Figure 23: The predicted and observed abundance for <i>Ae.vexans</i> in 2011 as an example. The panels are arranged so that the lengths on the x axis between two points in the weekly, biweekly and monthly models are the same. In the weekly and biweekly model, the predictions lagged the observations by about 1 time step. This was improved in the monthly model.	99
Figure 24: The correlation between the predicted and observed values changes as a function of time steps into the future for the growth rate and abundance from the best models.....	102
Figure 25: Comparison of the 7-day-ahead prediction using the daily observation and once-per-week observation	103
Figure 26: Results from co-prediction. Each point shows the correlation between the predicted and observed per capita growth rate. The size of the points is proportional to the values of the correlations. The plots should be read by row. For example: the row for <i>Cs.melanura</i> in the weekly model panel (in the grey box) shows the result of predicting the per capita growth rate of <i>Cs.melanura</i> by the lagged abundance of the 16 species...	105
Figure 27: a) scatter plots between r and $\ln(x_{t-1})$, conditional on $\ln(x_{t-2})$, and temperature; b) scatter plots between r and $\ln(x_{t-2})$, conditional on $\ln(x_{t-1})$ and temperature. The red lines are the smoothing curves using locally-weighted polynomial regression.	118
Figure 28: Nonlinear correlation between rainfall and soil moisture for site Gorino Veneto 2010 as an example.....	118

Figure 29: The hierarchical state space model was run 100 times using the synthetic data whose values represent those of the observed dataset. The plot shows the differences between the true parameters and modeled parameters. The dots are the mean of the absolute difference and the segments are the 95% credible intervals of the absolute difference. The difference is larger for $\alpha_{0,j}$ which has larger values.	120
Figure 30: The IBS models explicitly describe three mosquito life stages: egg, larva/pupa, and adult. Each stage is characterized by a distribution of the time spent in that stage, dependent on physiology, environmental conditions, and population density. Each stage is characterized by a survival rate, also a function of environmental conditions. A proportion of the emerged female adults are successful in blood feeding and oviposition. I further assumed that the observed population is a varying fraction of the underlying actual adult population represented by an activity factor.	121
Figure 31: Spectral power for the weather observations.	122
Figure 32: Relations between the activity factor and rainfall	126
Figure 33: ACF and PACF of Gompertz models for <i>Ae.vexans</i> with different density dependence (results for the Ricker model, not shown, are analogous)	127
Figure 34: ACF of observed abundances for <i>Ae.vexans</i> and <i>Cs.melanura</i> , ((a) and (f)), for IBS model realizations including activity ((b) and (g)), IBS model realizations without activity ((c) and (h)) ; Gompertz model realizations with density dependence at lag=0 days ((d) and (i)) , and Ricker model realizations with density dependence at lag=0 [57] and (j)).	128

Acknowledgements

I would like to express my deepest gratitude and appreciation to my committee members Marco Marani (advisor), William Pan (co-advisor), Song Qian, Sonia Silvestri, and Gabriel Katul, without whose guidance this research could not have been accomplished. Thank you very much, Marco, for your support and encouragement. You provided indispensable advice for my study, encouraged me to explore new research paths, and steered me in the right the direction whenever I needed it. I feel very fortunate to have you as my advisor. I would like to thank William Pan who freely shared his expertise on epidemiology and mosquito-borne diseases, which helped me to develop a more comprehensive understanding of the studied topic. I'm very grateful to Song Qian who shared his incredible abilities in statistics and modeling with me, and provided insightful suggestions for the Bayesian approaches I used in this dissertation. I would like to express my many thanks to Sonia Silvestri, whose amazing knowledge on remote sensing and incisive comment on the research inspired me throughout my study at the Nicholas School. I'm very grateful to Gabriel Katul, who as my committee member, and as the previous Director of Graduate Studies (DGS) for the Environmental Science and Policy Program at the Nicholas School, supported and encouraged me through difficulties during my study at Duke.

Many thanks to the Nicholas School of the Environment for supporting and funding this work. I am also very grateful for Duke Graduate School for providing

travel awards for me to attend related scientific conferences. I would like to deeply thank the Mosquito Control Department of Brunswick County, North Carolina, who freely shared their valuable long term daily mosquito samples for my research. In particular I would like to thank Jeff Brown and Rick Hickman for their continuous efforts in mosquito sampling and identification, and great patience for sharing their knowledge in mosquito biology. I would like to thank Marcee Toliver from NC Division of Public Health for providing valuable suggestions and information about mosquito sampling and mosquito-borne diseases. I also thank Enrica Belluco from University of Padova, Italy, for her modeling work on soil moisture, which provided basis for comparison the effect of soil moisture and rainfall on predicting mosquito abundance.

I would also like to extend sincerest appreciation to my colleagues in the Nicholas School. I would like to thank Joel Meyer the current DGS of the Nicholas School for supporting my study and research here. I would like to thank Wenhong Li, assistant professor of climate, for providing information of future climate for my study. I deeply appreciate the efforts of Meg Stephans who patiently helped me through the administrative bureaucracy. I would like to thank Andy Minnis and other members of Nicholas OIT for their technical support. I would like thank my friends from Marani's lab: Fateme Yousefi, Massimiliano Ignaccolo, and Gabriele Manoli as well as my friends in the previous Reckhow' lab: Ibrahim Alameddine,

Farnaz Nojavan, Kris Voss, YoonKyung Cha, BoknamLee, Roxolana Kashuba, and Rui Wu for their valuable comments and help for my research.

My family and friends are also great supports during my PhD study. Thank you mom (Ruimin Li) for your love to me. Thanks you dad (Wenyi Jian), for believing in me and for supporting me endlessly. Thanks you grandpa (Xueqin Li) for always encouraging me to enjoy learning. Thanks you grandpa (Zhongchi Jian) and grandma (Wanzhen Zhang) for rearing me up. Thank you my aunt (Linlin Li) for taking care of my mom and grandpa when I was away from home and study at Duke. Thank you my mother in-law (Fenglian Chang) for taking care of Jasmine when I was at work. Also many thanks to my fellow alumni in the Department of Environmental Sciences at East China Normal University. Last but not least, I would like to deeply thank my incredibly husband Jun Zhang. Your constructive feedbacks for my research, your patience for my practice presentations, and your love and belief in me always encouraged during my study at Duke.

1. Introduction

1.1 Mosquito – borne diseases in temperate regions: an emerging challenge

Mosquito – borne diseases are one of the most fatal challenges worldwide (Pascual et al. 2006, Enserink 2008, Alonso et al. 2011, Kilpatrick 2011). In 2012 alone, about 207 million clinical episodes of malaria were reported, among which more than 600 thousands death occurred (U.S.Centers for Disease Control and Prevention 2014b). The estimated yearly occurrence for dengue is 50 to 100 million, with the number of human death around 22000 (U.S.Centers for Disease Control and Prevention 2014a). While most of these mosquito diseases were first discovered in tropical areas, where they are still causing high mortality rates, their diffusion to temperate regions due to globalization and climate change has caused global concerns (Spielman and D'Antonio 2001, Jones et al. 2008, Randolph and Rogers 2010). The processes involved in mosquito arrival, establishment and diffusion in temperate regions are the subject of much ongoing work, especially in areas with high human population density.

A well-known example of mosquito-borne disease appearing in temperate regions concerns West Nile Virus (WNV). The WNV outbreak in New York City in 1999 was followed by widespread diffusion in the whole country. Only six years later, this mosquito – borne disease was discovered in almost every state of the country (Hayes et al. 2005, Jones et al. 2008). By the year 2010, the estimated number of infected people with WNV reached approximately 3 million in the U.S., with about 780,000 illnesses in

total (Petersen et al. 2013). Even with the relatively advanced surveillance network and control methods deployed in the U.S., WNV remains endemic and had a second peak of occurrence in 2012 (U.S. Centers for Disease Control and Prevention 2014c). Dengue and Chikungunya are other examples of mosquito-borne diseases which originated in tropical areas and are now spreading to temperate regions in connection with the mosquito species *Aedes albopictus* (Enserink 2008). Native of tropical and subtropical regions, this species was first documented in the U.S. in 1983 where it probably arrived in used tires transported on boards. It was found in 36 U.S. states by 2007. *Aedes albopictus* also became established in most of Italy and invaded many countries in Europe and South America (Enserink 2008, Randolph and Rogers 2010). Other mosquito-borne diseases, such as Eastern Equine Encephalitis, Japanese Encephalitis, La Crosse encephalitis, St. Louis encephalitis are also found in temperate regions (U.S. Centers for Disease Control and Prevention 2007). Though their occurrence is less common and endemic regions are more restricted, these diseases cause severe symptoms and high mortality rates, and represent serious local and regional problems.

Despite the expansion of the areas in temperate regions threatened by mosquito-borne diseases, studies on the population dynamics of mosquito vectors in these regions have only recently started to appear (e.g. (Day and Shaman 2009, Jian et al. 2014a). The accumulated research results about population dynamics of mosquito vectors in tropical regions cannot be directly transferred to temperate regions, due to

differences in biological controls of the mosquito vectors, unknown host-vector relations, intricate exogenous regulation mechanisms and heterogeneity in mosquito habitats (Jones et al. 2008, Randolph and Rogers 2010, Kilpatrick 2011). Unlike tropical areas, where controlling factors (such as water availability) have a clear-cut effect on mosquito population dynamics, it is more likely that mosquito dynamics be governed by the interplaying of multiple environmental forcings in temperate environments, and that no single factor become limiting. The artificial/urban surroundings and intensive agricultural practices in temperate regions also greatly modify water availability for mosquito oviposition and development. As a consequence of the complex interplay of numerous overlapping exogenous factors, of a relatively large inter-annual variability in environmental forcing (e.g. temperature, rainfall, length of the growing season, etc.), and of the potential health hazard associated with mosquito population outbreaks in densely populated areas, a much improved understanding of mosquito population dynamics in temperate regions is an urgent and important priority.

1.2 An overview of our current understanding of mosquito population dynamics

In general, the life cycle of mosquitoes includes four stages: egg, larva, pupa and adult, among which the first three are under water for most mosquito species (Clements 1992). Thus water availability, controlled by interplaying natural and artificial processes, is essential for mosquito development. Each of the stages is also characterized by a development rate which determines how long the stage lasts approximately. The speed

of mosquito development is found to be positively related to temperature and duration of day times under laboratory conditions, and is also influenced by nutrients availability under natural environment (Trpis and Shemanch.Ja 1970, Horsfall 1973, Clements 1992, Mahmood and Crans 1998a, Becker et al. 2003). Thresholds in temperature and oxygen concentration (detected by mosquitos as an evidence of ponding) are also found to govern the start of mosquito development, in other words, the hatch of mosquito eggs (Becker et al. 2003, Crans 2013a). The mortality rate at each stage is controlled by multiple biological and environmental factors. Among them the effect of temperature is nonlinear, and the temperature values corresponding to the maximum survival rate vary for different species (Clements 1992, Becker et al. 2003, Ermert et al. 2011a). Mosquito species also differ in their strategies through unfavorable environmental conditions. Most species overwinter as eggs, while a few species having high tolerances with cold weather overwinter as larva or adult (such as *Culiseta melanura* and *Culex salinarius*). The typical life span of mosquito lasts about 1 to several months. After emergence, female mosquitoes begin their gonotrophic cycle which includes copulation, blood searching and digestion, and egg development in the their body (Clements 1992). The number of eggs laid by female mosquitoes varies significantly across species, and within a species it depends on blood sources for the female mosquitoes and water availability in the habitats (Horsfall 1973, Scott and Lorenz 1998, Becker et al. 2003).

These understanding of mosquito population dynamics are the basis of abundance models to predict fluctuations in mosquito populations, which would be of fundamental importance to contrast and manage mosquito – borne diseases. In fact, existing modeling approaches to mosquito abundance prediction can usually be categorized as either “entomological” or empirical approaches (LaDeau et al. 2011). The first approach uses detailed descriptions of the mosquito life cycle and consequently involves a relatively large number of parameters which need to be calibrated with observed data or inferred from the literature (Bomblies et al. 2008, Linard et al. 2009, Cailly et al. 2012). This approach is effective when a large amount of data is available to constrain model parameters and when controlling factors are known in detail. Very often this is not the case, because of observational limitations (of both mosquito abundance and environmental forcings) and because of the difficulty of transferring to field conditions parameter values obtained from controlled lab experiments. Furthermore, detailed formulations of mosquito life cycles do not typically allow for stochastic components, thus not allowing the incorporation of ever-present noise and giving rise to a quite fundamental mismatch between model assumptions and actual population behavior.

Empirical models, at the other end of the spectrum, may be able to explain a large proportion of the observed variability by simply using meteorological and habitat information. However, forecasting skills are typically poor beyond the conditions under

which the model is calibrated, because of the intrinsic lack of an explicit basis in the governing physical mechanisms (LaDeau et al. 2011). Furthermore, empirical models do not allow insights into the relative importance of competing controlling mechanisms because such mechanisms are not explicitly resolved in the model structure. A balance is thus desirable between a very detailed process-based model, posing fundamental problems of parameter identification, and completely empirical models, lacking a robust process basis.

Given the heterogeneity in mosquito habitats, an increasing number of studies uses spatially-distributed environmental descriptions obtained from Remote Sensing and GIS analyses to provide mosquito habitat characterizations (Rogers et al. 2002, Overgaard et al. 2003). One common application is the use of NDVI, Tasseled Cap (soil-vegetation-water characterization) and other satellite-derived indices to identify hotspots for mosquito habitats (Rogers et al. 2002, Lacaux et al. 2007, Rahman et al. 2011, Yamana and Eltahir 2011). These indices, included in GIS or hydrological models, can provide dynamic and high-resolution information of resource availability for mosquito populations. In fact, land use and land cover have been found to be important factors influencing mosquito distributions. In particular, agricultural areas are found to sustain high mosquito abundance because of the irrigation and fertilization activities (Munga et al. 2006, DeGroot and Sugumaran 2012).

Significant gaps, however, persist in our understanding of the driving factors of fluctuations in mosquito populations. In particular, in order to develop a predictive framework for mosquito abundance, we need to tease out the relative importance of endogenous and exogenous factors, and to better understand their interplay in determining mosquito population dynamics under field conditions. In the present dissertation I use an interdisciplinary approach, incorporating hydrological modeling, GIS and remote sensing information, statistical tools, and process-based population models to improve our predictive understanding of mosquito population dynamics. The adopted approach takes advantage of both process-based and empirical methods. Thus it allows clear analyses of the regulating mechanisms, while at the mean time pools information from both observed mosquito samples and existing literature. These quantitative methods are used to model mosquito abundance sampled under different strategies and analyze the influence of sampling frequency on mosquito models. The spatial temporal stochasticity in the governing environmental forcings and in the populations is also incorporated in analyses for a realistic representation of the population dynamics under natural conditions. The skills gained from multiple fields provide efficient tools for an comprehensive understanding of mosquito life cycles which is regulated by competing biological and environmental factors.

1.3 Density dependence in mosquito population dynamics

The change of population size for a species can be regulated by its own abundance, which is often referred as density dependent growth (Turchin 2003). The possible presence of density dependence in mosquito populations in their “natural” environment lies at the very heart of our understanding of mosquito ecological processes and is critical to our ability of predicting mosquito abundance. This topic is usually studied as the relation between abundance (N_t) and per capita growth rate ($r_t = \log(N_{t+1}) - \log(N_t)$) over time (Turchin 1990, Berryman and Turchin 2001, Turchin 2001, Turchin 2003). Various functions between per capita growth rate and population abundance have been proposed in general (but not targeting at mosquito species) (Fowler 1981, Turchin and Taylor 1992, Sibly et al. 2005). In an early study, Fowler (1981) show that the relationship is related to life history of a species: the per capita growth rate-abundance relationship tends to be convex (displaying negative second derivative) in larger mammals with low reproductive rates and long life spans. Smaller animals are more likely to display a concave form probably due to their large reproduction rates (Fowler 1981). However, a later synthesis by Sibly show that the concave shape is the general form for most of the specie they analyzed (Sibly et al. 2005). This relation between per capita growth rate and abundance is fundamental to understand population fluctuations over time, and it is the basis for different density dependent models, such as the logistic model, the Gompertz-logistic model and the theta-logistic

model (Turchin 2003, Yang et al. 2008a, Russell et al. 2011). These different models can result in very different patterns of population fluctuation and stability, thus leading to divergent conclusions and testable assumptions. The understanding of density dependence is also essential for the efficient pest controls. The timing and amount of pesticide applied not only determine the mortality of current pest population, but also largely influence the growth of the population in the future, if the per capita growth rate itself is a function of population size. Efficient mosquito control practices must avoid reducing current mosquito abundance only to generate a steep increase in the overall population abundance at subsequent times (Ricker 1954, Juliano 2007).

The delay with which density dependence becomes manifested (the memory in the system) is largely dependent on the duration of the life cycle of a species (Turchin 2003). Under nearly constant lab conditions the duration of a life cycle is limited to a narrow range, and the presence of density dependence is relatively clear (Turchin 2003). Under natural conditions, the role of density dependence remained unclear, as the variability in environmental forcings can lead to a wide distribution of development time (Jian et al. 2014a, Jian et al. 2014b) and mask the signs of density dependence and its functional form (Turchin 1990). Furthermore, both the carrying capacity and the maximum growth rate in density dependent dynamics can change with habitat type (Yang et al. 2008b, Jian et al. 2014a). Development rates for egg, larval and pupal phases are reported to be accelerated by higher temperature in many mosquito species

(Clements 1992), but warmer conditions can also reduce mosquito body size and thus lower their survival possibility (Loetti et al. 2007, Loetti et al. 2011). Hence, for a more accurate prediction of mosquito abundance as well as a better understanding of their life cycles, density dependence and environmental forcings need to be considered simultaneously in our representation of mosquito population dynamics.

Evidence of density dependence in mosquito populations has been proposed in some previous studies (Clements 1992, Juliano 2007, Yang et al. 2008a, Yang et al. 2008b, Russell et al. 2011). Self-limiting growth of mosquito populations is often found for life stages taking place in the water, as a result of cannibalism and competition for nutrients (Church and Sherratt 1996, Koenraad and Takken 2003, Bomblies et al. 2008). A negative relation between the per capita growth rate and abundance is also found in adult mosquito populations through explorative plots (Yang et al. 2008a, Yang et al. 2008b). However, despite the accumulating evidence in support of density dependence, this concept was only recently included in mosquito abundance models (Yang et al. 2008a, Yang et al. 2008b, Jian et al. 2014a). Many questions remain open, such as whether accounting for density dependence can improve the predictive skills of modelling representation. What is the relative importance of density dependence and of exogenous environmental forcings in governing mosquito populations? Thus one goal of the dissertation is to investigate the role of density dependence in mosquito population dynamics in temperate regions and its impact on abundance models of adult mosquitos.

1.4 Hydrologic controls in mosquito population dynamics

Although the preferred habitat types of mosquito species differ considerably, most of them spend the first three stages (egg, larva, and pupa) under water (Clements 1992). Hence water availability is essential for understanding the fluctuations in mosquito populations. Typically, rainfall intensity is used as a representation of water amount in mosquito habitats (Yang et al. 2008b, Chaves et al. 2012, Gao et al. 2012). Yet, in recent years, hydrological models estimating soil wetness began to receive more attention because they could provide a physically-based description of a fundamental forcing term. Some studies show that modeled soil moisture is better correlated with biting and entomological inoculation rates than rainfall for anopheles mosquitoes in Kenya (Patz et al. 1998). Bomblies et al (2008) proposed a detailed simulation of local malaria transmission as influenced by hydrological and climatological factors in a semiarid environment. Trawinski and Mackay (2008) use a modified Penman-Monteith equation to estimate actual evapotranspiration, which is then incorporated in a predictive model of mosquito abundance in New York . Soil wetness and thermal conditions generated by the Topographically Based Hydrology model (TBH) has been used to drive models for St. Louis encephalitis (SLEV) and West Nile Virus (WNV) occurrences and the vector mosquito abundances (Shaman et al. 2002, Shaman et al. 2004, Shaman and Day 2005, Shaman et al. 2005, Day and Shaman 2009).

Although explored in previous studies, the control of water availability on mosquito population dynamics still remains one of the most challenging topics. This is especially true under natural conditions of temperate regions, because of the nonlinear regulating mechanisms, the interactions of multiple environmental forcings and the scale-dependent relation between water availability and mosquito abundance (Chaves and Kitron 2011, Jian et al. 2014a). Wet conditions are necessary to maintain mosquito habitats, but excessive water can also wash out larvae, dilute food concentration or increase the risk of predation for mosquito larvae (Shaman and Day 2005). Severe and sustained drought can reduce mosquito habitats, but temporarily dry periods can also induce the convergence of mosquito vectors and host animals, leading to an increase in the overall population (Shaman et al. 2004, 2005). Apart from water amount in soil, temporal distribution of water can also be critical to mosquito life cycle. Advanced or delayed wet conditions can result in very different mosquito abundance and disease transmission, due to their coupled effects with temperature and light (Day and Shaman 2008, Shaman et al. 2011). In addition, responses to soil moisture vary for different species. Wetter conditions are reported to increase the abundance of swamp species, such as *Aedes vexans* and *Anopheles walkeri*, while decrease eutrophic species like *Culex pipiens* (Shaman et al. 2002). Thus a detailed examination of the influence of soil water content is desirable for mosquito predictive models.

Furthermore, despite the recent applications of hydrological models in predicting mosquito abundance, few studies have compared the importance of soil moisture in explaining mosquito dynamics with that of rainfall (Patz et al. 1998). On one hand, soil moisture is likely a more direct physical parameter than rainfall for water availability in mosquito habitat. Thus its incorporation may provide more accurate information about the mosquito development and oviposition under water. On the other hand, rainfall, with a wider and easier availability, can not only influence actual fluctuations in mosquito populations because of its impact on habitats, but also affect mosquito behaviors by such as flight. In tropical arid regions, where water is the primary limiting factor, soil moisture is found to be the dominant driver of the fluctuations in mosquito abundance (Bomblies et al. 2008). However, in temperate regions, the effect of soil water content on mosquito population dynamics is unclear, and needs a more careful examination

1.5 The representativeness of adult mosquito observations

Representative mosquito observations are the prerequisite for developing and calibrating predictive models for mosquito abundance. Mosquito traps are the commonly used methods for sampling adult mosquitoes. However, only a few studies investigate the efficiency and representativeness of mosquito samples (Reisen and Pfuntner 1987, Reisen et al. 1999, Reisen and Lothrop 1999, Reisen et al. 2000). These studies mostly focus on the spatial arrangement and design of mosquito traps (Reisen

and Pfuntner 1987, Reisen et al. 1999, Reisen and Lothrop 1999, Reisen et al. 2000, Zhang et al. 2013, Azil et al. 2014, Johnston et al. 2014). For example, Reisen et al. (1999) compares the effectiveness of three different mosquito traps (New Jersey (NJ) light trap, dry ice baited trap, and gravid female trap) for collecting adult mosquitoes. Johnston et al. (2014) studies the effect of trap height on adult mosquito collecting. Azil et al. (2014) explores the spatial auto-correlations of adult mosquito samples.

However, in the case of adult mosquito populations in natural conditions, an important open issue concerns the choice of the sampling frequency which can capture the relevant mosquito population dynamical mechanisms. For studies on the yearly scale, adult mosquitoes are most commonly sampled, through trapping devices, over a single night with a weekly or even monthly frequency (Yang et al. 2008b, Shaman et al. 2011). Long-term studies of adult mosquito populations in their environment at the daily scale are rare. Thus a pertinent and important question is whether adult mosquito population dynamics, as they occur in nature, are fully captured when a weekly sampling frequency is adopted. In fact, many mosquito species have relatively short generation times. For example, laboratory experiments show that, under the most favorable conditions, the generation time for *Ae. vexans* can be less than 3 weeks (Becker et al. 2003). Furthermore, the activity of adult mosquito can (such as host seeking) respond quickly to environmental forcings (Clements 1992, Becker et al. 2003), thus imposing even more stringent requirements on the sampling frequency.

Another important issue related with mosquito sampling is the relation between the sampled and the underlying abundance. One implicit assumption usually adopted in adult mosquito collecting is that the ratio between the observed and the true abundance is relative constant, so that the fluctuations in the observation can reflect the changes in the actual population dynamics. However, it has been reported that the behavior of adult mosquitoes can also response to fast changing environment (such as light, temperature, relative humidity, rainfall and wind) thus pose a question on the assumption of fixed proportion (Bidlingmayer 1971, Nayar and Van Handel 1971, Clements 1992, Chaves and Kitron 2011, Spitzen et al. 2013). Previous studies show that the flight muscles of mosquitos cannot function efficiently at low temperature, reducing their flight activity (Clements 1992). Larger catches of adult mosquitoes are reported to be linked with lower moonlight when light traps are used for collecting the sample (Clements 1992). Furthermore, high relative humidity, and low wind speed are permissive for mosquito flight, while rainfall shows a nonlinear effect, promoting flight at lower intensity but inhibit it at extremely high intensity (Clements 1992). However, these results have seldom been incorporated in mosquito abundance models to separate the fluctuations in the abundance caused by true population change and by mosquito behavioral events.

The responses of mosquito activity to environmental forcings can impede the understanding of the true population fluctuations and reduce the accuracy of mosquito

models because they change the relation between the observations and the underlying population. However, this effect has not been explored in previous studies and its influence on predicting abundance is unknown. The only work I found which includes activity in predicting mosquito abundance is by Bomblies et al (2008), which models the location of adult mosquitoes as a function of wind and CO concentrations. In the general field of ecology, animal behaviors and sampling errors have been explored in Bayesian state space models (Clark 2007), which provide interesting insights to the question. However, a better understanding of mosquito population dynamics needs a more detailed investigation about the relation between the observed and the underline abundance.

1.6 Dissertation Objectives and Organization

In this dissertation, I combine different quantitative methods to understand mosquito population dynamics and to improve predictive models for adult mosquito abundance in temperate regions. Specifically I work on the following topics to address some of the open questions in the field. (1) How are mosquito populations in temperate regions regulated by density dependence, and how can mosquito models be improved by incorporating it? Although biological processes causing density-dependent growth have been observed in mosquito populations (Clements 1992, Church and Sherratt 1996, Koenraad and Takken 2003), few works have investigated its effect using formal statistical and/or process-based modeling approaches. Furthermore, the interactions of

density dependence with environmental forcings and habitat characteristics still remain elusive under natural conditionings. (2) What is the relative importance of soil moisture and rainfall in driving mosquito models in temperate regions? This has not been tackled before, likely because of the added complexity of hydrologic regimes frequently switching between soil controlled (dry) and atmosphere controlled conditions. Due to this complexity rainfall data are often used as a surrogate of soil water availability as a driver of mosquito abundance. However, the more direct hydrologic forcing of mosquito dynamics is arguably soil moisture, e.g. through the formation of ponding. Therefore, hydrological modeling to estimate the soil water status is a promising tools to advance our ability to predict mosquito abundance. (3) What are the temporal scales of variability in mosquito populations and what are the regulation mechanisms of the variability at different scales? This is an important but unaddressed question in mosquito population dynamics, and its answer forms the basis for determining the temporal scales of mosquito sampling and modeling. Although the number of mosquito models at a single time scale is increasing, no previous study, as far as we know, has explored the full temporal spectrum of variability in mosquito populations. (4) What sampling resolution can fully resolve population dynamics in adult mosquito? Fast fluctuations have been observed in mosquito abundance (Jian et al. 2014b). But most long-term mosquito abundance observations are often sampled at once-per-week or even long time intervals, without any investigation of the representativeness of the

samples. Thus a research is necessary to study the effects of sampling resolution on the understanding of mosquito dynamics and on the accuracy of their predictive models. (5) How does the predictability of mosquito abundance change over the predictive horizon? With the increasing number in mosquito models, we have seen a variation in the temporal scales of these models and differences in their predictive skills. However we still lack a systematic understanding of how the predictability of mosquito abundance changes with modeling scale, especially at what time scale we can reliably predict the rate of change in population size.

My dissertation is divided into five chapters. The first 2 research questions are addressed in chapter 2, where a hierarchical Gompertz-based approach is used to include density dependence in predicting mosquito abundance and evaluate its relative importance vs. environmental forcings. Realistic descriptions of hydrologic processes are also incorporated in the model and soil moisture is evaluated as a more direct driver of mosquito population dynamics. The model is based on a hierarchical state-space structure to pool information from multiple mosquito traps. It is applied to the description of the abundance of *Culex pipiens* - a West Nile Virus vector - in the Po River Delta region (Northeastern Italy). Much of the work was developed in collaboration with Dr. Marco Marani, Dr. Sonia Silvestri, Dr. Enrica Belluco, Dr. Andrea Saltarin, and Mr. Giovanni Chillemi.

The 3rd and 4th research questions are addressed in chapter 3. In this chapter, I analyze a long term daily time series of abundance data for multiple adult mosquito species in North Carolina, focusing in particular on *Aedes vexans* and *Culiseta melanura* (vectors of West Nile Virus and East Equine Encephalitis). The temporal spectrum of fluctuations in mosquito abundance is studied using Fourier Transform. Time series analysis is applied to compare the information obtained from weekly samples and daily samples. Individual-based simulations are used to investigate the driving mechanisms of the fluctuations by selectively turning off the effects of endogenous or/and exogenous controls. A component representing mosquito activity is also added to the individual-based simulation to study the effect of mosquito behaviors on model building. This and the following chapter were developed in collaboration with Dr. Marco Marani, Dr. Sonia Silvestri, Mr. Jeff Brown, and Mr. Rick Hickman.

In chapter 4, I address the 5th research question using a state space reconstruction (SSR) approach to compare the predictability of mosquito abundance at weekly, biweekly and monthly scales. Among the methods for SSR, the simplex projection (SP) method is used to forecast near future abundance change using the mosquito data from the Brunswick County. The result of the SP method is compared with random walk models in their ability to capture short-term population fluctuations. In addition, species interactions for multiple mosquito species across temporal scales are investigated using the co-prediction method based on the SSR approach. Finally, in chapter 5, the overall

results and conclusions of the dissertation are summarized and the major contributions of this dissertation to the literature are listed.

2. Environmental Forcing and Density-dependent controls of *Culex pipiens* Abundance in a Temperate Climate (Northeastern Italy)

2.1 Introduction

Emerging and re-emerging mosquito-borne diseases in temperate regions have become progressively more common in recent years as ever increasing human and vector mobility creates conditions which are favorable for their diffusion (Enserink 2008, Randolph and Rogers 2010). This is a source of concern, particularly in areas with high human population density characterized by low immunity and uncertain vector-host relationships (Hayes et al. 2005, Enserink 2008, Lafferty 2009, Randolph and Rogers 2010). Well-known and relevant examples include the West Nile Virus (WNV) diffusion in the United States and Europe, mostly associated with the *Culex* genus (Hayes et al. 2005), and the increasingly frequent and numerous Chikungunya and Dengue fever cases in Europe, spread by *Aedes albopictus* (Enserink 2008).

A fundamental step towards understanding and predicting mosquito-borne disease transmission in temperate climates requires the development of a mechanistic modeling framework of vector population dynamics (Stenseth et al. 2002, Jones et al. 2008). However, work on modeling mosquito population dynamics in temperate climates remains relatively limited. It is often based on empirical regressions of mosquito population on environmental drivers, and usually assumes a fast response of population abundance to meteorological forcings. However, this assumption is unlikely

to hold in temperate which areas are characterized by subtle links between mosquito population dynamics and highly heterogeneous environmental drivers (e.g. due to a lack of sharp transitions between dry/wet rainfall regimes). Temperate regions also usually exhibit a high human density and degree of anthropogenic control on water availability (e.g. irrigation, diffuse water impoundments, etc.). As a result, reliable models of mosquito abundance remain elusive in temperate areas (Shaman et al. 2006, Linard et al. 2009).

Given the importance of water availability in mosquito development and the intricate soil water balance in temperate regions, it is critical to provide a realistic representation of water dynamics in the soil and at its surface, jointly controlled by several hydrologic processes, such as infiltration, evapotranspiration and runoff generation. However, most approaches to modeling water controls on mosquito population dynamics simply use rainfall as a direct driver (e.g. Yang et al. 2008b, Chaves et al. 2012) and relatively few contributions use explicit hydrological models (Shaman et al. 2006, Bomblies et al. 2008, Day and Shaman 2008, Montosi et al. 2012) and/or satellite remote sensing (Chuang et al. 2012, Midekisa et al. 2012) to drive mosquito population models.

The importance of endogenous controls, such as density dependence and delayed population responses (Fowler 1981, Turchin 1990, Sibly et al. 2005) should not be underestimated either. Only recently have they been recognized as important

regulatory mechanisms of mosquito population and they have been rarely incorporated in modeling formulations (Yang et al. 2008a, Yang et al. 2008b, Chaves et al. 2012). I hypothesize that endogenous controls may be particularly important in humid temperate climates, where water is less often limiting and the interaction of multiple environmental controls may result in a wider distribution of adult emergence times with respect to those occurring under more homogeneous environmental conditions (e.g. in tropical climates).

Based on the above considerations, the goals of this dissertation chapter are: i) explore the relative importance of endogenous (e.g. density dependence) vs. exogenous (meteorological and hydrological forcing) factors. I explore in particular the relationship between per capita growth rate and population abundance, the magnitude of the delays with which population responses become manifested, and how they are influenced by environmental factors; ii) evaluate if and how the use of a full-fledged hydrological model of infiltration, percolation, and runoff to estimate soil moisture affects the model ability to explain the variability in mosquito population abundance in a temperate climate; iii) develop a sound hierarchical modeling approach (Clark 2007) to optimally exploit spatially-distributed observations and minimize the impact of mosquito population sampling schemes which do not fully represent all scales of spatial and temporal heterogeneity.

2.2 Materials and methods

2.1.1 Study area and data collection

Western Europe in general is identified as a hotspot for the emergence and re-emergence of vector-borne diseases (Jones et al. 2008), spread by 96 endemic mosquito species. Of these species, 62 were found in Italy in 1999 (Snow and Ramsdale 1999), and this number has probably increased significantly since then. The Po river delta in Northeastern Italy, where study site of this chapter is located (Figure 1), is in particular characterized by a high mosquito abundance, due to favorable climatic and environmental conditions (Enserink 2008, Schaffner 2009). I focus on the species *Culex pipiens*, one of the main vectors of WNV (Vinogradova 2000, Dohm et al. 2002, Hamer et al. 2008) and the most common species in the Po river delta area. *Culex pipiens* mainly feeds on birds, but also on mammals and humans (Vinogradova 2000, Hamer et al. 2008, Crans 2013b). It is highly adapted to various types of agricultural, urban and natural habitats and is active from late April to September (Madder et al. 1983, Vinogradova 2000, Becker et al. 2003, Crans 2013b). *Culex pipiens* preferably lives in vegetated areas (which provide shelter from predators and direct sunshine) close to water ponds rich in nutrients (Vinogradova 2000, Becker et al. 2003, Crans 2013b). Females lay eggs in small rafts on the water surface. Pupae and larvae subsequently develop in the water and adults emerge after several weeks, depending on environment factors (temperature and daylight hours) (Vinogradova 2000, Becker et al. 2003). Under optimal conditions,

typical of the summer period, the total time needed for an adult to emerge from an egg can be as short as one week (Becker et al. 2003, Loetti et al. 2011). Temperature is also reported to influence the adult survival probability and individual size (Oda et al. 2002, Loetti et al. 2007, Loetti et al. 2011). The flying ability and oviposition of *Culex pipiens*, like other mosquito species, can be limited by high wind speed (de Meillon et al. 1967, Clements 1992, Becker et al. 2003).

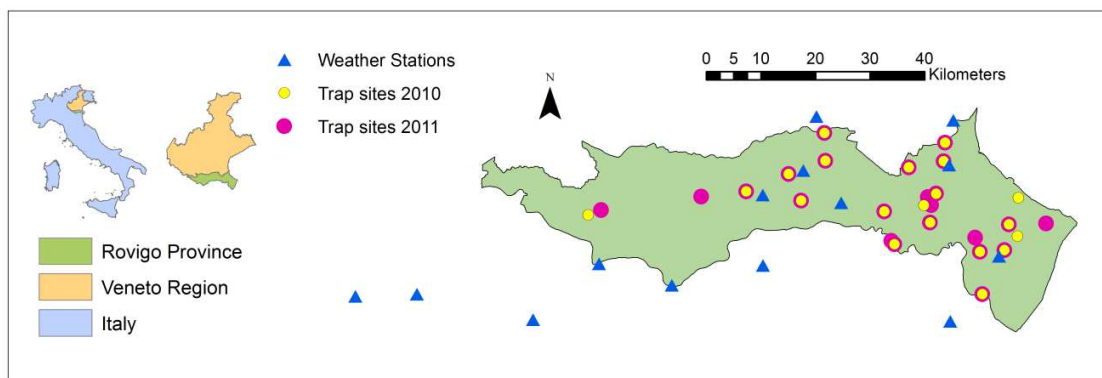


Figure 1: Study area, spatial distribution of mosquito trap sites, and weather stations in the Po River delta area Italy.

I used mosquito abundance observations performed from May to September in 2010 and 2011, sampled with CO₂ traps. Female individuals and species presence were subsequently identified in the lab. The sampling was performed weekly between 8:00 pm and 7:00 am the next morning at 20 sites in 2010 and 23 sites in 2011 (Figure 1). *Culex pipiens* accounted for approximately 90% of the more than 300,000 total captures. I excluded from the analyses data from 5 sites in 2010 and 6 sites in 2011, because of the known application of pesticides, even though details on how and when they were

applied are not available. Sites for which land use and land cover information could not be established through GIS and remote sensing were also removed. Data from 15 sites in 2010 and 16 sites in 2011 remained after this initial filtering.

Meteorological data were gathered from 14 stations in the study area, including temperature, wind speed, humidity, precipitation and global solar radiation (Figure 1) (data provided by Agenzia Regionale per la Protezione Ambientale del Veneto, ARPAV, and by Agenzia Regionale per la Protezione Ambientale dell'Emilia-Romagna, ARPAE). Ordinary Kriging was used to interpolate meteorological conditions at the sampling sites (Pebesma 2012) adopting an exponential variogram with a correlation scale of 8 km, as deduced from an analysis of the experimental variograms. A leave-one-out cross validation of the ordinary Kriging procedure yielded Root Mean Square Errors (RMSE) of 0.74mm/hr for rainfall, 1.1 C° for temperature, 0.6 m/s for wind speed, and 52.9 W/m² for solar radiation. These values of the RMSE indicated that the Kriging interpolation provided reliable local estimations of the environmental forcings. The Kriging interpolation and the validation were performed in R 2.5.1 with the package gstat (Pebesma 2004). Daylight hours, later used as an explanatory variable, were calculated using latitude and Julian date (Allen et al. 1998).

GIS information and remote sensing data were gathered to address the effects of land use and to support hydrological modeling (data provided by Consorzio di Bonifica del Delta del Po). Such information included a 5m Digital Terrain Model, shape files of

land use, soil type, permeability, geomorphology and population density, as well as 9 ASTER (Advanced Space-borne Thermal Emission and Reflection Radiometer) acquisitions from 2005 to 2011. The land use vector dataset, with scale 1:10000 and minimum mapping unit of 0.25 hectares, was obtained from the Veneto Region administration. Land use classes for this map were identified from SPOT 5 satellite images, DEM data, and other vector spatial information such as road and forest maps. The classes on the map were consistent with those from the CORINE Land Cover (CLC) database established by the European Environment Agency (<http://www.eea.europa.eu/publications/COR0-landcover>). NDVI values were computed from ASTER data acquired from May to July 2010 over 75m x 75m windows around the sampling points using the ENVI Classic application. The computation of mean local human population densities, performed under ArcGIS 10, is based on data provided by the Veneto Region.

2.1.2 Modeling Approach

I used the Gompertz-logistic model which was externally forced using soil water content obtained from hydrological modeling and meteorological observations. The hierarchical approach adopted also addressed issues connected with spatial and temporal heterogeneities and explicitly models observation and process uncertainties.

2.1.2.1 Soil moisture dynamics

The soil moisture status at the sampling sites was evaluated using a finite element numerical method to solve the 2-dimensional equation of water flow in variably saturated porous media. The algorithm employed a Galerkin finite element formulation for the spatial discretization and used a weighted finite difference method and an implicit backward Euler scheme in the time domain. The resulting discrete equation was solved by Picard-Newton iteration (Paniconi and Putti 1994, Camporese et al. 2010).

The soil moisture dynamics at each mosquito sampling site were evaluated by considering a representative transect, in which the initial depth of the water table was assigned on the basis of the local values of mean depth to the water table provided by the Consorzio di Bonifica Delta Po and by ARPAV. The area of the Po river delta was characterized by a very small relief and diffuse crops. I assumed a simplified geometrical setup consisting in a 20 m long flat transect, drained at the sides, a typical configuration in the agricultural study site at hand. The model was forced with the kriged precipitation estimates obtained at each site and with site-specific surface evaporation and vegetation transpiration rates (a function of vegetation cover and type - crop, arboreal or herbaceous - as derived from remotely sensed data, aerial photographs, and from direct knowledge of the sites). The boundary conditions at the outer edge of the computational domain were fixed to the value of the known mean depth to the water table. This approach, even though it idealized the saturated/unsaturated flow

through the soil, referred to a realistic configuration incorporating readily available site-specific hydrologic information (soil type, depth to the water table, vegetation, temperature, rainfall). The simulations were started on the first day of March and run until 30 September. The soil moisture dynamics of the topmost soil layer at the point most prone to saturation (at the center of the domain) was considered to be representative of soil saturation in the area near the sampling site. A direct validation of the hydrological model output in the study area was not possible due to a lack of appropriate hydrologic observations of soil moisture and water table depth. However, the hydrological model has been previously applied to several case studies and its successful validation in those cases (e.g. Camporese et al. 2010, Weill et al. 2013) supports its use to provide estimates of hydrological forcings to mosquito population dynamics.

2.1.2.2 Mosquito population modeling

One of the aims of the present work is the evaluation of the relative importance of endogenous mechanisms in determining mosquito abundance dynamics. Prior to model formulation, I first investigated the existence of detectable lag effects and density dependence through an autocorrelation analysis of the data. I analyzed, in particular, the Autocorrelation Function (ACF) and the Partial Rate Correlation Function (PRCF). The latter is a partial autocorrelation, i.e. its k -th value is the correlation between mosquito abundance at time t , x_t and x_{t-k} , once the correlations between x_t and x_{t-1} through x_{t-k+1} are

removed (Box et al. 2008). In the case of the PRCF one considers the partial correlation between the per capita growth rate ($r_{t-1} = \ln(x_t / x_{t-1})$) and the logarithm of the abundance at current and previous times: $\ln(x_{t-1})$, $\ln(x_{t-2})$... (Berryman and Turchin 2001). The PRCF is a direct index of density dependence effects as it relates the current rate of change of the population with its size at previous times. It is seen that the ACF's show positive correlations for about 3-4 weeks in most cases, and subsequently negative correlations up to a lag of 7-10 weeks (Figure 2a). However, this is largely due to the serial correlation induced by the individuals surviving between time $t-k$ and time t . Once the correlation with intermediate time steps is removed, through the computation of the PRCF, density regulation is only seen at the 1 week lag (see Figure 2b). Density dependence is also evidenced by conditional scatter plots exploring the possible relationships between two of the relevant variables (growth rate, abundance at current and previous times, temperature) when the remaining variables are constrained within narrow ranges (Appendix A, Figure 17a). This analysis shows that growth rates significantly decrease as abundance at the previous time increases, irrespective of $\ln(x_{t-2})$ and temperature. On the contrary, no visible dependence exists between r and $\ln(x_{t-2})$, for all values of $\ln(x_{t-2})$ and temperature (Appendix A, Figure 17b).

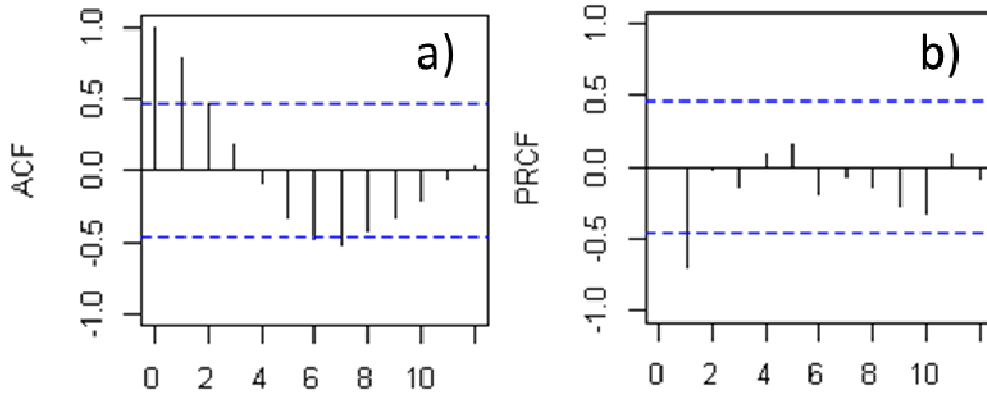


Figure 2: (a) Autocorrelation function (ACF) and (b) partial rate correlation function (PRCF) for site 8 (Taglio di Po). The blue dashed lines represent 95% confidence intervals for the ACF and PRCF. The remaining sites, not shown here for brevity, display similar patterns

The exploratory analyses on log-transformed data provided strong support to the existence of a density dependence mechanism with a memory of about one week. On this basis I assumed a basic Gompertz-Logistic (GL) model structure:

$$r_{t-1} = dx/x_{t-1} dt = \ln(x_t/x_{t-1}) = r_m(1 - \ln(x_{t-1})/\ln(K)) \quad (1)$$

where r_m is the maximum per capita growth rate and K is the carrying capacity.

In order to connect observations, $y_{t,j}$ (the subscript ' j ' indicates the j -th site), to the actual abundance $x_{t,j}$, I assume $y_{t,j}$ to be distributed according to a Poisson distribution with mean $x_{t,j}$, i.e. $y_{t,j} \sim \text{Poisson}(x_{t,j})$ (' \sim ' represents equality in distribution). This assumes given the underlying abundance, the observed abundance is observed as a Poisson distribution.

Next, I assumed that both the per capita growth rate and the carrying capacity should be functions of exogenous environmental forcings. The environmentally-forced GL model can now be written as:

$$\ln(x_{t,j}) = \alpha_{0,j} + \alpha_{1,j} \ln(x_{t-1,j}) + \beta E_{t-1,j} + \epsilon_x \quad (2)$$

where $\alpha_{0,j}$ and $\alpha_{1,j}$ were model coefficients, $E_{t-1,j}$ was a vector containing the relevant exogenous environmental factors evaluated at time $t-1$, β was a vector of parameters to be estimated for the exogenous controls. ϵ_x was the process error and referred to the variability that is not captured by the model due to its structure, e.g. because of an incomplete or improper model formulation. ϵ_x was assumed to be normal with standard deviation δ_x .

The fundamental role of environmental controls in the formulation can be made explicit by considering that the maximum per capita reproduction rate (defined by $\ln(x_{t-1,j}) = 0$) is now $r_{m,j} = \alpha_{0,j} + \beta E_{t-1,j}$ and the carrying capacity (defined, as before, by the condition $\ln(x_t) = \ln(x_{t-1})$) is now $K = \exp((\alpha_{0,j} + \beta E_{t-1,j}) / (1 - \alpha_{1,j}))$. Under this formulation, a value of $\alpha_{1,j}$ between 0 and 1 implies density dependence, i.e. a per capita growth rate, $r_{t-1,j} = \ln(x_{t,j} / x_{t-1,j}) = \alpha_{0,j} + (\alpha_{1,j} - 1) \ln(x_{t-1,j}) + \beta E_{t-1,j} + \epsilon_x$ which is a decreasing function of the current population abundance.

I considered the following exogenous forcings: temperature, wind speed, precipitation, modeled soil moisture, solar radiation and daylight hours. The variables expressing environmental forcings were normalized with respect to their mean and

standard deviation prior to their use in eq. (2), to ensure a similar dynamic range across different variables, favoring a faster convergence and ensuring a clear interpretation of the relative importance of different factors. The effect of temperature on mosquito populations is known to exhibit threshold behaviors and to lead to a maximum net reproduction rate for large temperatures (Becker et al. 2003, Ermert et al. 2011a, Loetti et al. 2011). By plotting the abundance of *Culex pipiens* vs. daily average temperature (not shown), I found that population abundance was negligible below a threshold of 19 °C. I hence represented the influence of temperature through the accumulated daily average temperature above 19 °C.

Finally, to capture across-site heterogeneities, I allowed $\alpha_{0,j}$ and $\alpha_{1,j}$ to vary across sites as a function of land use and land cover. The maximum per capita growth rate, $r_{m,j}$, and carrying capacity, K_j , are functions of $\alpha_{0,j}$ and $\alpha_{1,j}$ and thus this formulation assumes that density dependence controls vary for different sites. Under this model structure group level coefficients ($\alpha_{0,j}$ and $\alpha_{1,j}$) were not exchangeable. Rather, site-level environmental conditions were accounted for by expressing parameters in Eq. (2) as linear functions of local factors: $\alpha_{0,j} = \theta\alpha_0 L_{\alpha 0,j} + \epsilon_{\alpha 0}$ and $\alpha_{1,j} = \theta\alpha_1 L_{\alpha 1,j} + \epsilon_{\alpha 1}$. $L_{\alpha 0,j}$ and $L_{\alpha 1,j}$ were vectors of local factors, which, after exploring a wide range of potentially relevant environmental forcings (e.g. human population, distance to the nearest wetland, forest, water body, agricultural area, and urban area, topographic slope and curvature) included just the factors that were found to be influential: i) vegetation cover as

expressed through NDVI (Normalized Difference Vegetation Index, a remotely sensed index of vegetation cover) for $\alpha_{0,j}$ ii) distance to the nearest rice fields for $\alpha_{1,j}$. $\theta\alpha_0$ and $\theta\alpha_1$ were vectors of coefficients estimated through calibration. $\epsilon_{\alpha 0}$ and $\epsilon_{\alpha 1}$ are normally distributed error terms with standard deviations $\delta_{\alpha 0}$ and $\delta_{\alpha 1}$ respectively. In the following, I used Eq. (2) to predict the mean of *Culex pipiens* abundance ($x_{t,j}$) using information acquired at previous time steps.

With the above assumptions the model used in this study can be summarized as

$$y_{t,j} \sim \text{Poisson}(x_{t,j})$$

$$\ln(x_{t,j}) = \alpha_{0,j} + \alpha_{1,j} \ln(x_{t-1,j}) + \beta E_{t-1,j} + \epsilon_x$$

$$\alpha_{0,j} = \theta\alpha_0 L_{\alpha 0,j} + \epsilon_{\alpha 0}$$

$$\alpha_{1,j} = \theta\alpha_1 L_{\alpha 1,j} + \epsilon_{\alpha 1}$$

In order to determine whether an explicit spatial correlation should be accounted for in model development, I studied the spatial correlation between mosquito abundance observed across the sampling sites. The results of this analysis did not evidence a strong influence of the distance on the correlation between recorded abundances, even at small spatial scales (less than 1 km). Furthermore, after model fitting, I studied the spatial correlation of model residuals, finding that indeed no spatial structure could be identified. These findings are coherent with the short typical flight distance of *Culex pipiens* individuals, observationally found to be of the order of 500 m (Lindquist et al. 1967, Becker et al. 2003, Crans 2013b). These analyses show that spatial

correlations in the *Cx.pipiens* population were negligible at the scales considered here and hence I would not need to consider explicit spatial relations in the modeling framework (though spatial dependence did enter the proposed model through the inclusion of land use effects).

The posterior distributions of parameters were approximated with a sequence of random samples obtained in a Markov Chain Monte Carlo (MCMC) processes. Non-informative priors were used for the parameters, which allowed their values to be estimated from the data. The MCMC process was run with three chains, each containing 10,000 iterations to ensure convergence. The potential scale reduction factor was used as an indication of convergence (Gelman and Hill 2007). To summarize the posterior distributions, every other 15 values from the last 5000 iterations were used to eliminate the influence of initial values and autocorrelations in the MCMC samples (burning=5000 and thin =15). Details of the model can be found in Appendix A as WinBUGS code.

To compare the contribution of rainfall and/or soil moisture, the model was run with two configurations, one driven by estimated soil moisture and one by observed rainfall. Model evaluation was performed using artificial data simulation. Synthetic data were drawn with known model coefficients. The data were then used to estimate the coefficients in the above model structure, which were then compared with the actual values assumed in the generation phase (Gelman and Hill 2007). The results of this evaluation suggested that the model was able to capture the values of the actual

parameters for the synthetic generation exercise (see Appendix A for details). The estimation and evaluation procedures were performed with MCMC as implemented in R 2.13.1(R Core Team 2012) and WinBUGS (Lunn et al. 2000)).

2.2 Results

In general, mosquito abundance in both years started from about zero in May, reached a peak in late June–early July and then gradually decreased in August and September (Figure 3). The variation among sites was very significant. The number of captured *Culex pipiens* in a given night ranged between 0 and 4000. However, consistency was observed across the two years: sites displaying high abundance maintained this characteristic in both years.

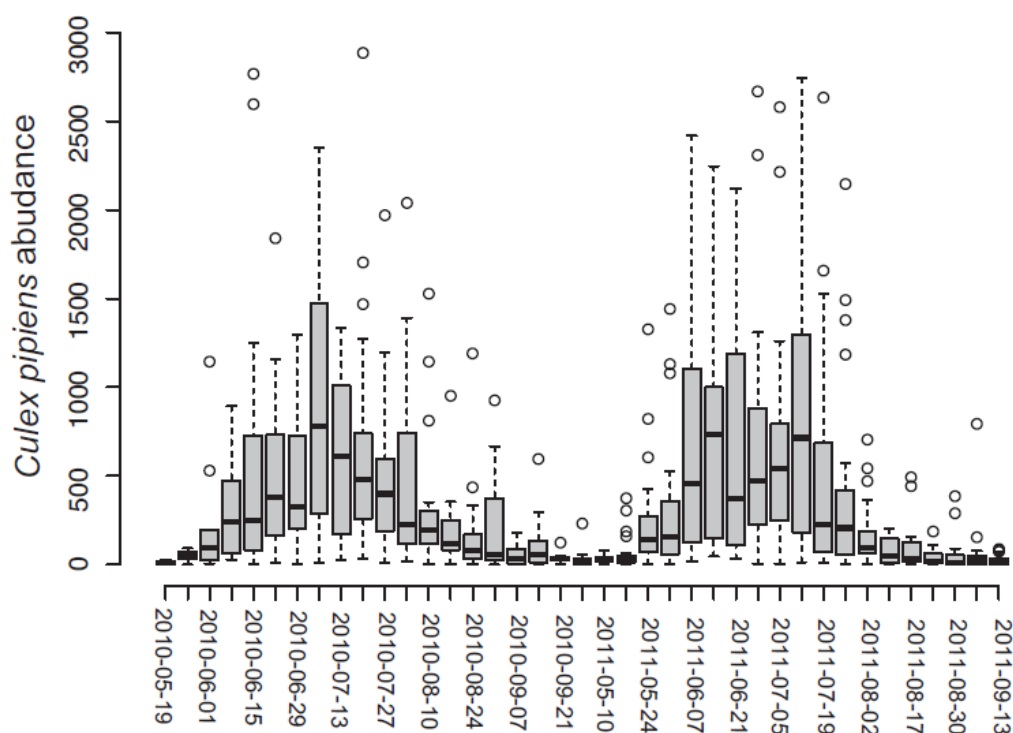


Figure 3: Box-plot of observed *Culex. pipiens* abundance as a function of time. Horizontal segments represent the median across observation sites. Box edges indicate the 25% and 75% quantiles. Whiskers represent 1.5 times the interquartile ranges.

The model performance was first evaluated in terms of predicted vs. observed per capita population growth rate, $r_t = \ln(x_{t+1}/x_t)$ between time t and time $t+1$ (Figure 4 a and b). The value of r_t is an approximation of $1/N \cdot dN/dt$, in other words, this is defined as the change of population size normalized by the size itself. The correlation between fitted values and observations is relatively good for small to intermediate population changes, most common in the observations (the red/yellow dots in Figures 4 a and b, clustered around the 1:1 line. Colors code the density of points within small neighborhoods in the graph). The model does not seem to be able to capture the largest values of the per capita growth rate, both for negative and positive fluctuations (blue/gray dots away from the 1:1 line). While this is of course undesirable, it is, to our knowledge, a limitation affecting all current mosquito population models (e.g. see Chaves et al. 2012). Large rates of population change are indeed not common (as indicated by color coding in Figure 4), but are nevertheless important as they potentially mark abrupt changes in the population abundance (outbreaks or population collapses) possibly associated with changing environmental forcings. Finally, even though a slight bias is present for low abundances (Figure 4 c and d), the model overall explains most of the variance in the data and captures seasonality and site differences (Figure 5).

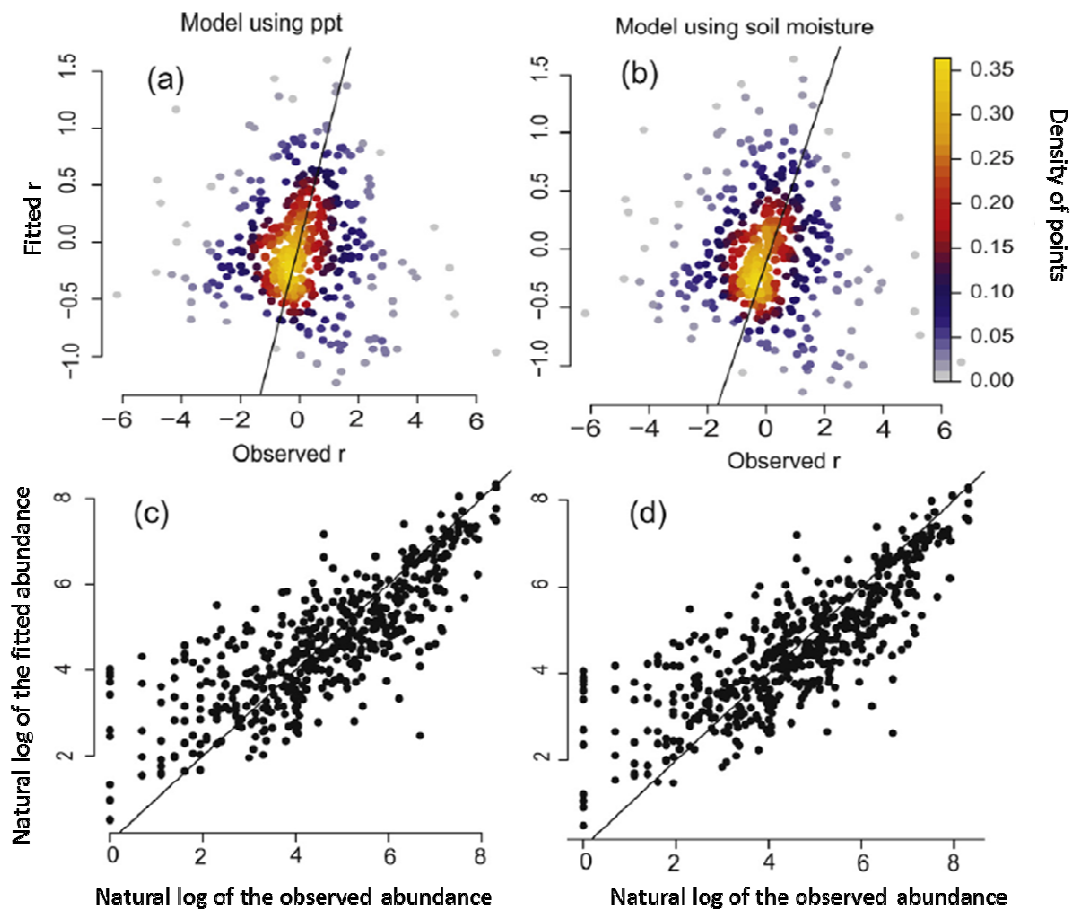


Figure 4: Predicted vs observed values of *Culex pipiens* abundance and per-capita growth rates under different model formulations. a) and c) include rainfall as a predictor, while b) and d) refer to the inclusion of estimated soil moisture. Colors in a) and b) encode the density of points in the graph. Yellow indicates that a large amount of modelled vs observed points fall in that specific area of the graph. Grey points indicate that no other point lies in the immediate neighborhood. Solid lines indicate 1:1 correspondence.

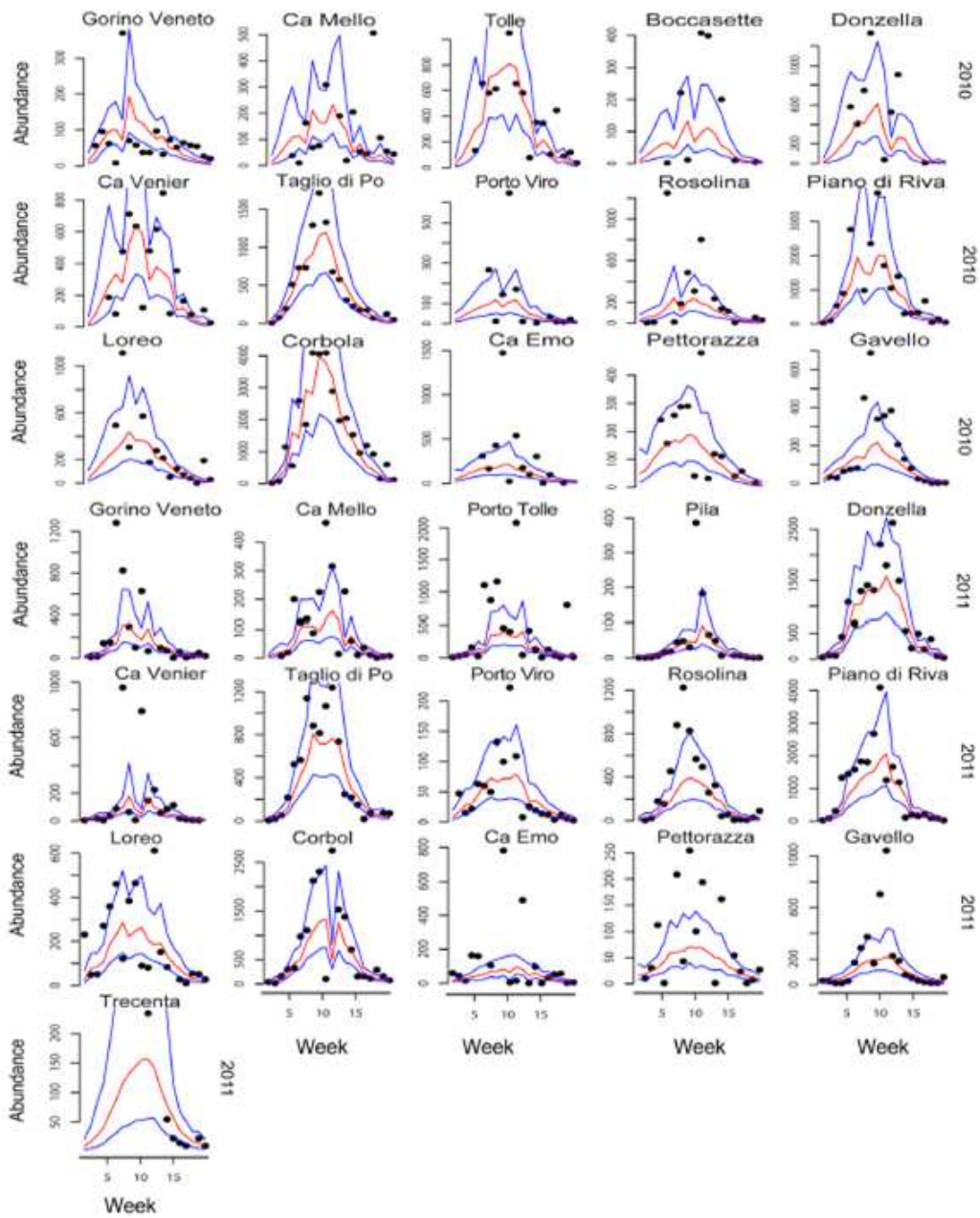


Figure 5: Time series of predicted and observed abundance. The first 3 rows are for 2010 and the last 4 rows are for 2011. Black dots are the observed values. The red lines are the mean predicted values and the blue lines are the 95% credible intervals of the predicted values based on the MCMC samples.

Model formulations forced using soil moisture or precipitation display similar performances (Figure 4 a-b and c-d), the use of soil moisture leading to slightly lower Deviance Information Criterion values (DIC, a Bayesian metric, which simultaneously considers model fitness and the number of effective parameters, e.g. (Gelman and Hill 2007)) and Root Mean Square Error (RMSE) values (Table 1). This similar performance can be attributed to i) the absence of a strong water limitation in the study area, ii) the presence of a moderate (nonlinear) correlation between rainfall and soil moisture (see appendix A); iii) the abundance of artificial habitats associated with towns and residential areas. Given the similar performance of the two models I will focus the further discussion on the results from the soil-moisture forced model alone.

Table 1: Model performance when soil moisture or rainfall was used as predictors.

	SM	Rainfall
RMSE	350.0	354.8
DIC	4263.9	4270.4

The values of $\alpha_{1,j}$, the prefactor of the abundance at the current time in Eq. (2), vary from -0.09 to 0.41 across sites, with a mean of 0.23 (Figure 6). The fact that this parameter values are in all cases significantly smaller than 1 (corresponding to a free exponential growth) reinforces the indication of a density dependence in the mosquito population dynamics, as previously discussed. Values of $\alpha_{1,j}$ close to 0 (e.g. compatible with values found at Porto Viro, Rosolina, Ca Emo, Pettorazza, Gavello, Loreo, Corbola

and Trecenta see Figure 6) indicate sites where abundance is primarily limited by exogenous environmental factors. The values of $\alpha_{1,j}$ are consistent across the two years (Figure 6), suggesting that *Culex pipiens* abundance at most sites is jointly controlled by endogenous and exogenous factors.

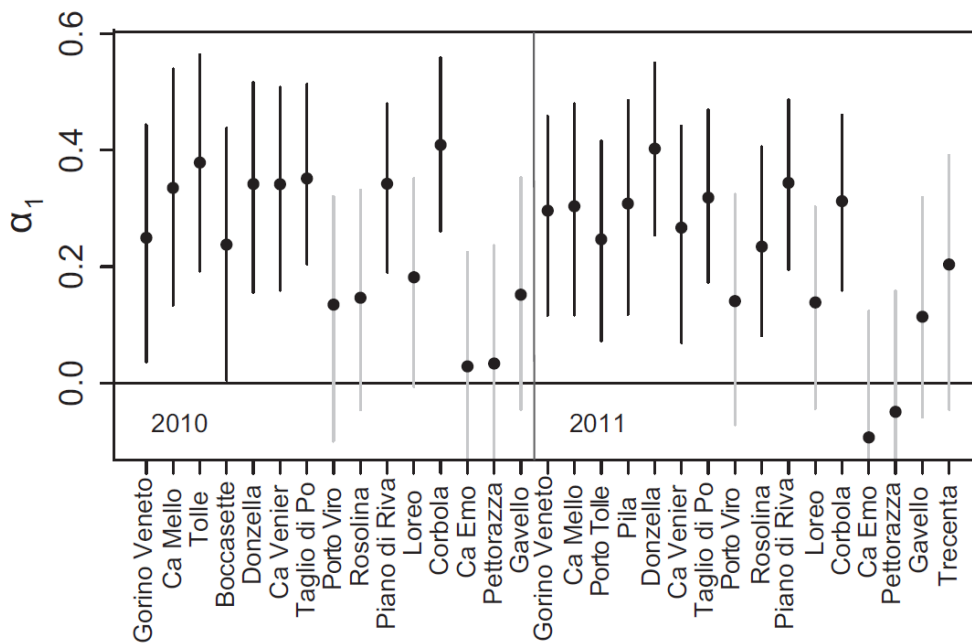


Figure 6: α_1 for different sites. α_1 is the coefficient for mosquito abundance one week before present, i.e. it represents the magnitude of density dependence. The black dots are the mean values and the segments are the 95% credible intervals based on the MCMC samples. α_1 values for the sites with the black segments are significantly larger than 0 while α_1 values for the ones with grey segments are not. The left panel shows the result for 2010 and the right panel shows that for 2011.

Among exogenous controls, I find daylight hours to be the most influential predictor of *Culex pipiens* abundance (see Table 2), while soil moisture is the second most important forcing factor. The negative correlation exhibited by *Culex pipiens* abundance with soil moisture, a possibly surprising finding, is likely related to the water available

in ponded areas (e.g. due to irrigation) even when the average soil moisture is low. The model parameter values do not suggest a significant influence of temperature, radiation or wind speed on mosquito population dynamics on weekly time scales.

Table 2: Mean and standard deviation of multiplicative coefficients of exogenous factors in eq. (4). Soil water content, radiation, hours and wind speed were calculated as the average values one week before mosquito samplings. NDVI was calculated for a 75m x 75m window around each sampling site. (levels of significance are: * p <0.1, ** p<0.05, and * p<0.01)**

	Mean	SD
Temperature	-0.02	0.06
Soil moisture	-0.27	0.14*
Radiation	-0.03	0.07
Daylight hours	0.78	0.07**
Wind speed	-0.05	0.07
Distance to the nearest rice field	-0.11	0.04***
NDVI	0.41	0.15***

The significant control exerted by daylight hour illustrates the strong seasonal cycle in *Culex pipiens* dynamics, either directly regulated by daylight hours or by variables strongly correlated to it. The lack of significance of the factors related with temperature, radiation, and wind speed may be partly due to the fact that mosquitoes were mostly sampled in the summer period, when meteorological factors were consistently within a range favorable to sustain a mosquito population: as long as the values of these parameters lie within acceptable bounds they do not affect mosquito population dynamics. In fact, the 5% and 95% quantiles of the distribution of the average

daily temperature were 15.2 °C and 27.8 °C respectively. The reported lower and upper thermal death conditions for females of *Culex pipiens* were 9.8 °C and 34.2 °C (Loetti et al., 2011). Colinearity with day length may be another reason for the insignificant coefficient representing the effect of temperature. The 5% and 95% quantiles of average daily wind were 0.3-2.2m/s: wind conditions were thus favorable for mosquito activity most of the time and hence the possible influence of extreme winds was not picked up by model calibration, which is sensitive to the most common environmental conditions. Finally, as pointed out by Chaves et al. (2012), mosquito species are more sensitive to climatic factors that have high variability. Since the environmental conditions in the Po River Delta were relatively stable during the summer, they may not significantly contribute to explaining the fluctuations in *Culex pipiens* population.

The hierarchical model structure allows the model coefficients to vary across sites according to the specific environmental conditions. Here, after an initial exploration of a wider set of environmental descriptors, I consider the distance to the nearest rice field and the Normalized Difference Vegetation Index (Table 2 and Figure 7). NDVI ranged from 0.17 to 0.55 and the distance to rice field ranged from 0 to 21.5 km. I find a significant positive effect of NDVI on $\alpha_{0,j}$, and a significant suppressive effect of the distance to the nearest rice field on $\alpha_{1,j}$ (Figure 7). The intercept α_0 represents the maximum per capita growth rate when environmental conditions are at their average value. The positive effect of NDVI on α_0 suggests that areas with better vegetation

conditions are preferred habitats, which have larger carrying capacity. α_1 is larger at sampling sites closer to rice fields. Because high values of α_1 (i.e. closer to 1) indicate closeness to a free exponential growth while lower values of α_1 indicate a stronger exogenous constraint, I suggest that the relative importance of density dependence is a function of habitat characteristics. Additionally, since α_1 is positively related to the carrying capacity, this result implies that rice fields, which provide both water and nutrients, can sustain larger *Culex pipiens* populations.

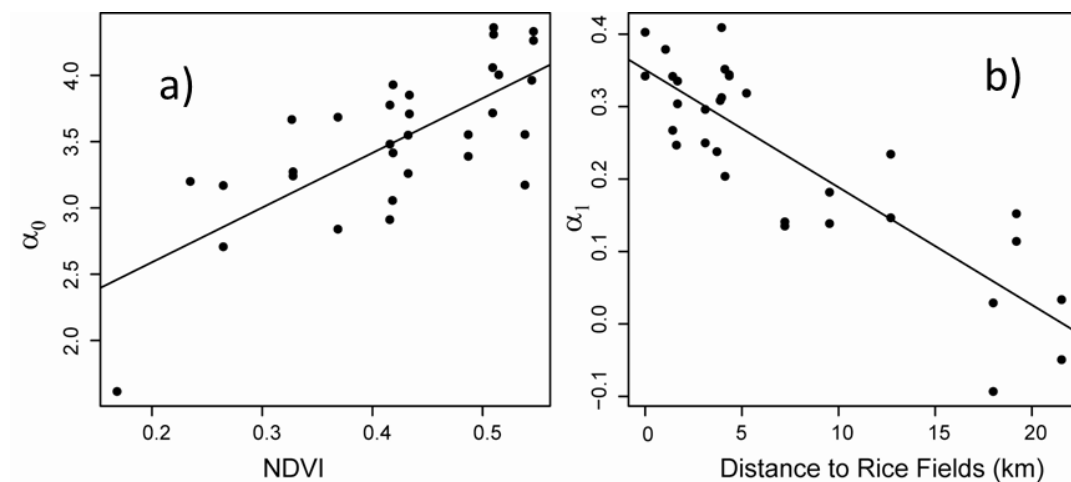


Figure 7: Land use land cover effects on *Culex pipiens* abundance. Panel a) shows α_0 increases with NDVI. Panel b) shows α_1 decreases with distance to the nearest rice field.

2.3 Discussion and conclusions

The analysis of the data through a new model of mosquito population dynamics shows that endogenous and exogenous factors are both important regulators of mosquito abundance and that they interact in a complex way. Density dependence is observed under laboratory conditions for *Culex pipiens* larvae: higher larvae density lead

to larger mortality of the immature stages and longer development times (Vinogradova 2000). However, the relevance of density dependence mechanisms in the field has not been previously evaluated for *Culex pipiens*, particularly within a framework that includes both endogenous and exogenous controls.

In particular, I find that endogenous regulations induce dependence on previous system states with a maximum lag of about one week. *Culex pipiens* is shown to have a relatively short generation time under lab conditions (Becker et al. 2003, Loetti et al. 2011). Indeed, laboratory experiments show that the development time for *Culex pipiens* is much shorter than that for many other mosquito species, such as *Aedes vexans* and *Ochlerotatus cantans* and is close to about one week when temperature is above 25°C (Vinogradova 2000, Becker et al. 2003, Loetti et al. 2011). The daily temperature in the study period lies in the interval 13°C – 29.5°C, and hence the fast growth and density response of *Culex pipiens* can partly explain the short memory I observe in the data. A clear explanation for the observed 1 week characteristic time scale in the mechanism of density dependence is not entirely straightforward. In fact, (1) space-time heterogeneity in habitat characteristics can result in widely varying hatching and development times, (2) different generations of *Culex pipiens* overlap at any given observation time. However, the correspondence between the observed characteristic time scale for density dependence and the typical duration of the *Cx.pipiens* life cycle hardly seems coincidental.

Even though endogenous and exogenous factors have been separately addressed in previous work for other mosquito species (such as in Shaman et al. 2002, Yang et al. 2008a), a better understanding of their relative role and interactions can only be obtained when they are modeled simultaneously (Yang et al. 2008b, Chaves et al. 2012). The most common modeling assumption is that exogenous factors rigidly dictate mosquito abundance fluctuations. However, the work shows that ignoring endogenous controls will: i) neglect critical information in the observations, thereby amplifying the predictive uncertainty, ii) lead to erroneous identifications of the role of exogenous factors because part of the variability associated with internal population dynamics will be attributed to changes in environmental factors. Hence, neglect of the role of endogenous drivers of mosquito population dynamics has significant implications for mosquito control and for our understanding of mosquito population's response to environmental changes (Juliano 2007).

Because the parameters are biologically interpretable in the model, I am able to identify how environmental factors may affect the relative importance of endogenous vs. exogenous controls. In fact, the hierarchical structure of the model allows the growth rate, the carrying capacity, and the lagged abundance effect to vary across sites, according to different land use and land cover properties. In particular, we have seen how vegetation abundance and distance from rice paddies may significantly alter both the maximum reproduction rate and the carrying capacity of the system, thus placing

the mosquito population in regimes characterized by varying degrees of internal dynamical control.

A second significant finding is the relatively small influence of rainfall/soil moisture on mosquito abundance. Compared to areas in which sharp transitions between dry/wet weather regimes make soil moisture the predominant controlling factor of mosquito abundances (Bomblies et al. 2008, Montosi et al. 2012), my study area does not display a similarly marked control of soil water content. More frequent and evenly distributed rainfall, as well as human activities (irrigation, gardening, etc.) typically make available adequate amounts of water in the densely populated temperate regions. High soil moisture values caused by recent rainfall events become, over the background of an already sufficient moisture availability, a suppressive factor of the active mosquito population. This consideration points to the limitations associated with the fact that y_t may represent a varying proportion of x_t as a function of current conditions. The negative correlation between *Culex pipiens* abundance and soil moisture thus supports the notion that factors other than water availability, such as nutrients and organic material availability, are likely to be limiting its population in the temperate study area. Unlike swamp species, *Culex pipiens* prefers high concentrations of organic matter in water bodies (Vinogradova 2000, Becker et al. 2003). High soil moisture related to rainfall events may act to dilute organic matter, thus reducing *Culex pipiens* abundance (Shaman et al. 2002, Day and Shaman 2008, Crans 2013b). High rainfall can

also favor flushing of water which would otherwise be stagnant, leading to larger larval mortality rates (Becker et al. 2003). We note that this result does not necessarily or readily extend to other mosquito species in temperate regions, for which more clear-cut water limitations can exist (such as flood water species and species living in more pristine environmental settings). Furthermore, the relative importance of some exogenous and endogenous controls of mosquito population may be different from the case examined here in temperate regions displaying a drier climate and a less pronounced anthropogenic influence (e.g. less intense irrigation)

I also find that use of rainfall or inferred soil moisture to force mosquito dynamics does not produce significantly different model predictive skills. This is somewhat counterintuitive, as one expects soil moisture to be a more direct driver of mosquito populations and because of recent results suggesting the importance of hydrologic processes for mosquito modeling. However, a large part of the previous literature focuses on arid environments (Bomblies et al. 2008), and very rarely soil moisture and rainfall effects are compared (Patz et al. 1998), such that my finding does not seem to contradict previous results. Hence, I conclude that an important implication of the work is that *Culex pipiens* abundance in temperate and humid areas responds to rainfall data, and does not necessitate explicit hydrological modeling of soil moisture content. It should be pointed out, however, that some currently temperate areas (e.g. northern mediterranean Europe) are predicted to become significantly drier under

projected climatic changes (IPCC 2007), such that controls of water availability on mosquito population dynamics may increase in the course of the next century. It should also be noted that the values of soil moisture used here are outputs from a hydrological model applied to each mosquito sampling site, rather than actual measurements. Hence, some of the estimation error variance is attributable to an imperfect estimation of the soil moisture state. A further improvement of the model ability to explain observed mosquito variability should be expected when in situ (or, at a larger scale, remote sensing) observations of soil water content can be used.

The hierarchical approach adopted here provides a way to pool together information from different sampling sites and to overcome limitations associated with short sample lengths by exploiting a set of concurrent observations. The predictive power at each site can be increased by the use of data from sites with similar local environmental properties, while preserving track of site-specific features. This is possible because the coefficients $\alpha_{0,j}$ and $\alpha_{1,j}$ (which define the maximum per capita growth rate and the influence of endogenous control) are modeled through site-level regressions.

The limitation of the model during large population change may be attributed to a lack of correspondence between the number of individuals captured by the traps and the actual underlying mosquito population. In fact, rapid changes in the proportion of active individuals (captured by the traps) may be due to the occurrence of rainfall, which

leaves the actual population size in the area unaffected, leading to the mismatch between modeled (relatively low) and observed (relatively high) per capita growth rates. This further necessitates the studies on how mosquito activity and sampling uncertainties can influence the understanding of mosquito population dynamics. The hierarchical model assumes the observed abundance to be approximately Poisson-distributed, with a mean equal to the actual underlying abundance. Because the Poisson distribution does not supply an independent variance parameter, the abundance may be over-dispersed. This assumption remains difficult to validate with the limited amount of data available at each station and is ultimately tested through the correspondence between model runs and observations. Further tests for this hypothesis can be performed as more data become available.

The model exhibits significant potential to aid in understanding the population dynamics of *Culex pipiens* in the Po river delta. However, current limitations in mosquito population modeling approaches are confirmed, particularly when dealing with very large rates of change in mosquito abundance. This is a crucial issue in mosquito modeling and control, which will require further observational/modeling work.

3. The Temporal Spectrum of Adult Mosquito Population Fluctuations: Conceptual and Modeling Implications

3.1 Introduction

A detailed understanding of mosquito population dynamics under natural environmental forcing requires the observation and understanding of ecological processes over a wide range of time scales. For example, the effect of rainfall on mosquito oviposition has been documented to be dependent on the time scale: the effect is negative over short and intermediate time scales, due to diluted nutrients, reduced mosquito activity, and egg removal, and it is positive over long time scales because of increased habitat extent and relative humidity (Chaves and Kitron 2011). Adult mosquito activity (such as host seeking) can also respond quickly to meteorological forcings (Clements 1992, Becker et al. 2003), thus inducing fast response times of apparent population abundance. Many mosquito species have relatively short generation times. Laboratory experiments show that, under favorable conditions, less than 3 weeks may be required between two successive generations of *Ae. vexans* (Becker et al. 2003). Mosquito oviposition and feeding processes occur at hourly and daily scales (Chaves and Kitron 2011, Sanford and Tomberlin 2011, Chadee et al. 2014), and endogenous and exogenous driving factors typically vary on weekly to monthly scales (Shaman and Day 2007, Yang et al. 2008a, Yang et al. 2008b, Hart and Gotelli 2011, Chaves et al. 2013, Zhang et al. 2013, Jian et al. 2014a).

The sampling resolution should of course adequately cover such a wide range of scales, but few studies address the role of temporal resolution in mosquito sampling

(Reisen and Pfuntner 1987, Reisen et al. 1999, Reisen and Lothrop 1999, Reisen et al. 2000, Zhang et al. 2013), which is most commonly carried out over one single night with a weekly frequency (Gu et al. 2006, Bomblies et al. 2008, Yang et al. 2008b, Ermert et al. 2011b, a, Shaman et al. 2011, Chaves et al. 2013, Jian et al. 2014a). Daily, long-term studies of adult mosquito populations in their environment are, in fact, the exception rather than the rule. Among the exceptions is the work by Shaman et al. (2002), who focus on linking water availability and mosquito abundance at the monthly scale. Daily data are also used in Chuang et al (2012), who aggregate them into weekly means to explore the merit of using satellite and in situ weather measurements as drivers for mosquito modeling. Both these contributions take advantage of the increased reliability of weekly/monthly abundance estimates afforded by averaging daily data, but do not explore the full extent of the temporal scales covered by a daily dataset.

Indeed, particularly in the case of adult mosquito populations in natural conditions, an important question concerns the choice of the sampling frequency which can capture the governing population dynamical mechanisms. In fact, the degree with which observations represent the population being studied is a general and fundamental problem that should always be explicitly addressed in ecological studies (MacKenzie et al. 2002, Clark 2007, McCarthy et al. 2013). In the present case, the representativeness of observations of adult mosquito abundance with respect to the underlying population dynamics depends crucially on the time scales over which the size of the population changes, and on the factors that may affect the relation between observations and the actual abundance.

In this framework, the aims of this chapter are the identification of the range of temporal scales over which mosquito population variability occurs, the attribution of these temporal scales of fluctuation to the exogenous and endogenous dynamical mechanism generating them, and the inference of implications for observational requirements and modelling approaches. To this end I analyze, through Fourier Transform and mechanistic population models, a unique 9-year time series of uninterrupted daily abundance observations in North Carolina involving a large number of mosquito species, produced and maintained by the Mosquito Control Department in Bolivia (NC).

3.2 Materials and methods

3.2.1 Study area and data

The Mosquito Control Department in Brunswick County (North Carolina – USA) was established to monitor and prevent mosquito-borne diseases, with particular reference to Eastern Equine Encephalitis (EEE) and West Nile Virus (WNV), among the most severe mosquito-borne diseases in temperate semi-humid areas. The ornithophilic *Culiseta melanura*, and several other species, including *Aedes vexans*, have been implicated as mammalian bridge vectors of EEE, as well as of other arboviruses such as WNV (Maloney and Wallis 1976, Mahmood and Crans 1998a, Buckner et al. 2012, Crans 2013c). Since 2004, the Mosquito Control Department of Brunswick County has been routinely collecting daily abundance of adult mosquito at three locations (Figure 8) using New Jersey Light Traps (NJLT) all year around. NJLT's were placed 4 feet off the ground at chest height. The trap light source is a 25 watt frosted incandescent light bulb.

All traps were hard wired and plugged into a 120V all-weather outlet. The light source and fan were run continuously. Trap collections are made every morning between 8 and 10 am, 7 days a week, and female mosquitoes are identified and counted. The mosquito sampling was carried out on the Brunswick county government property (the “Chicken Trap”, 34.059°, -78.168°, contact Jeffrey Brown Jbrown@brunsco.net for future permissions) as well as on private property (the “Fox trap”, 34.216°, -78.000°, and “X-roads trap”, 33.930°, -78.611°, for future permissions contact Jeffrey Brown Jbrown@brunsco.net and Rick Hickman rickhickman@atmc.net). Field studies did not involve endangered or protected species.

Mosquito Traps
Brunswick County
North Carolina

- Weather stations
- Groundwater level station
- ▲ Mosquito traps
- Brunswick county
- NC boundary

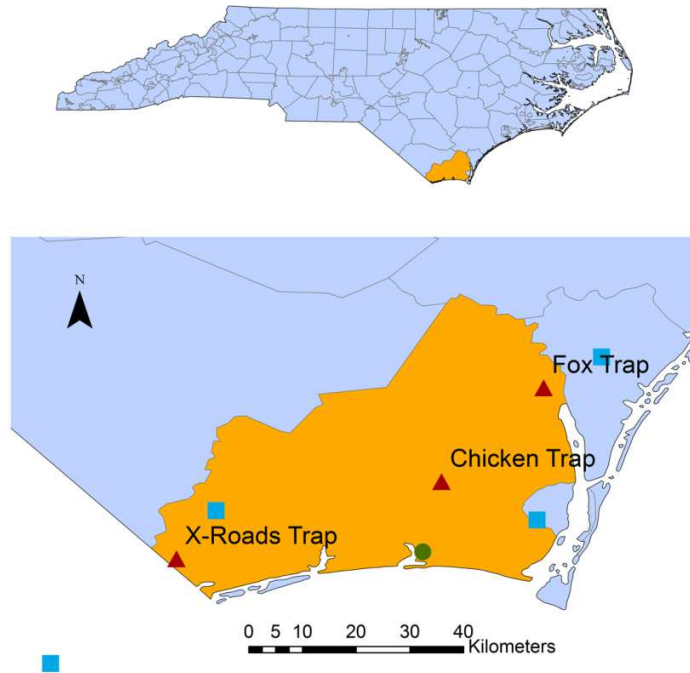


Figure 8: Study area, sampling sites and weather stations in the Brunswick County North Carolina, U.S.

I focus here on the “Chicken Trap” site (close to several woodland pools and to a sentinel chicken site providing blood bait) because of the comparatively large sample size and because expert opinions at the Brunswick County Mosquito Control Department suggest that the population dynamic recorded at the "Chicken trap" sentinel site is well-aligned with changes in mosquito population abundance over large areas of

the County. Daily weather data (temperature, precipitation, dew point, and wind speed) at the closest National Climate Data Center (NCDC) station were acquired (Station USW00013748, about 34 km from the “Chicken Trap” site, <http://gis.ncdc.noaa.gov>). Ground water level observations were also downloaded from the U.S. Geological Survey real-time groundwater level network (Station 335629078115407, 13 km from the “Chicken Trap” site <http://groundwaterwatch.usgs.gov/>). These data were used to study the role of exogenous environmental controls as drivers of mosquito population dynamics.

Cs.melanura is identified as the primary vector of EEE disease. This mosquito species feed primarily on birds and lay eggs in underground crypts. It is a multivoltine species with an exceptionally low development rate and a tolerance to cold weather. It can overwinter in multiple larval stages (Mahmood and Crans 1997, 1998a, b, Brunswick County Government 2011, Crans 2013c). *Ae.vexans* is a floodwater mosquito species ubiquitously found in the USA. It is important because of its abundance, widespread distribution, and role as the vector of multiple diseases. This species lays eggs in soils subject to transient flooding. The eggs hatch and complete their development when submerged under water. Unlike *Cs.melanura*, *Ae.vexans* overwinters as eggs (Horsfall 1973, Becker et al. 2003, Crans 2013a).

3.2.2 Data analysis

Various time series analysis approaches have been developed and applied in the context of population ecology (e.g. phase space models, autoregressive models, and Bayesian dynamic linear model (Sugihara et al. 1990, Kantz and Schreiber 2004, Hsieh et

al. 2005, Shumway and Stoffer 2006, Clark 2007, Box et al. 2008, Chaves et al. 2012, Sugihara et al. 2012, Tzeng et al. 2012, Deyle et al. 2013)). The objectives of this work require the identification and analysis of the characteristic scales of fluctuation of mosquito abundance. I tackled this problem by first applying Fourier analysis to detect and identify, in the observed adult mosquito abundance and environmental forcing time series, characteristic fluctuation time scales. I then experimented by artificially reducing the data resolution to the weekly scale to observe how fluctuations happening at high frequency and inferred statistical properties changed with observation frequency. Finally, I used an Individual Based Simulation model (IBS model), as well as density-dependent population models, to comparatively explore the relative importance of mosquito activity and of endogenous and exogenous controls in determining the observed scales of fluctuation and the overall population dynamics.

3.2.3 Fourier analysis

Discrete Fourier Transform (DFT) decomposes a time series into the sum of sinusoidal functions with varying periods $T_i = (N \cdot \Delta t) / i$ ($i=0, \dots, N/2$) (Press 2007) (where N is the sample size and Δt is the sampling interval). This representation is very useful to detect seemingly irregular hidden periodicities. DFT provides, as a result of the analysis, the amplitude of the fluctuations corresponding to each discrete period T_i , hence allowing identification of possible dominant periodicities (i.e. having relatively large amplitudes). Other analysis methods, such as wavelet analysis, provide further sophistication, e.g. in analyzing non-stationary time series (Shumway and Stoffer 2011). However, the focus here is the identification of characteristic periodicities in adult

mosquito populations (which may e.g. arise due to the presence of characteristic time scales in environmental forcings and/or in mosquito life cycles), and the DFT (employed in previous population ecology studies, e.g. see (Carpenter and Brock 2010, Polansky et al. 2010, Shumway and Stoffer 2011)), is the simplest, and possibly most robust, tool that suffices this objective. One important notion related to the DFT is the Nyquist theorem, which establishes that the shortest periodicity (i.e. the fastest dynamics) that can be captured when a process is sampled at a resolution Δt is equal to $2\Delta t$ (corresponding to the *Nyquist frequency*, $1/(2\Delta t)$). In the case of mosquito abundance observations, when adult mosquitoes are collected once per week, the shortest periodicity that can be resolved is 2 weeks: fluctuations occurring over shorter time scales will remain undetected in the data and will be seen as “noise”. The dataset used here has a resolution of 1 day, such that the shortest periodicity that can be resolved is equal to 2 days: this dataset allows us to explore, in the field and under natural conditions, the full range of periodicities that may be present in population dynamics of adult mosquitoes. As customary, I represent results from the DFT through the power spectrum, $S(T)$, which represents the square of the oscillation amplitude of the sinusoidal component of period T in the Fourier decomposition of the time series studied.

3.2.4 Autocorrelation, partial correlation, and data splitting

I split the daily observation time series at a 7-day frequency to evaluate how a degraded temporal resolution affects the temporal scales of fluctuation captured by the time series. I obtained 7 time series, each “collected” on a different day of the week. I computed the AutoCorrelation Function (ACF) and the Partial AutoCorrelation

Function (PACF) for the original dataset and for the once-per-week samples. The k -th element of the ACF provides a measure of the average correlation between the abundance values x_t , and x_{t-k} , k time steps apart. The PACF is obtained by removing from the correlation between x_t and x_{t-k} the indirect correlation associated with the intermediate terms $x_{t-1}, x_{t-2}, \dots, x_{t-k+1}$, such that only the direct correlation between x_t , and x_{t-k} is retained (Box et al. 2008).

3.2.5 Models

3.2.5.1 Individual-Based life cycle simulation model

With the aim of identifying the statistical properties in the observed abundance of adult mosquitoes associated with distinct population dynamical mechanisms, I constructed Individual-Based life cycle Simulation (IBS) models for *Ae.vexans* and *Cs.melanura* populations. The IBS models explicitly describe three mosquito life stages: egg, larva/pupa, and adult (Becker et al. 2003). Each stage is characterized by a distribution of the time spent in that stage, dependent on physiology, environmental conditions, and population density (see Figure 9 and Appendix B). Each stage is characterized by a survival rate, also a function of environmental conditions (Figure 9). I based my description of the distributions of the time spent in each stage and of the survival rate for each stage on existing literature, to minimize the number of parameters which require ad hoc assumptions (Figure 9). No calibration of the models was performed as the objective is here to obtain a realistic representation of adult mosquito abundance fluctuations, rather than the numerical reproduction of a specific sample.

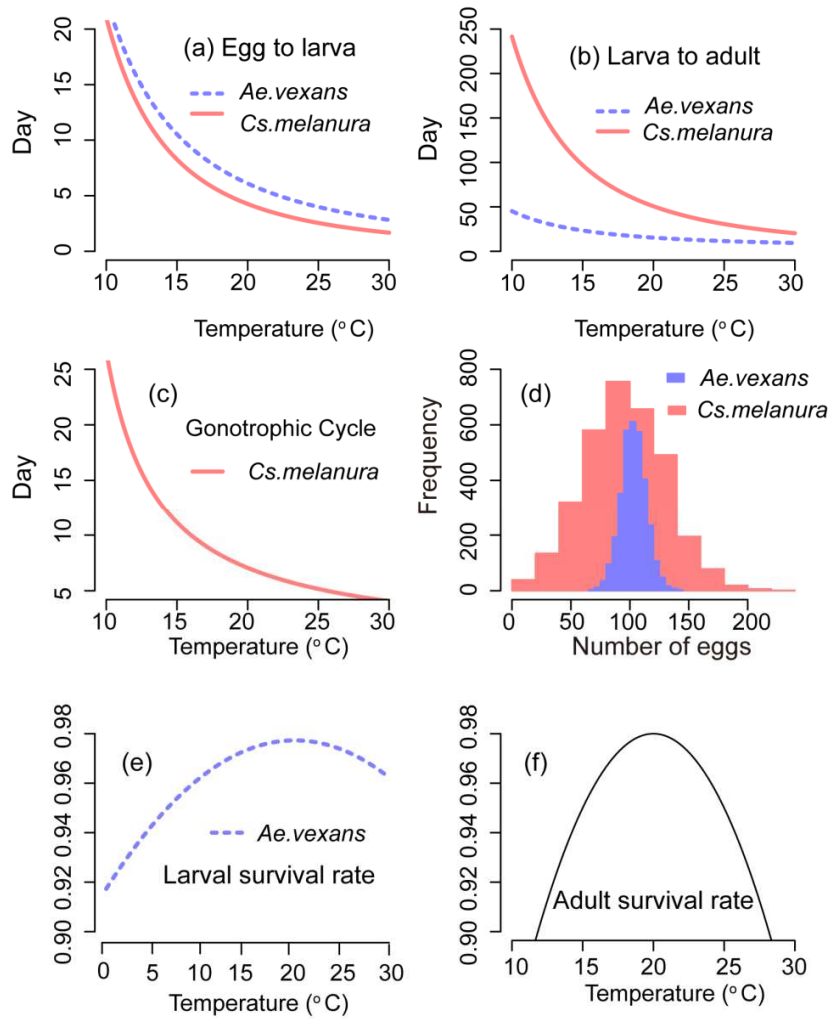


Figure 9: Main biological parameters as assumed in the IBS model. (a) Transition time from egg to larva as a function of temperature. (b) Transition time from larva to adult as a function of temperature. (c) Length of gonotrophic cycle for *Cs.melanura* as a function of temperature. (d) Marginal distribution of the number of eggs laid per batch. (e) Larval survival rate as a function of temperature for *Ae.vexans*. (f) Adult survival rate as a function of temperature for both *Cs.melanura* and *Ae.vexans*.

The time spent in each life stage by each individual is drawn from a normal distribution whose mean depends on the temperature averaged over a 10-day window (to represent temperature conditions throughout the developing period), and a fixed

standard deviation (1 day). The mean “residence” time (d) in each stage is assumed to decrease with the average temperature according to a power law (Figure 9): $d = A \cdot T^{-a}$ (Becker et al. 2003). The literature-derived exponents adopted are as follows: $a=1.90$ for *Ae.vexans* embryogenesis, $a=1.86$ for *Ae.vexans* larval / pupal stage, $a=.30$ for *Cs.melanura* embryogenesis, and $a=2.25$ for *Cs.melanura* larval / pupal stage (Trpis and Shemanch.Ja 1970, Horsfall 1973, Mahmood and Crans 1998a, Becker et al. 2003). The gonotrophic cycle in adult mosquitoes includes copulation, blood search, blood digestion, and egg development in the female body. The length of the gonotrophic cycle for *Cs.melanura* is assumed to be drawn from a Gaussian distribution with a mean which decreases with increasing temperature and a unit standard deviation (Mahmood and Crans 1997). The length of the gonotrophic cycle for *Ae.vexans* is assumed to be a truncated normal distribution with a mean of 10 days, standard deviation of 1 day, upper bound of 13 days and lower bound of 7 days (Horsfall 1973, Becker et al. 2003) (see Figure 9 and appendix B). The survival rates for the larval/pupal and adult stages of *Ae.vexans*, and the adult stage of *Cs.melanura* are quadratic functions of the 10-day moving average temperature (Figure 9) (Trpis and Shemanch.Ja 1970, Horsfall 1973, Mahmood and Crans 1997). The larval/pupal survival rate of *Cs.melanura* is assumed to be 1 when the current larval abundance is zero and 10-day moving average of precipitation is larger than 1 mm/d as there is no information for this species. I further assume that the survival rates of larvae and adults for both species decreases when the 10-day moving average of precipitation is below 1mm/day to mimic a documented sensitivity of survival rates on moisture and water availability (Clements 1992, Bomblies et al. 2008).

Finally, survival rates for egg and larval stages for both species are assumed to decrease linearly with abundance to reflect documented density dependence effects (Jian et al. 2014a) (see Appendix B).

Under natural conditions only a fraction of female mosquitoes is successful in obtaining a blood meal and are able to oviposit. The probability of success is represented by a Bernoulli distribution with a mean that linearly increases with the 10-day moving average of relative humidity for *Ae.vexans*, and a mean which is an increasing quadratic function of the 10-day moving average of temperature for *Cs.melanura* (Appendix B) (Mahmood and Crans 1997, Becker et al. 2003). After oviposition, engorged females can start another gonotrophic cycle until they die. This model representation realistically reproduces (under current weather conditions) the fact that the large majority of females only have the opportunity of one blood meal and oviposit only once during their lifetime (Horsfall 1973). Only a small proportion of females succeeds in obtaining a second blood meal and oviposit a 2nd batch of eggs. The number of eggs laid by each adult per batch is assumed to have a normal distribution, with a mean that increases with precipitation amount, as water is more likely available for oviposition (Figure 9).

Details on the development rate and the values of the controlling factors for each development stage can be found in Appendix B. Such values were obtained from the wide relevant literature, as noted above, and I purposely avoided ad hoc calibrations because the objective is to identify the signature of each individual developmental process on the resulting population variability, rather than to maximize the ability of the model to reproduce a specific observed time series. The models (i.e. defined by one set

of parameter values for each species) were run under three configurations: (1) observed environmental forcings (temperature and rainfall in 2004-2012) (2) observed temperature forcing only (effect of rainfall on survival rate, oviposition and egg hatching “ turned off ”) (3) endogenous dynamics only (fixed temperature - $T=18^{\circ}\text{C}$ - and rainfall effect turned off). The three model configurations allow us to separate and identify the population fluctuations and periodicities caused by endogenous and environmental controls.

The IBS models produce, at each time step, the abundance of the “actual” adult mosquito population (the abundances of the other life stages, also computed at each time step, are not analyzed here due to a lack of the corresponding observations). I further assumed that the observed population, i.e. the number of adults that would be attracted and captured by a trap, is a varying fraction of the underlying actual adult population. The dependence of this “activity fraction” on rainfall was estimated based on observations as follows. I first calculated the ratio of the current abundance to the maximum abundance in a moving window of 31 days. The rationale for this estimate is that the maximum abundance over a relatively homogeneous period should be a good proxy for the fraction of the underlying population that can be captured under the most favorable environmental conditions. The median of the activity ratio computed over discrete intervals of rainfall intensity was then plotted against current day rainfall. This analysis (see Appendix B) indicates that the activity ratio increases with rainfall at low intensities and decreases steeply for rainfall intensities above a threshold. This nonlinear

dependence of the activity ratio on rainfall was used to represent rainfall-activity effects in the IBS model.

I note here that, while the activity component in the IBS model formulation indeed includes several assumptions, I have extensively explored a wide variety of such assumptions. These included the use of a uniform distribution in the interval $[0, f_{\max}]$, where f_{\max} is dependent on daily rainfall, and the use of a normal distribution with parameters dependent on weather forcing. The method based on the moving average of 31 days was finally chosen because it allowed the assumptions to be based on the available observations. Overall, I found the impact of these different assumptions on the emerging dynamical time scales, and particularly on the fastest and slowest time scales of population fluctuations, to be limited. Because of the stochastic nature of the IBS models, I ran the models 20 times for each species, to obtain ensemble means as a basis for further discussion. I used a sample size of 20 because each run of the IBS model generated daily abundances of eggs, larvae and adults for ten years, and because a large number of eggs is needed to reproduce an adult abundance which has similar size with the observed abundance. This choice of size allows effectively approximations of the observed population dynamics.

3.2.5.2 Density dependent population models

Two classic and commonly used population models were applied to the daily abundance observations of *Ae.vexans* and *Cs.melanura*: the Ricker model and the Gompertz-logistic model (Clark 2007, Yang et al. 2008a) (Table 3). These models are defined through specific relations between per-capita growth rate and abundance: the

relation is linear in the Ricker model and log-linear in the Gompertz formulation.

Through the application of these models I tested for the existence of density dependence with lag between 0 ($\log(N_t)$) and 5 days ($\log(N_{t-5})$), to explore the possible effects of delayed density control. The logarithmic abundance at lag 0 (i.e. at current time, $\log(N_t)$) is included as the value of the current per capita growth rate, $r_t = \log(N_{t+1}) - \log(N_t)$ is defined as the change from current to future abundance and it can depend on the current population size. I also compared the statistical properties of the population dynamics generated by these models with those from observations, to identify which features can indeed be reproduced using canonical population modeling. Environmental forcings were included in the models as multiplicative terms, to account for the dependence of the carrying capacity and the maximum per-capita growth rate on environmental conditions (Yang et al. 2008b, Jian et al. 2014a). These models were calibrated (in R 2.15.1) as linear models using the least squares method (see Appendix B for estimated parameter values). Although it is known that least square methods do not always lead to the most accurate estimates of parameter values (Ives and Zhu 2006), they are known to be robust with respect to the available sample size and have been widely applied to density-dependent models (Sibly et al. 2005). Furthermore, the focus of the analyses is not the identification of “true” parameter values, but the evaluation of the ability of density-dependent population model formulations to capture observed correlation structures. I will thus focus on comparing modeled and observed correlation structures rather than on quantifying bias in parameter estimates. The calibrated density-dependent models were used to generate synthetic time series, and their ACF

and PACF were compared with those of the original observations and of the time series produced using the IBS model.

Table 3: Density-dependent models (showing lag 0 as examples), where t is index of sample date; N is adult mosquito abundance; r_m is the maximum per capital growth rate; K is the carrying capacity

Model name	Recursive form
Ricker model	$N_{t+l} = N_t \times \exp(r_m (1 - N_t / K))$
Gompertz-logistic model	$N_{t+l} = N_t \times \exp(r_m (1 - \log N_t / \log K))$

3.3 Results

I analyze the observed statistical properties of the four most abundant species in the studied area: *Aedes vexans*, *Culex salinarius*, *Culiseta melanura*, and *Psorophora columbiae* (Figure 10). *Cs.melanura* and *Ae.vexans* are connected with EEE and WNV diseases, hence the additional interest and further analyses reported later. Figure 10 shows large and very rapid fluctuations in the daily abundance of adult mosquitoes: for example, more than 800 individuals of *Ae.vexans* were collected on Oct-27-2010, while only about 50 individuals were collected 2 days before and after. This dramatic change in the abundance is much more rapid than would be allowed by physiologically possible generation times (about 3 weeks under favorable conditions (Becker et al. 2003)). Indeed, large differences (several order of magnitudes in 1-2 days during the growing season) are present throughout the 9-year dataset (Figure 10), which are likely attributable to the changing proportion of active individuals rather than to changes in the actual population.

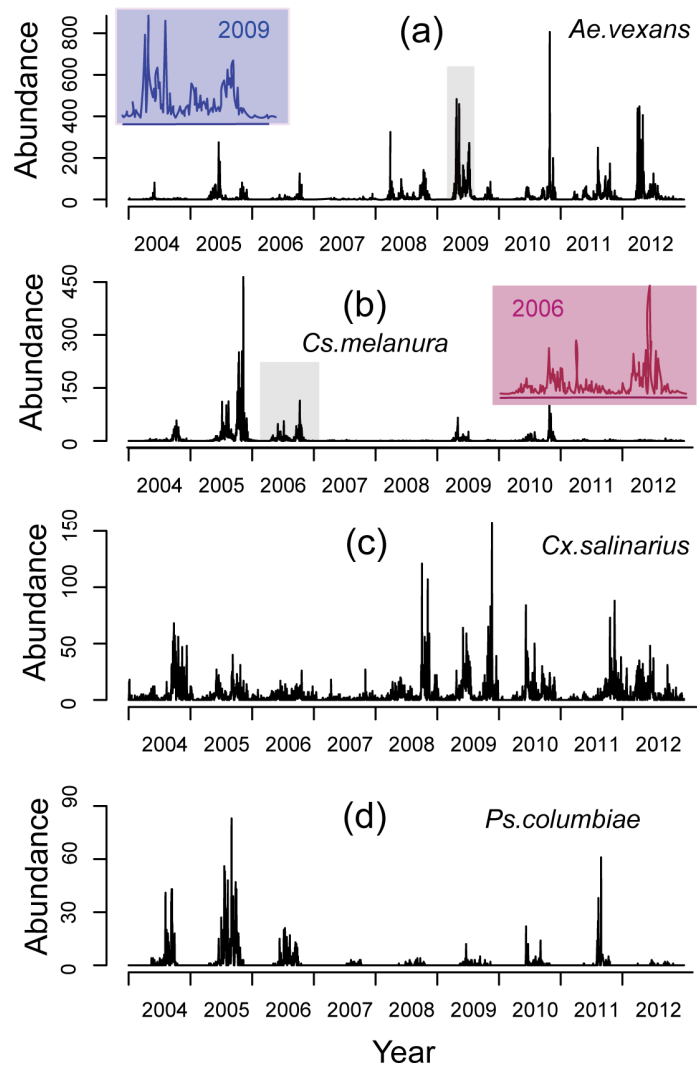


Figure 10: Observed abundance for the 4 dominant species at the Chicken Trap site in the period 2004 – 2012. The subpanels show details of the abundance fluctuations for two specific periods identified by the grey windows in (a) and (b).

The results of DFT analysis differ for the four species (Figure 11). A Peak at yearly time scales in the power spectrum is found for *Ae.vexans*, *Cx. salinarius* and *Ps. columbiae*, but it is less obvious for *Cs.melanura*. The lack of detected cycles at yearly scales for *Cs.melanura* may probably be attributed to the large differences in its inter-

annual abundance (e.g. see the particularly low abundance during the 2007 drought), as well as to more widely varying overwintering times (Figure 11). At the scale of 1 to several months, major peaks can be seen for *two* of the studied species (70 days and 30 days for *Ae.vexans*, and 110 days and 30 days for *Cs.melanura*). This intermediate range of time scales includes realistic durations of the life stages in mosquito life cycle (Clements 1992, Becker et al. 2003). At shorter time scales (less than 1 month), peaks in the Fourier spectra are found for *Cs.melanura* and *Ps.columbiae*. In particular, peaks at wavelenghts shorter than 2 weeks are identified for *Cs.melanura*. Spectral power at daily scales does not exhibit significant preferred scales of fluctuations. The power spectra of temperature, rainfall and relative humidity exhibit a major annual cycle (Appendix B). The spectrum of rainfall also shows peaks at time scales of several days, while the power spectrum of groundwater is very smooth with no obvious cycles during the study period. Interestingly, the peaks in the power spectra of mosquito abundance at monthly scales are not matched by major peaks in the power spectra of weather forcings. This suggests that fluctuations over these time scales are caused by internal dynamical mechanisms.

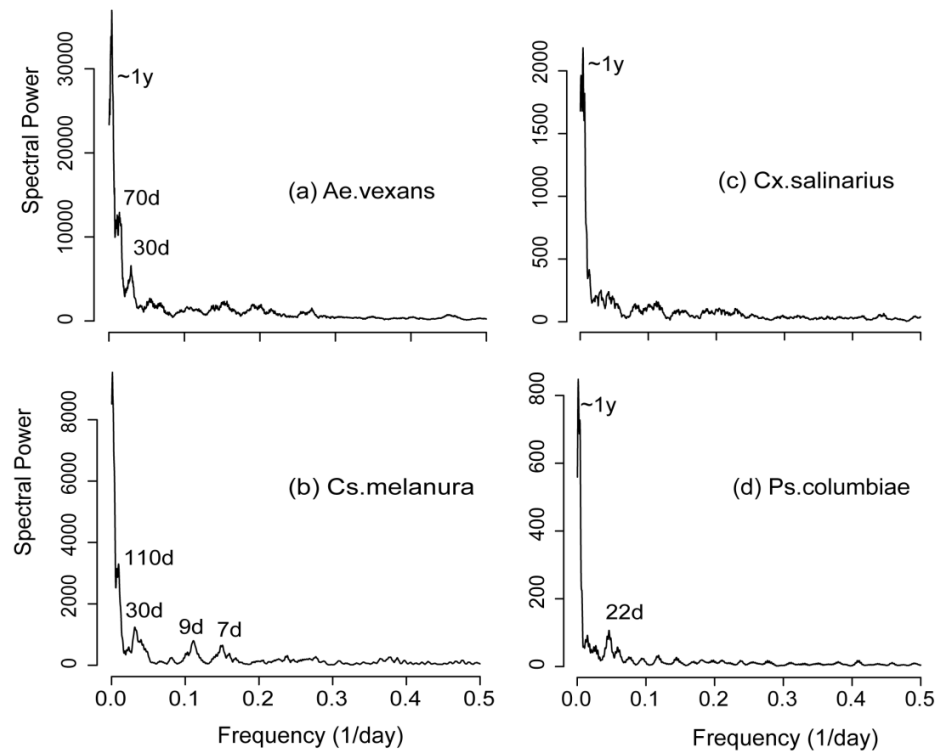


Figure 11: Power spectra for the 4 dominant species. The text marks the approximate locations of major peaks.

Analysis of the ACF's highlights significant differences between the daily data and the once-per-week subsamples, and among the once-per-week subsamples (Figure 12). I focus here, and in most of the following, on the two most relevant species, *Ae.vexans* and *Cs.melanura*. The ACFs of the daily *Ae.vexans* observations are significantly positive for time lags up to about 11 weeks, while, for example, the “Wednesday” samples for the same species only show a significant positive autocorrelation for lags up to 3 weeks. Furthermore, the ACFs of different once-per-week subsamples exhibit very wide differences. For example, the positive autocorrelations of the “Sunday” sample are both larger and more persistent than those in the “Wednesday” sample. A quite similar

situation is seen in the case of *Cs.melanura*, some once-per-week samples suggesting a much shorter memory than others (Figure 12 c and d) and, in particular, a shorter memory than indicated by the more statistically representative daily observations. Furthermore, the peaks in the ACF of daily sampled *Cs.melanura* at about 1 and 3-4 weeks (Figure 12, c) correspond to the peaks identified in the Fourier spectrum, as theory requires. Such peaks are lost in the once-per-week ACF. It is clear from these results that the apparent statistical properties of the adult mosquito population are extremely different depending on the specific weekly time series which happens to be sampled.

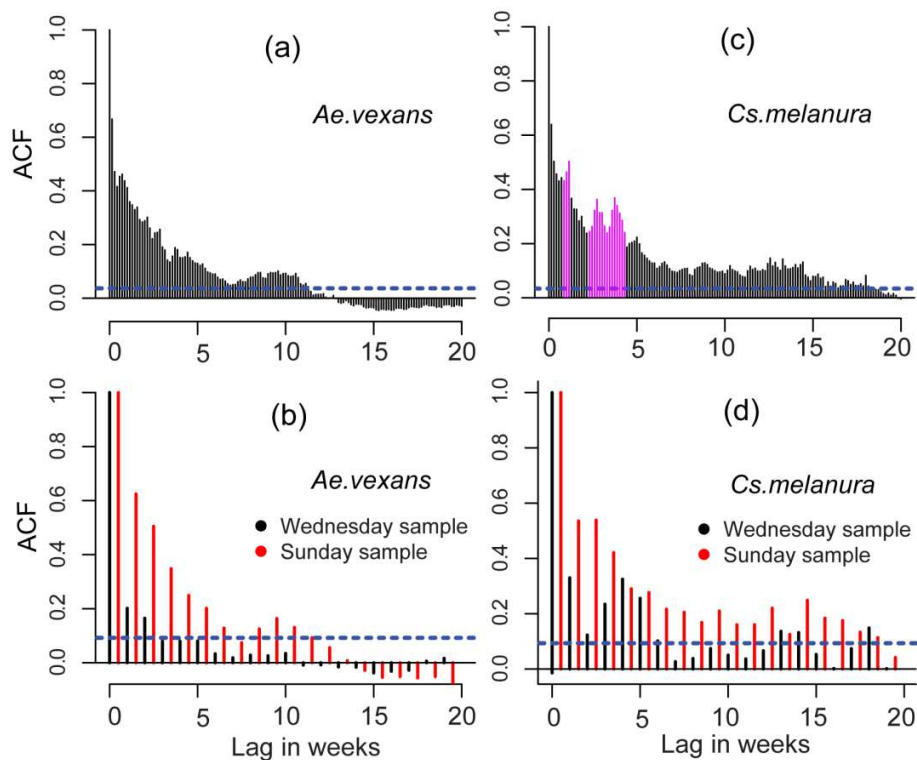


Figure 12: ACF for daily observations ((a) and (c)) and for subsampled weekly data ((b) and (d)). The dashed blue lines represent the 95% confidence intervals for the ACF. Significant peaks around 1 and 3-4 weeks, marked magenta in (c), are partly lost in the subsampled weekly data.

I now turn to the analysis of the synthetic time series generated using the IBS models. I again underline that the IBS models were run in an “unconstrained mode”: I used literature values of the parameters and I did not update the model state (number of eggs, adults, etc.) using observations during the simulations. The time series generated by the IBS models with observed environmental forcings with and without the activity term exhibit realistic annual peaks and reproduce the influence of dry and cold weather conditions (Figure 13). However, the fast time scales of fluctuation in the observed abundance are realistically represented only by the IBS model which includes an activity term modelling the variable vagility of adult mosquitoes (Figure 13).

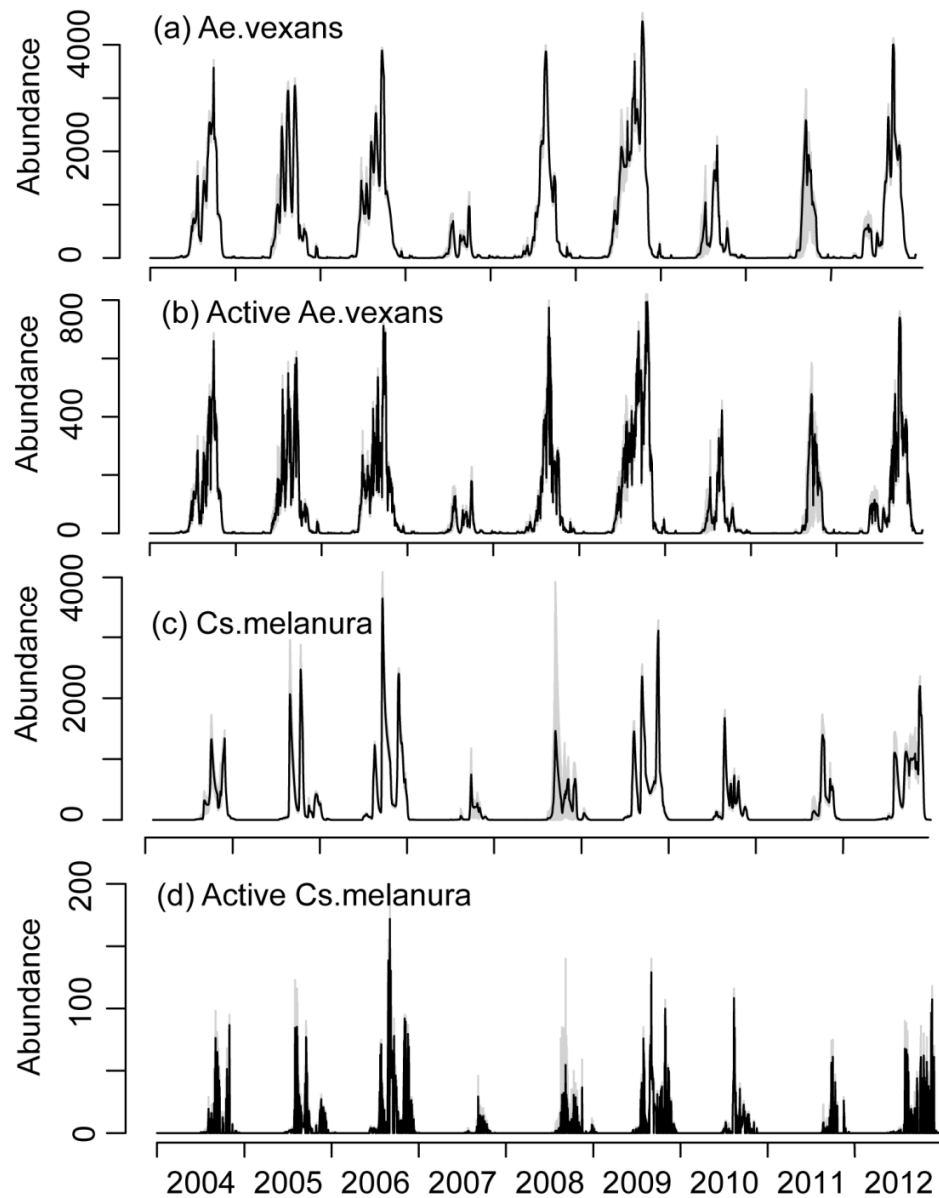


Figure 13: The mean abundance from 20 runs of IBS model driven by observed weather forcings for *Ae.vexans* and *Cs.melanura*: simulations without ((a) and (c)) and with ((b) and (d)) activity component. The grey lines represent the range (minimum and maximum) of 20 simulated values.

I also compared the PACFs of the observations, of the IBS simulations, and of the output of canonical population models. The PACFs for the daily observations are positive for both species up to about one week, while the PACFs generated by the

Ricker and Gompertz models with density dependence dictated by the current abundance (lag 0) are negative at the same temporal scale (Figure 14 d, e, i, and j). Models which embed density dependence at the 1 day or 5-day lag exhibit similar results (Appendix B). Moreover, adding multiple lags (lags 0-5) to the density dependence representation does not produce a better match of the observed correlations, as it increases the short term correlations but model outputs are less correlated in time than measured abundance (Appendix B).

The PACFs for the IBS model without the activity component also show negative correlations at short temporal scale (Figure 14, c and h). However, when the activity component is included in the formulation, the resulting dynamics show significant, and realistic, positive correlations at time scales up to about one week (Figure 14, b and g). This suggests that the apparent correlation properties in the observed population at short time scales (< 1 week) are highly influenced by adult mosquito activity and do not reflect fluctuations in the actual population.

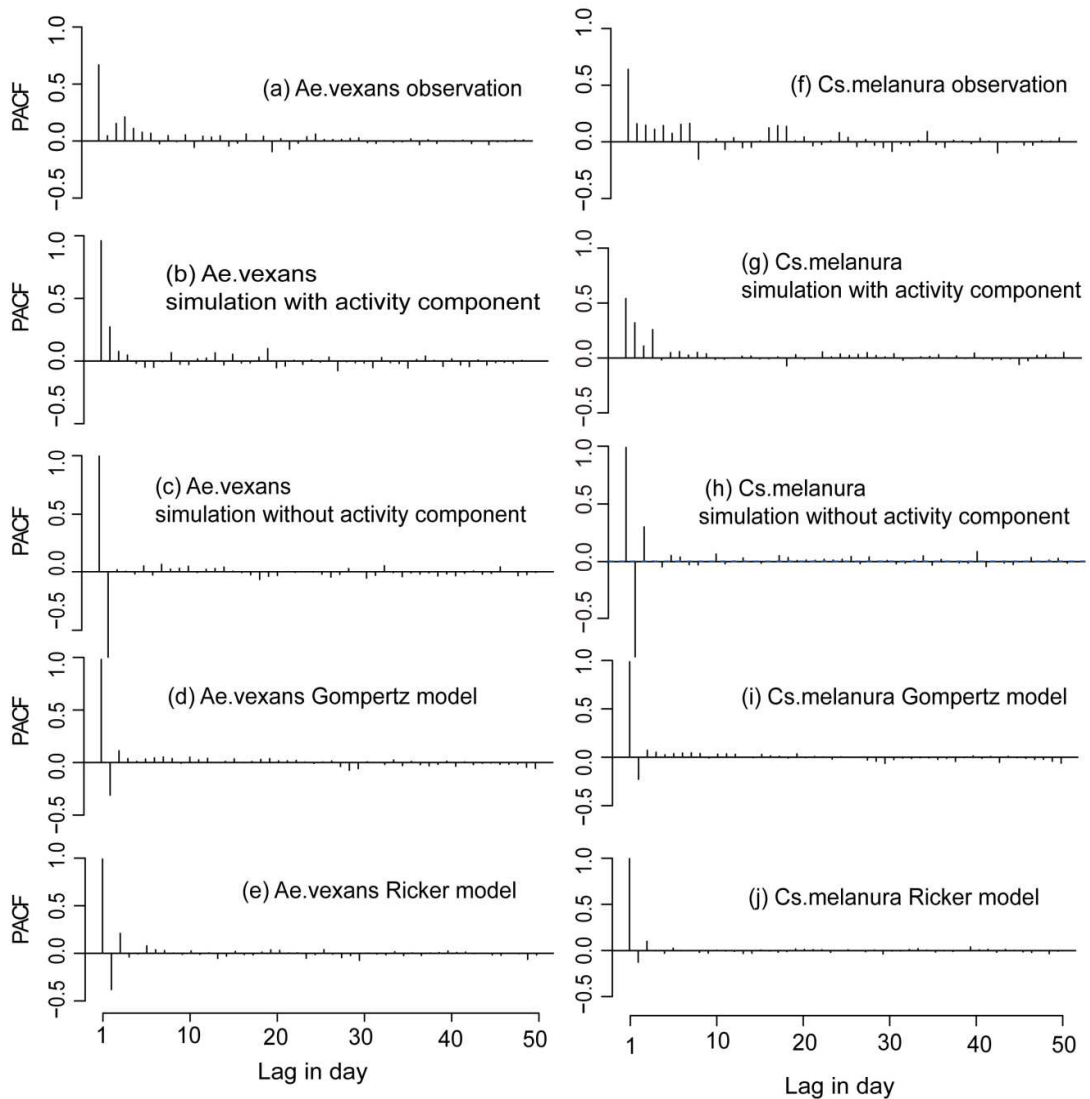


Figure 14: PACF of observed abundances for *Ae.vexans* and *Cs.melanura*, ((a) and (f)), for IBS model realizations including activity ((b) and (g)), IBS model realizations without activity ((c) and (h)); Gompertz model realizations with density dependence at lag=0 days ((d) and (i)), and Ricker model realizations with density dependence at lag=0 days (Heptonstall (England : Parish) and Horsfall) and (j))

I finally compare the power spectra of the simulated abundance generated with the three model configurations that include the activity component with those obtained by “turning-off” mosquito activity (Figure 15). For simplicity I use *Cs.melanura* as the

illustrative example. Under constant environmental forcings, a major peak is found at time scales of about 180 days (Figure 15 a and d), which is a result of endogenous controls as exogenous factors do not fluctuate under this environmental setting ($T=18\text{ }^{\circ}\text{C}$, and no rainfall effect), with the population oscillating around the carrying capacity. When the observed temperature is included in the model, an annual peak appears due to the yearly cycle in this forcing (Figure 15 b and e). Under the same setting, the spectra also exhibit another peak at a monthly scale (about 35 days), which is the joint result of interacting endogenous and exogenous controls. The added rainfall effects reduce the size of the peaks at the yearly scale and introduce a peak at about 70 days (Figure 15 c and f). The annual cycle in the population abundance becomes less obvious because the interannual rainfall variability induces large uncorrelated variations in bloom times and abundance across different years. Finally, when activity is added to the model, the height of the peaks at longer time scales (>1 month) are reduced considerably while their position and shape are preserved. The amplitude of short time scale fluctuations increases (at the high-frequency end) relative to longer time scale periodicities, yielding a relatively low difference in amplitude across scales. While this is a qualitative observation, we note that model formulations including adult mosquito activity lead to power spectra in which energy decreases less steeply with increasing frequency, similarly to what happens for observations.

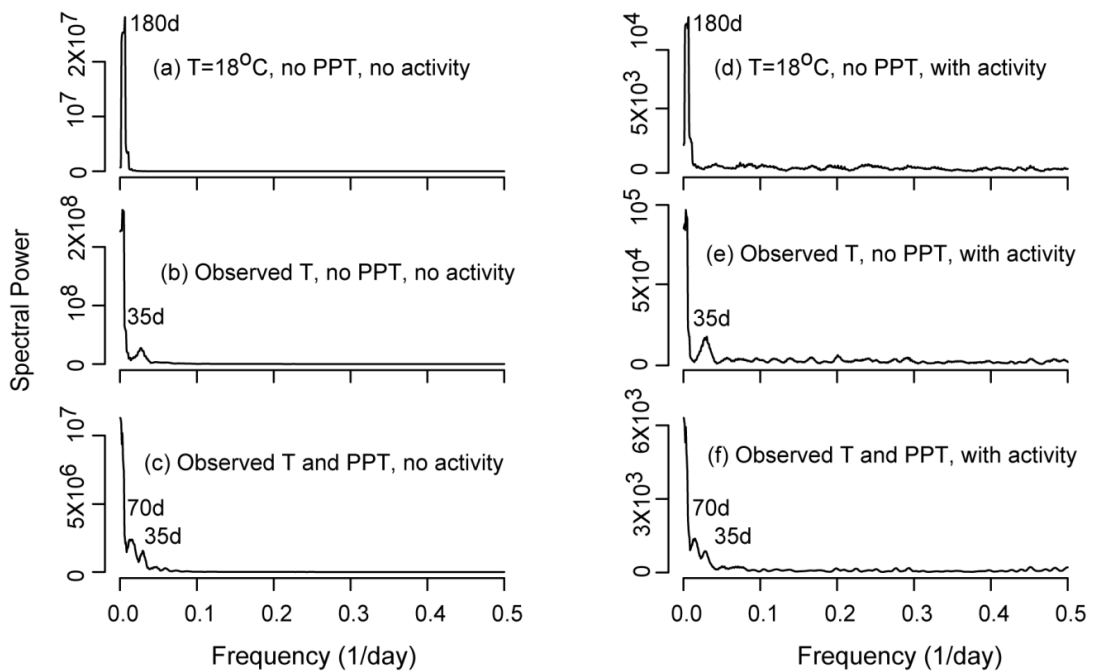


Figure 15: Power spectrum of IBS model outputs with ((a), (b), and (c)) and without ((d), (e), and (f)) activity component. Panel (a) and (d): IBS model with constant temperature (18°C) and no rainfall effect; panel (b) and (e); IBS model with observed temperature, and no rainfall effect; panel (c) and (f) IBS model with observed temperature, and with rainfall effect on death rate, oviposition, and egg hatching driven by observed rainfall.

3.4 Discussion and conclusions

A coherent picture of adult mosquito dynamics, for the species examined here, emerges from the analysis of daily data and the use of a variety of modeling tools.

First, the analysis of the autocorrelation properties suggest that the relatively large “memory” in the observations (represented by positive values in the PACF for several time lags, Figure 14) can hardly be reproduced by density dependence mechanisms, even when multiple lags are involved. On the contrary, the inclusion of weather-driven activity does produce a modelled PACF which more realistically

reproduces observed partial autocorrelations (see the supplementary material for a detailed comparison). The influence of mosquito activity on the ACF and PACF has implications for empirical analyses of mosquito populations. Observational ACFs and PACFs, in fact, importantly depend on the sampled abundance (as influenced by activity) and their interpretation as representative of the “memory” in the actual underlying population abundance can lead to erroneous conclusions regarding population dynamical mechanisms, e.g. in terms of reproductive time scales or of the time lags at which density dependence operates. The availability of daily observations allowed us to show that autocorrelation structures estimated on once-per-week data may vary widely and may be quite different from the “actual” autocorrelation structure estimated using daily data (Figure 12). Hence, even when relatively long time scales are of interest, a high sampling frequency is highly beneficial to obtain realistic estimates of abundance autocorrelation properties and of density dependent population regulation mechanisms.

Spectral analysis reveals a coherent structure of the temporal organization of adult mosquito population dynamics (Figure 16). I find that mosquito activity, forced by short time scale weather, is most likely responsible for the observed population variability at fine time scales (< 1 month). This is a sort of “microscale” at which variability is “injected” into the system. At monthly time scales coherent temporal structures and characteristic time scales emerge. These periodicities are here explained by the interplay of exogenous forcing and endogenous mechanisms. My results suggest that the organized character of mosquito dynamics at the intermediate scales ranging from one to several months is jointly determined by the characteristic time scales of

endogenous regulations (of survival, death rate, development, and reproduction) and by population responses to temperature and rainfall fluctuations. At even longer time scales, mosquito population fluctuations mirror seasonal, annual, and inter-annual environmental patterns.

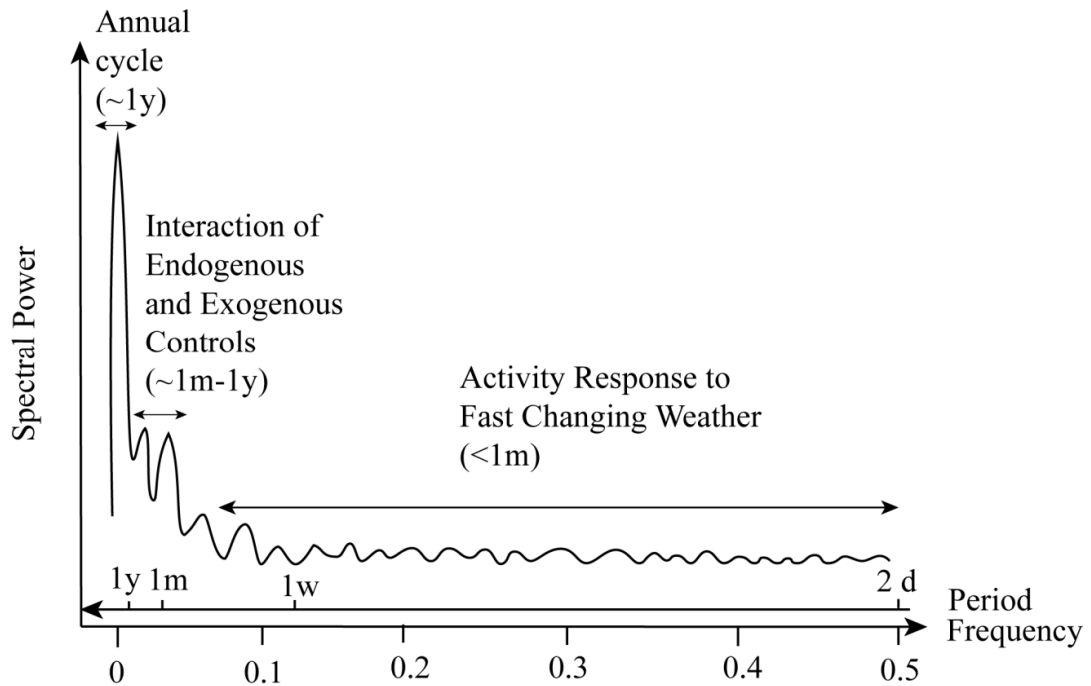


Figure 16: A conceptual spectrum highlighting the ecological/environmental processes driving mosquito dynamics at different time scales.

This interpretative framework provides guidance in choosing the observational temporal scale required to resolve the relevant population dynamics and possibly improve the prediction of adult mosquito population abundance. Clearly, if the mosquito species of interest exhibits characteristic scales of variability shorter than 2 weeks (such as in the case of *Cs.melanura*), my results imply that weekly observations, typical in adult mosquito studies in the field, are unsuitable to describe the full extent of

the mosquito population variability, as they can only capture periodicities longer than two weeks.

Generation times in mosquito populations typically range between weeks and months (Clements 1992, Becker et al. 2003) and are thus not consistent with the rapid fluctuations we have observed in mosquito abundance on daily time scales. This discrepancy emphasizes the importance of understanding the relation between captured adult individuals and the actual underlying population. Non-detection by a trap does not imply the absence of the targeted animal (MacKenzie et al. 2002, MacKenzie 2006), and the number of captured individuals does not necessarily reflect true abundance fluctuations (MacKenzie et al. 2002, Clark and Bjornstad 2004, MacKenzie et al. 2005, Dennis et al. 2006, Clark 2007, Royle and Dorazio 2008, Nadeem and Lele 2012). Hence, adult mosquito activity is a fundamental property of mosquito populations and fundamentally affects the observation process. Observations with weekly (or lower) resolution tend to overestimate population variability/responses because large observational fluctuations due to adult mosquito activity are erroneously attributed to changes in the actual population. Furthermore, I find that the inclusion of a weather-forced activity component allows the reproduction of realistic density dependence, autocorrelation functions, and power spectra.

My results indicate that the dynamics of mosquito populations may not be understood separately from the mechanisms driving the activity of individuals. Current models for adult mosquitoes often appear unable to generate seemingly fast abundance fluctuations, and have difficulties in predicting observed per-capita growth rates at

relatively short temporal scales (Russell et al. 2011, Chaves et al. 2012). I suggest that this apparent lack of predictive ability may be due to a changing proportion of the active mosquito individuals, which should be included as a fundamental ingredient of mosquito population models, conceptual or mechanistic, particularly at the short temporal scales.

4. Predicting Mosquito Abundance across Temporal Scales

4.1 Introduction

Mosquito population dynamics is an important and active field of research, with implications in ecology, entomology, social science, human health and environmental management. An interdisciplinary approach is increasingly required, and adopted, in order to make significant advances in our ability to predict mosquito population abundance. With the emergence and reemergence of mosquito-borne diseases worldwide, predictive models for mosquito abundance have been developed at various temporal scales based on different sampling strategies (Pascual et al. 2006, LaDeau et al. 2007, Bomblies et al. 2008, Randolph and Rogers 2010, Chuang et al. 2012, Jian et al. 2014a). In the previous chapter I investigated daily mosquito abundance and found that fast fluctuations over short time scales can be attributed to mosquito behavioral responses to environmental conditions which do not involve a change in the population abundance. In fact, despite the fast fluctuations in mosquito population dynamics, the abundance models at the daily scale are rarely seen. Predictive models based on weekly samples are most common for long term studies of mosquito abundance, such as the work of Bomblies et al (2008) and Shaman et al (2011). Monthly data are also widely used to investigate fluctuations in mosquito populations and the related diseases (Shaman et al. 2004, Day and Shaman 2009, Montosi et al. 2012). Less frequently, daily abundance observations are used or are aggregated to weekly and monthly time scales,

to take advantage of the increased reliability obtained by averaging high-resolution data (Shaman et al. 2002, Chuang et al. 2012).

In fact, fluctuations in mosquito abundance over different time scales are driven by different mechanisms. Hence, models developed and calibrated at different time scales are indeed desirable to fully account for endogenous and exogenous controls on fluctuations of mosquito abundance. However, predicting mosquito population dynamics remains a very challenging task. Detailed comparisons between predicted and observed abundance (e.g. (Jian et al. 2014a)) are seldom seen and this seems to imply modest predictive skill of our current models. Moreover, mosquito population abundance is highly serially correlated such that models which are progressively updated with the latest observed abundance can be mistakenly assumed to display some predictive skill. A more reasonable test of model predictive skills must, instead, be based on comparing observed and predicted rates of change of population abundance. Works that compare population rates of change (or, more accurately, per capita growth rate) are extremely rare (examples include (Russell et al. 2011, Jian et al. 2014a)), and clarify how current models are unable to provide reliable predictions of mosquito dynamics.

An important question in the present context is whether model predictive performance can be improved by using observations sampled at short time intervals (e.g. daily), as compared with common once-per-week sampling. In addition, we lack a systematic understanding of mosquito population predictability as a function of aggregation time scale and prediction horizon (how far into the future the prediction is performed). These are important and unaddressed questions, and their analysis can

provide a basis to choose appropriate time scales for observation and prediction, as well as highlight existing gaps in our understanding of population dynamical processes at various scales. In this part of this dissertation I approach these questions by analyzing a long term daily mosquito abundance data using a State Space reconstruction approach (Sugihara and May 1990). The predictability of mosquito abundance is compared at scale ranging from daily to monthly to answer the following three questions: (1) How is the predictability influenced by averaging mosquito abundance sampled at the daily scale over moving windows of varying lengths? (2) Can predictions of mosquito abundance be improved using daily samples compared to once-per week samples? (3) How does our ability to predict changes in mosquito population vary with prediction horizon?

4.2 Methods

4.2.1 Study area and data

A ten year (2004-2013) daily female mosquito abundance dataset collected by the Mosquito Control Department of Brunswick County in North Carolina was analyzed in this chapter. Details about the mosquito and weather dataset, as well as descriptions for the studied species can be found in section 3.2.1 in this dissertation.

4.2.2 State space reconstruction (SSR) and Simplex Projection (SP)

To explore the predictability of adult mosquito populations at different time scales, I consider observed abundances aggregated over non-overlapping periods of 7 days, 15 days, and 31 days to represent weekly, biweekly and monthly aggregation time scales. Furthermore, to investigate the potential benefit gained through daily sample

with respect to the commonly adopted once-per-week sample, I created 7 once-per-week abundance samples from the daily observation, and compare the prediction resulted from the once-per-week sample and the daily observation. I then used a State Space Reconstruction (SSR) method, applied at each aggregation scale as well as for the daily and once-per-week observations, with particular focus on the *Cs.melanura* and *Ae.vexans* time series.

A State Space (SS) representation considers the mosquito population and the conditions defining its environment as a dynamical system, in which its state is uniquely defined by the values of the state variables, here assumed to be: population abundance, temperature, daylight and rainfall. A possible state of the system is represented by one point in SS, and the time evolution of the system is represented by a trajectory in SS. An observational record thus describes one (complex) trajectory in SS and this observed trajectory can be used to estimate the future state once the current state is known (Sugihara et al. 1990, Kantz and Schreiber 2004). Usually we cannot be sure to know the “true” full dimension (all the governing factors) of a SS. However, its reconstruction can be obtained from one or multiple time series (in my case the mosquito abundance and/or weather forcings) by considering the known exogenous forcings and by including “delayed” values of the state variable (i.e. relative to the present, as well as to observational times $t-1$, $t-2$, etc.), to represent time derivatives of different orders. This reconstruction is usually considered to be equivalent to the unobserved full dimensional SS and is used for prediction as long as the order of the delays considered is large enough (Kantz and Schreiber 2004, Deyle and Sugihara 2011).

It is useful to note that the SSR approach used here is radically different from time series modelling methods, such as Auto-Regressive models (AR) or Moving Average models (MA). In these linear methods the prediction of future states is based on the linear combination of a number of states occurred over a fixed period in the near past, and the contribution of these states to the prediction remains constant over time. On the contrary, the SSR approach uses the past states that are closest to the present state *in the state space*. Such past states can have occurred at any time in the recorded history of the system and their weight in estimating future states depends on their proximity to the present state. SSR methods are thus inherently non-linear estimators.

Different SSR methods (i.e. approaches to reconstruct trajectories) exist. Here I use the Simplex Projection (SP) method (Sugihara and May 1990). This method is efficient for short term forecasting and can distinguish the effects of errors and of possible chaotic dynamics (Sugihara et al. 1990, Kantz and Schreiber 2004, Hsieh et al. 2005, Deyle et al. 2013, Perretti et al. 2013a). SP is especially appealing in ecological studies because of the potentially nonlinear and delayed response of the studied species to environmental forcings (Hsieh et al. 2005, Pascual et al. 2006). Furthermore, its non-parametric and model-free characteristics provide additional capability for describing partially-observed and high-dimensional systems (Perretti et al. 2013a). This method has been successfully applied to understand and predict population dynamics of zooplankton and fishes (Hsieh et al. 2005, Liu et al. 2012, Deyle et al. 2013, Liu et al. 2014), and has wide applications in the study of stochastic systems in a wide variety of fields (Kantz and Schreiber 2004).

In the SP method, a simplex¹ formed by neighboring points is used to envelop the current observations in the state space, and then a weighted average of the trajectories of neighboring points are used to project the trajectory starting from the current state of the system into the future (Sugihara et al. 1990, Deyle et al. 2013). To obtain an E-dimensional SSR from a single time series $\{x_t\}$, first a delayed vector is formed for the observation at each time step, $s_t = \{x_t, x_{t-1}, \dots, x_{t-E+1}\}$. This gives the coordinates for the state at time step t in SSR. Given an observed current state x_t and its delayed vector s_t to predict x_{t+1} , E+1 nearest points defined by their delayed vectors s_i 's (where i is the index of time for the nearest points in the state space) are chosen by their Euclidian distance to s_t . The E+1 points form the smallest simplex in the E dimensional state space which contains the point representing the current state of the system (Sugihara and May 1990). To obtain the predicted value for x_{t+1} , the trajectories of the E+1 neighboring points are tracked after 1 time step (x_{i+1}), and a weighted average of these values is used as the prediction (Sugihara and May 1990). For example, in a 2 dimensional SSR, the delayed vector is formed by the observations at the current and previous step, $s_t = (x_t, x_{t-1})$ (Figure 17). Three nearest neighboring points, s_{i1} , s_{i2} , and s_{i3} form the smallest triangle to contain s_t . The weights of these neighbors in predicting the future step are a function of their distance to s_t . For example the distance between s_{i2} to s_t is calculated as $d_2 = ||s_{i2} - s_t|| = \{(x_t - x_{i2})^2 + (x_{t-1} - x_{i2-1})^2\}^{1/2}$. The weight for s_{i2} is represented by $w_2 = \exp(-d_2/d_1) / \{\exp(-d_1/d_1) + \exp(-d_2/d_1) + \exp(-d_3/d_1)\}$. The weights for s_{i1} (w_1) and s_{i3} (w_3) are calculated in the same way. Moving one step ahead $s_{i2+1} = (x_{i2+1}, x_{i2})$, and the

¹ A k-simplex is a k-dimensional polytope which is the convex hull of its k + 1 vertices (Munkres 1984)

predicted value for x_{t+1} equals $w_1x_{i1+1} + w_2x_{i2+1} + w_3x_{i3+1}$. If multiple time series are available for SSR, the delayed vectors include the observations from other time series in a similar way.

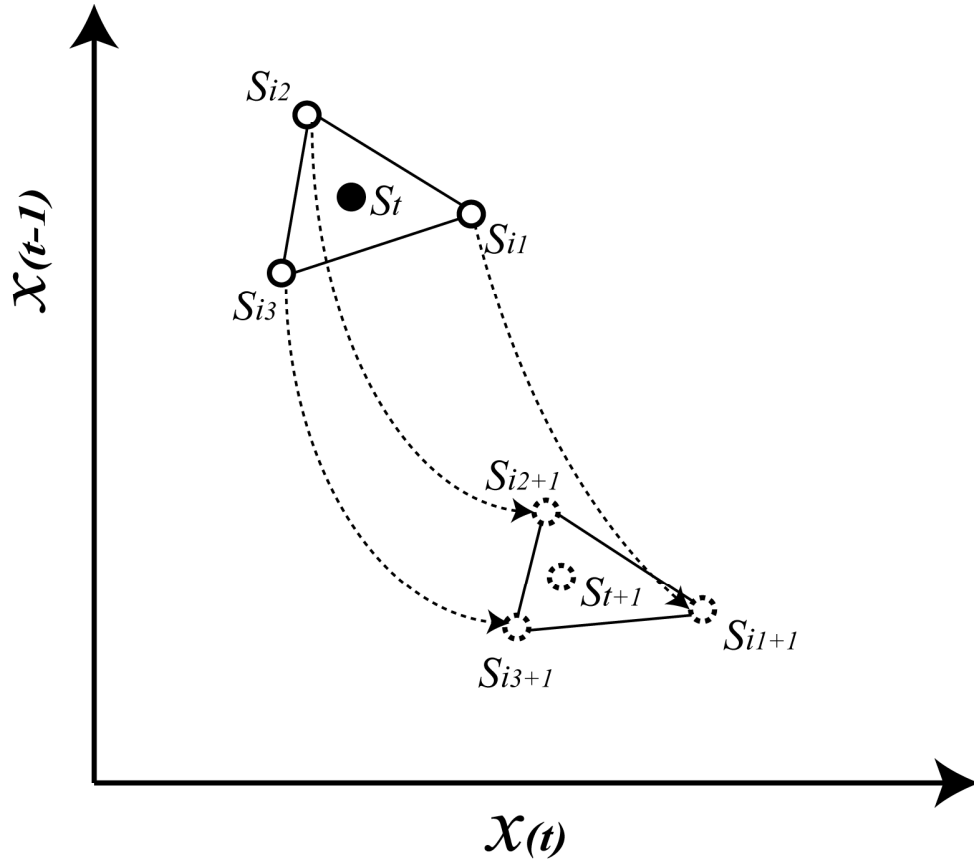


Figure 17: SSR from a single time series $\{x_t\}$ in the 2 dimensional case.

First, I applied this method to predict the weekly, biweekly and monthly mosquito growth rate ($r_t = \log(N_{t+1}) - \log(N_t)$). The SS was reconstructed using the delayed vector that includes the lagged abundance on the logarithmic scale ($\log N$), temperature (T), day length (D) and rainfall (P). Day length was calculated using the latitude of the trap and Julian date (Allen et al. 1998). The delayed vector was

represented as $\mathbf{s}_t = (\log(N_t), \log(N_{t-1}) \dots \log(N_{t-j}), T_t, D_t, P_t, P_{t-1} \dots P_{t-k})$, where $\log(N_t)$, T_t , D_t , P_t were mandatorily included in the models because of their known effects on mosquito population change (Horsfall 1973, Mahmood and Crans 1997, 1998a, b, Becker et al. 2003), and j (<10) and k (<4) were the maximum orders of delay for abundance and rainfall selected (see discussion below). I explored the effects of rainfall from lag=1 to lag=3 (1-3 weeks in the weekly model, 2-6 weeks in the biweekly model and 1-3 months in the monthly model), because of the relatively low autocorrelation in the rainfall time series and its potentially delayed influence on mosquito abundance.

I selected the lags for each of the variables (j and k , and the dimension of SSR $E=4+j+k$) by minimizing the root mean square errors of one-step-ahead prediction (the step is 1 week in the weekly model and 2 weeks in the biweekly model and 1 month in the monthly model) for the per capita growth rate using a leave-one-out cross validation. To predict r_t (which was later used to calculate N_{t+1}), I looked for the nearest $E+1$ neighbors \mathbf{s}_i 's in a library dataset which includes all the points except \mathbf{s}_t and the ones with the delayed vector containing any element in \mathbf{s}_t . After the \mathbf{s}_i 's were selected, the weighted average of their per capita growth rate r_i was calculated as the prediction for r_t . This was repeated for each point in the dataset. All the variables were centered with respect to their mean and scaled by their standard deviation before inclusion in the model (Sugihara and May 1990, Deyle et al. 2013). After obtaining a prediction for r_t , the prediction for N_{t+1} was calculated by adding the log abundance at current step N_t and the predicted value for r_t , and then taking the exponential of the resulting value.

To explore how the predictability may change with time steps into the future at each aggregation time scale, the selected models were then used to predict the per capita growth rates n ($n=1$ to 30) time steps ahead $r_t, r_{t+1}, \dots, r_{t+30}$, by tracking the per capita growth rate of the neighbors n time step ahead r_{i+n} using the model selected for 1 time step ahead prediction. Additionally, I also calculated the predicted abundance at 1 to 30 steps ahead by adding the current abundance (N_t) and the predicted growth rates ($r_t \dots r_{t+n-1}$), and then taking the exponential of the resulting values.

I subsequently applied this approach to compute 7-day-ahead predictions based on the once-per-week samples obtained by selecting one every seven daily samples in the observed sequence (i.e. the first two of the seven sub-series obtained with this procedure would be N_1, N_8, N_{15}, \dots , and N_2, N_9, N_{17}, \dots). Models based on the once-per-week samples were run and selected separately for each of the 7 realizations available. Results from these prediction experiments predict N_{t+7} using information at times $t, t-7, t-14$, etc. These results were compared with the result of a 7-day-ahead prediction using all the daily observations available (i.e. predicting N_{t+7} using information at times $t, t-1, t-2$, etc.). For comparison purposes, seven models based on the full set of daily observations were also set up to match the prediction dates of the once-weekly-based models above. In other words, in the model for daily data a first model was set up to predicting Monday abundance every seven days, but using all the daily information available. A second model was set up to predict Tuesday abundance every seven days, and so forth. Even though reference to the days of the week does not indicate that a

dependence on the specific day of the week is expected, but rather as a label to indicate the seven different realizations of the once-weekly series considered.

The Simplex Projection method uses a fixed number of points when looking for the nearest neighbors. In other words, in an E dimensional SSR, $E+1$ nearest points and their trajectories are used in the prediction of the target. The original SP method does not impose a threshold on distance to possibly exclude points in the library of trajectories which may be deemed to be too far from the current system state. However, I also explored a method of fixed distance (Kantz and Schreiber 2004), which searches simplex vertexes only within a neighborhood of the current system state, s_t , defined by a maximum threshold distance (ϵ). In this method the maximum distance is pre-determined but the number of neighbors can vary at each time step (and hence the geometry defined by the points enveloping the current system state need not be a simplex as before). I explored various values of the threshold distance, however, for the mosquito dataset, the SP method consistently yielded better predictions than the fixed distance method. Small values of ϵ incorporated no neighbor for some observations, thus inhibiting their prediction. Increasing values of ϵ resulted in a large number of neighboring points for other observations, and some trajectories of such neighbors were not representative of changes in the present. Therefore, in the following section the analysis was focused on the SP method.

Finally, to better assess the performance of the SP models, their results were compared with the results from a reference random walk model at corresponding temporal scales. The random walk model was calibrated as an Autoregressive integrated

moving average model ARIMA (0,1,0). This model uses the most recent observation as the prediction, and in a previous study it was shown to outperform both parametric and non-parametric methods for short-term forecasting for other population datasets (Ward et al. 2014).

Species interactions can play an important role in regulating population dynamics (Liu et al. 2012, Perretti et al. 2013a, Liu et al. 2014). I investigated the possible role of species interactions, and the potential to improve mosquito abundance models, by incorporating two mosquito species simultaneously into a single SP model at the three aggregation time scales (Liu et al. 2012, Liu et al. 2014). This was referred to as co-prediction hereafter. In this method, SP was used to investigate the pair-wised relations between the populations of different species. The lagged abundance of one species was used to predict the per capita growth rate of another species. The 16 most abundant species were considered in this analysis (Figure 18), resulting into 256 pairs of co-predictions at each time scale. To reconstruct the state space the order of lags for the abundance was fixed at 3 as suggested by explorative analysis. Thus, to predict $r_{p,t}$ (the per capita growth rate for species p at time t), a lagged vector of $s_{p,t}=(\log(N_{q,t}), \log(N_{q,t-1}), \log(N_{q,t-2}), \log(N_{q,t-3}))$ involving the lagged abundance for species q was constructed, and its nearest neighbors were searched SSR for species q . Environmental forcings were not included in this analysis because the purpose is to selected the most related species. A skillful prediction of the population change of species p by the lagged abundance of species q would indicate synchronized fluctuations in the abundance of the two species, which can either result from similar responses to environmental forcings, or from inter-

species interactions. The species found to be most related to *Ae.vexans* and *Cs.melanura* were then incorporated in the full single-species model (with lagged environmental forcings and the abundance of *Ae.vexans* or *Cs.melanura*), to investigate possible improvement in the prediction of per capita growth rate of the two species.

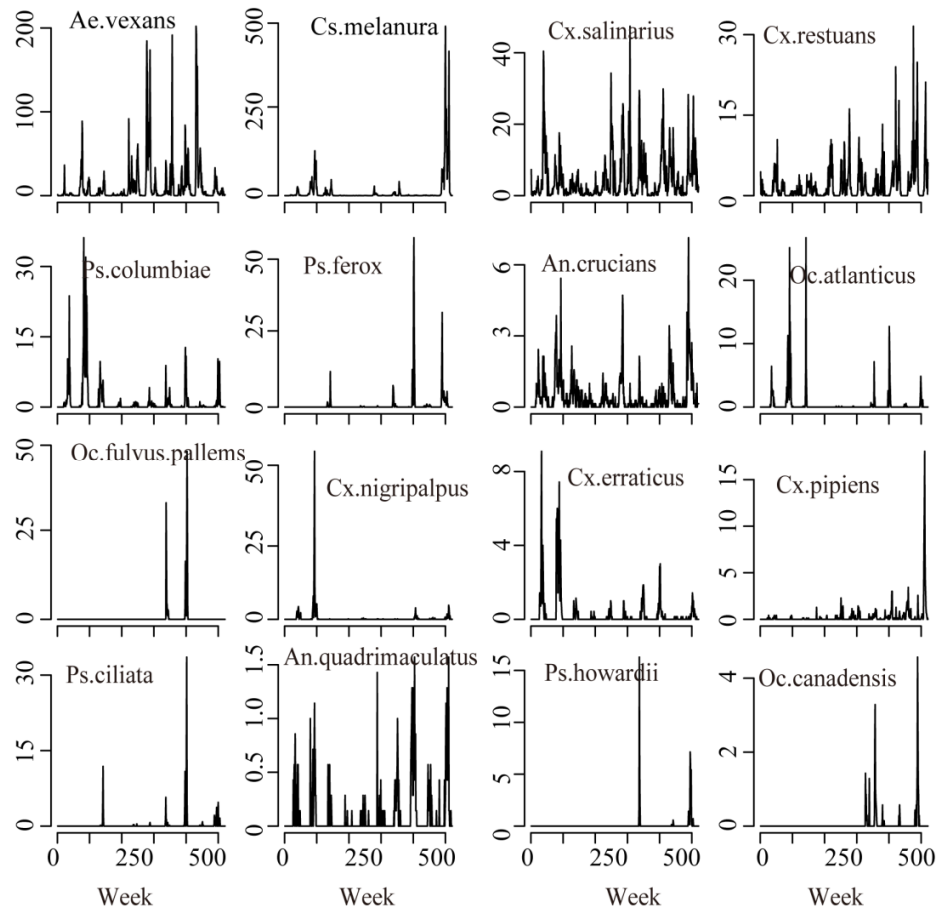


Figure 18: Time series of the 16 most dominant mosquito species in the Chicken site trap for the period 2004-2013.

4.3 Results

First, I investigated the predictability of mosquito abundance and growth rate for different aggregation time scales. The SP models resulted in high correlations between the predicted and observed per capita growth rates at monthly scale (Figure 19) and between the predicted and observed abundance at all three time scales (Figure 20). The correlations were higher for the abundance than for the per capita growth rates of both species, as expected, especially at weekly and biweekly time scales (Table 4, Figure 19-20), which illustrates the challenges in predicting the change in population size (Jian et al. 2014a)

Table 4: The correlations and RMSE for the best models at three time scales for *Cs.melanura* and *Ae.vexans*

Time scales	Correlation for N	Correlation for r	RMSE for N	RMSE for r
Week <i>Cs.melanura</i>	0.753	0.248	27.260	0.467
Biweek <i>Cs.melanura</i>	0.773	0.499	24.153	0.523
Month <i>Cs.melanura</i>	0.712	0.636	24.743	0.678
Week <i>Ae.vexans</i>	0.773	0.332	17.785	0.665
Biweek <i>Ae.vexans</i>	0.665	0.515	19.644	0.749
Month <i>A.vexans</i>	0.577	0.678	18.904	0.847

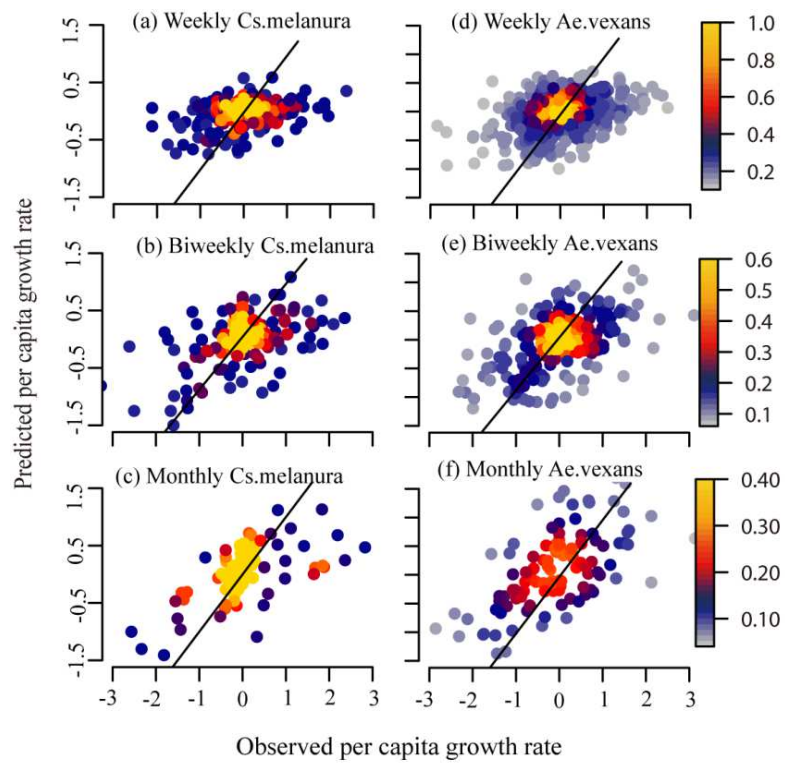


Figure 19: Predictions of the growth rate from the best SP models at weekly, biweekly and monthly for *Cs.melanura* and *Ae.vexans*. The colors indicate the density of the points available for the evaluation.

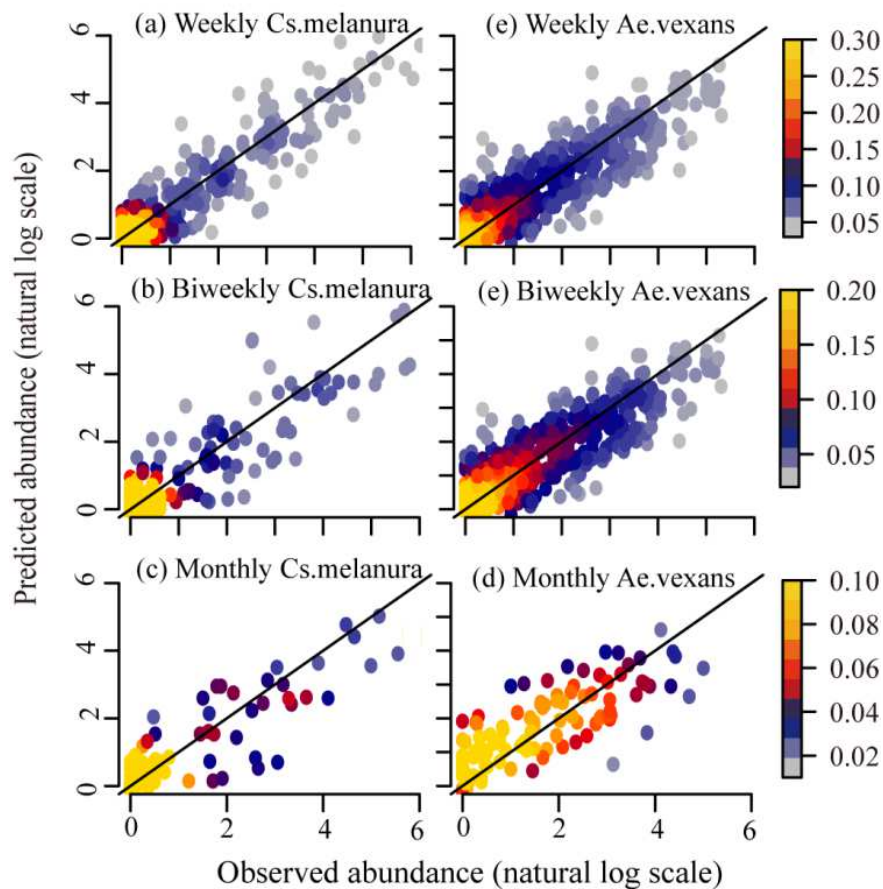


Figure 20: The predictions of abundance from the best SP models at weekly, biweekly and monthly for *Cs.melanura* and *Ae.vexans*

Overall, the correlations between the predicted and observed per capita growth rate increased from weekly to monthly time scales (Table 4, Figure 19). At weekly and biweekly time scales, mosquito per capita growth rates were highly fluctuating. The large changes in per capita growth rate were underestimated, while the small changes were overestimated by the SP approach, especially at the weekly scale (Figure 19, 21). In fact, the prediction explained about 10% (calculated as the coefficient of determination) of the variations in the observed per capita growth rate at the weekly scale, and about

25% at the biweekly scale for both species. However, the prediction of the per capita growth rate at the monthly scale was greatly improved and explained 41% of the variations in *Cs.melanura* and 43% in *Ae.vexans*. The low predictability of per capita growth rate at short time scales is also seen with other prediction methods (e.g. (Chaves et al. 2012, Jian et al. 2014a)).

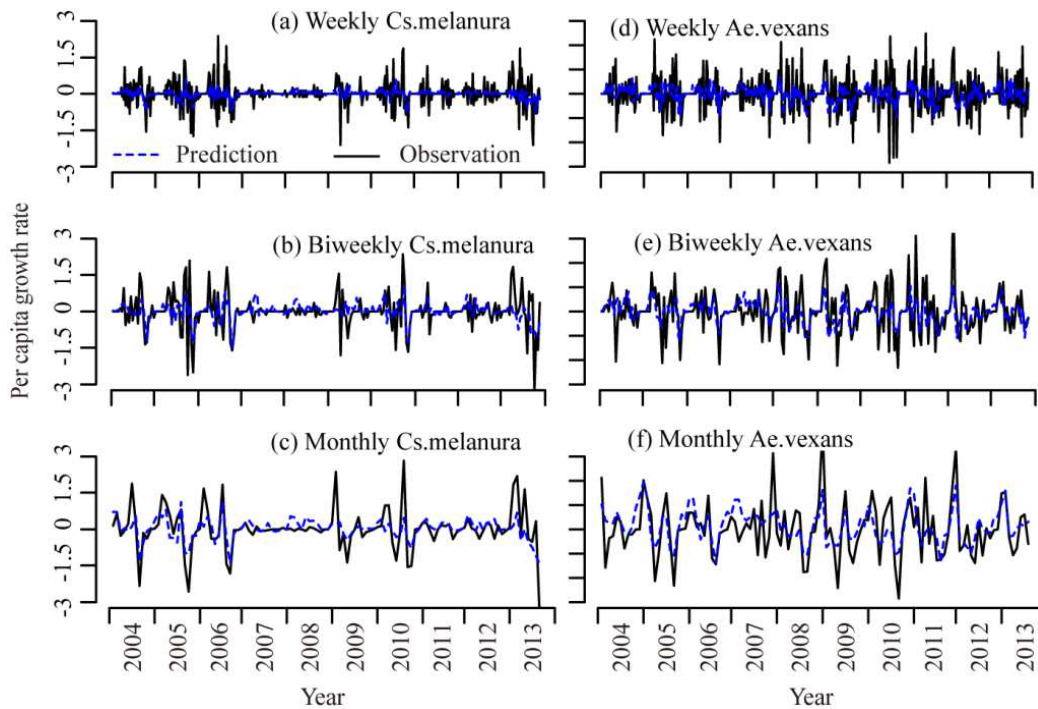


Figure 21: The time series of predicted and observed growth rates at different time scales.

The predicted abundance explained the majority of the variations in the observed abundance, 88%, 79% and 78% for *Cs.melanura* and 78%, 70%, and 60% for *Ae.vexans* at weekly, biweekly and monthly scale (Figure 20 and 22). Furthermore, the correlations between the predicted and observed abundance decreased from weekly to monthly scales (Table 4 Figure 20). However, a closer examination shows that the predicted abundance always lagged the observed abundance at the weekly and biweekly scales

(Figure 23), illustrating how the model predictive capability evaluated on the abundance are artificially high and mainly due to the high correlation between abundance in successive time steps. In fact, the decrease in the correlation can be attributed to the decreased autocorrelation in the abundance as the time scale increased. However, this lagged effect was reduced at monthly scale, where a better prediction of the per capita growth rate improved predictability of the abundance, especially with respect to the timing of abundance rises and falls (Figure 23).

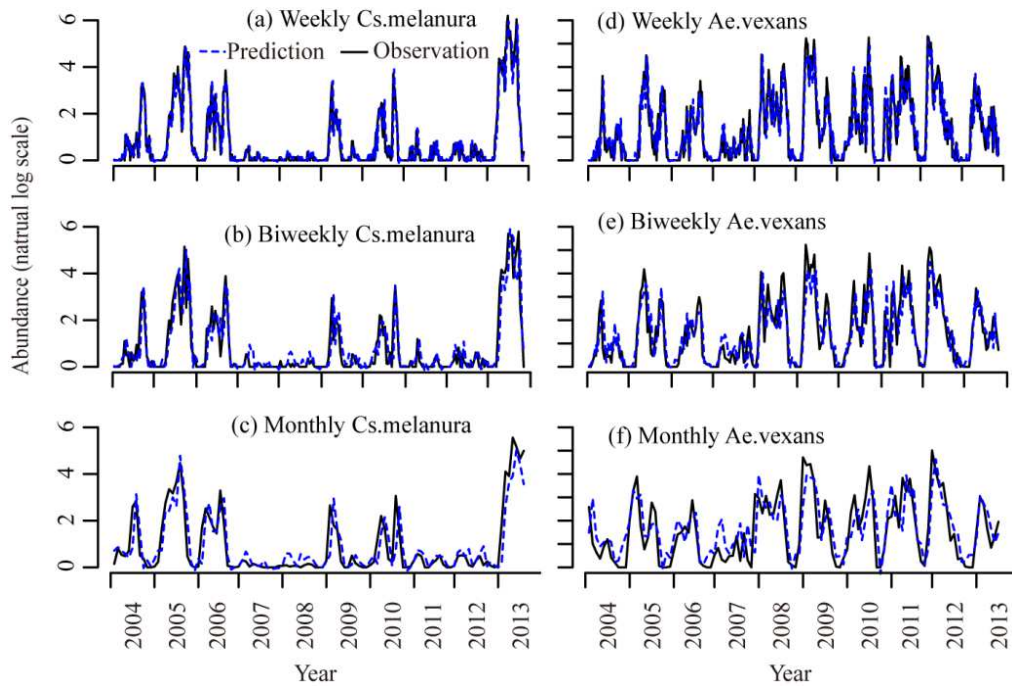


Figure 22 : The time series of predicted and observed abundance at different time scales.

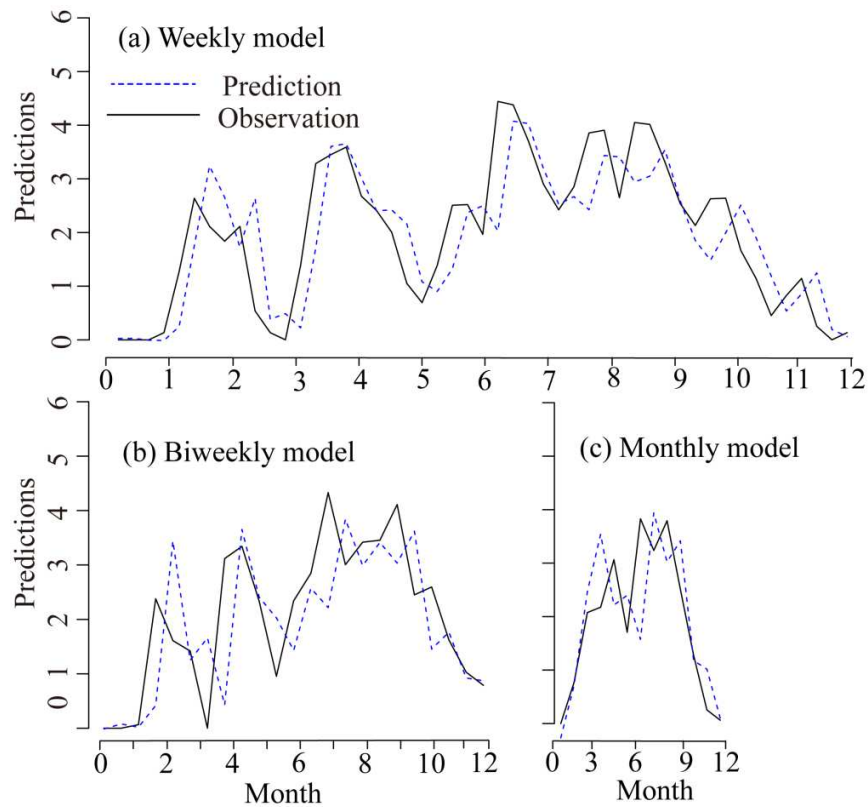


Figure 23: The predicted and observed abundance for *Ae.vexans* in 2011 as an example. The panels are arranged so that the lengths on the x axis between two points in the weekly, biweekly and monthly models are the same. In the weekly and biweekly model, the predictions lagged the observations by about 1 time step. This was improved in the monthly model.

The performance of SSR methods shows that the selected order of lags for abundance in the delayed vector (the value of j) decreased as the time scale increased (Table 5). This resulted in a relatively consistent length of time period (~1-2 months) over which historical abundance was found to be useful to predict future population changes. This approximately corresponded to the length of the life cycle of the 2 species (Jian et al. 2014b). Furthermore, multiple lags of rainfall were included in most of the selected models, consistently with known delayed effects of rainfall on mosquito dynamics

(Horsfall 1973). The change in the value of j as a function of time scale also contributed to the difference in the correlations between the predicted and the observed per capita growth rate across time scales. Because E (the dimension of SSR) is a function of j , at weekly and biweekly scales, larger values of j required more neighboring points to calculate the weighted average, which lead to a smoother series of the predicted values. Thus, most of the large fluctuations in the population were underestimated.

Table 5: The variables selected for the best models at three time scales for *Cs.melanura* and *Ae.vexans*

Time scales	logN	Rainfall
Weekly <i>Cs.melanura</i>	Lag 0-5	Lag 0-2
Biweekly <i>Cs.melanura</i>	Lag 0-2	Lag 0,1
Monthly <i>Cs.melanura</i>	Lag 0-1	Lag 0
Weekly <i>Ae.vexans</i>	Lag 0-8	Lag 0-3
Biweekly <i>Ae.vexans</i>	Lag 0-3	Lag 0
Monthly <i>Ae.vexans</i>	Lag 0-1	Lag 0-3

Compared to the results for *Cs.melanura*, the models for *Ae.vexans* exhibited higher correlations between the predicted and observed per capita growth rate, and lower correlations between the predicted and observed abundance (Table 4). This suggested faster but more predictable fluctuations in the abundance of *Ae.vexans*, which may be partly related to its shorter generation time (Becker et al. 2003). Wider inter-annual variability in the abundance of *Cs.melanura* was observed. For examples, in the dry year of 2007, only 31 *Cs.melanura* were caught, while in 2013 the annual abundance for *Cs.melanura* was around 25,000. This extraordinary inter-annual variability in the abundance of *Cs.melanura* increased the challenge to predict the change of its population

size, as extreme high and low values unobserved in the data library could not be captured by the weighted average of observed data points.

The correlation between predictions and observations changed as a function of the prediction horizon (Figure 24). It decreased sharply for the first few time steps and then remained relatively stable (Figure 24 and Appendix C). The gradual decrease of the correlation at larger time steps suggests slow divergence of the trajectories of nearby points in the SS at long time scales, which is a character of periodic systems and can be partly due to the seasonal cycle in the population dynamics (Kantz and Schreiber 2004). The fast decrease of the predictability in the near future is also coherent with previous analogous studies of other population time series (Sugihara and May 1990).

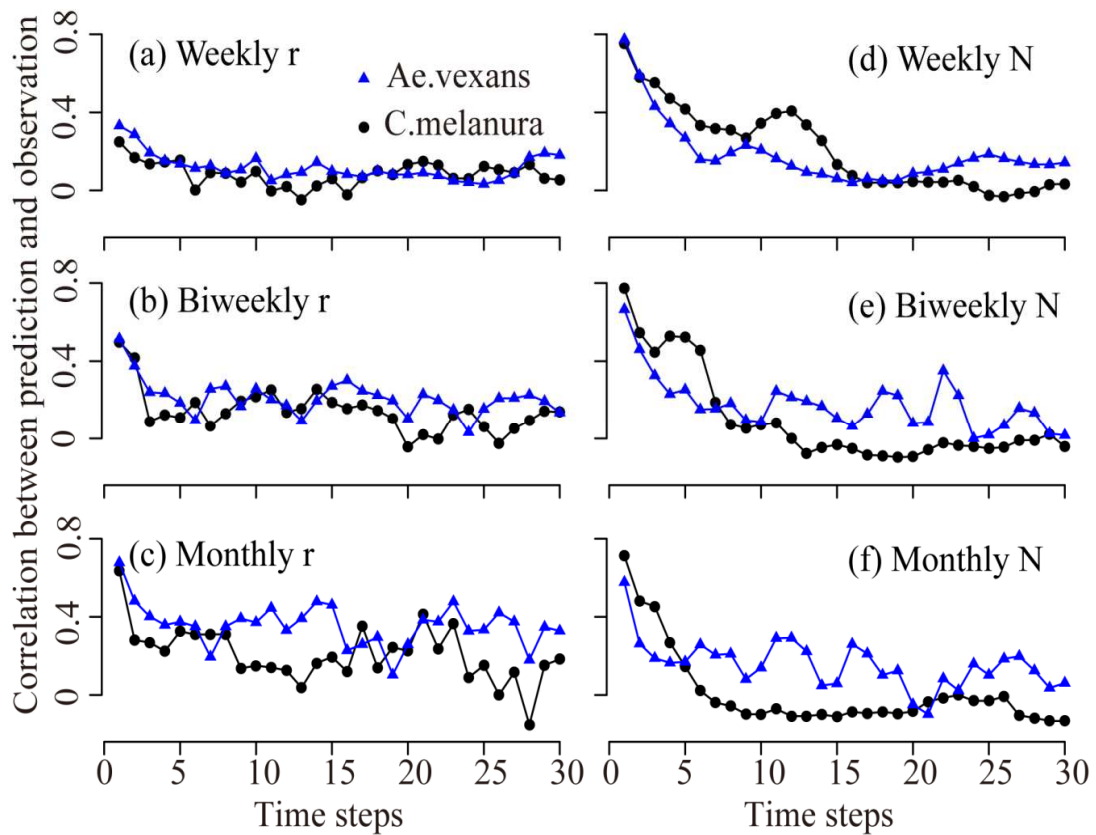


Figure 24: The correlation between the predicted and observed values changes as a function of time steps into the future for the growth rate and abundance from the best models

Now I turn to the comparison of the 7-day-ahead prediction obtained from daily observations and the 7-day-ahead prediction based on once-per-week samples. In general, daily observations allowed better predictions for the per capita growth rate of both species, as indicated by higher correlations between predicted and observed values, as well as lower root mean square errors (Figure 25). The improvement was less manifest in the prediction of abundance, but a better prediction of the abundance for *Cs.melanura* can also be obtained using the daily observation. The variables in the selected models for each realization of the once-per-week sample were also different, with the maximum lag of abundance ranged from 2 to 7 weeks for *Cs.melanura* and 0-7 weeks for *Ae.vexans* using the once-per-week sample. (Appendix C).

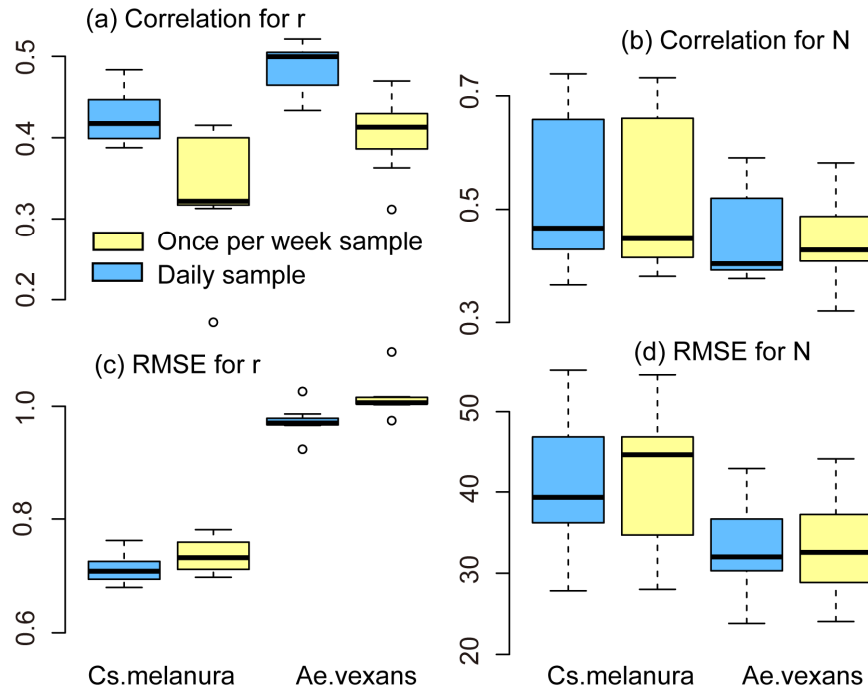


Figure 25: Comparison of the 7-day-ahead prediction using the daily observation and once-per-week observation

The method of co-prediction is a useful tool to identify species with similar population dynamics. We present its results using a matrix where row p shows the correlations between the observed and the predicted per capita growth rate of species p by using the lagged abundance of other species (Figure 26 and Appendix C). For most species the best prediction of their population change was achieved using their own lagged abundance (Figure 26, indicated by larger circles with warmer colors). The maximum correlations at off-diagonal locations may be partly explained by sampling uncertainties. Because mosquito species vary in their response to artificial light, the New Jersey light trap displays different efficiency in capturing their abundance (Reinert

1989). Thus a mosquito species which is modestly attracted by the trap may be better predicted by another species whose abundance can be more accurately collected.

The results also indicated more and larger positive correlations as the time scale increased from weekly to monthly in the pair-wise co-prediction (Figure 26). In addition, the rank of the correlated species also changed across time scales. For example, the per capita growth rate of *Ae.vexans* was found to be best predicted by its own lagged abundance at all three time scales, followed by *Cx.salinarius* at the weekly scale, and *Cx.pipiens* at the biweekly and monthly scale. The incorporation of the lagged abundance of the most correlated species in this analysis into the full single species model did not improve the prediction of the per capita growth rate of *Ae.vexans* and *Cs.melanura*. This result suggests that the synchronized fluctuations in the populations were more likely due to similar responses to environmental forcings rather than direct interactions among populations.

The “correlation matrix” resulting from the pair-wise application of co-prediction models is symmetric for some of the studied species. For example, at the monthly scale the per capita growth rate of *An. quadrimaculatus* can be best predicted by the lagged abundance of *Culex erraticus* (correlation = 0.51), and the per capita growth rate of *Culex erraticus* can also be best predicted by the lagged abundance of *An. Quadrimaculatus* (correlation = 0.52). In fact these two species share similar natural habitat at their larval stage (Horsfall 1955). Thus this symmetric result of prediction indicates their preference for similar environmental conditions. However, non-symmetric results are also found for other species, such as when the prediction of

Cx.restuans and *Ae.vexans* at monthly scale. The per capita growth rate of *Cx.restuans* can be best predicted by the lagged abundance of *Ae.vexans* (correlation = 0.51), but the per capita growth rate of *Ae.vexans* cannot be predicted using the lagged abundance of *Cx.restuans* (correlation = 0.14). One of the reasons for this asymmetry is related with sampling uncertainty. The abundance of *Ae.vexans* can be accurately sampled by New Jersey light trap while *Cx.restuans* abundance cannot (Reinert 1989).

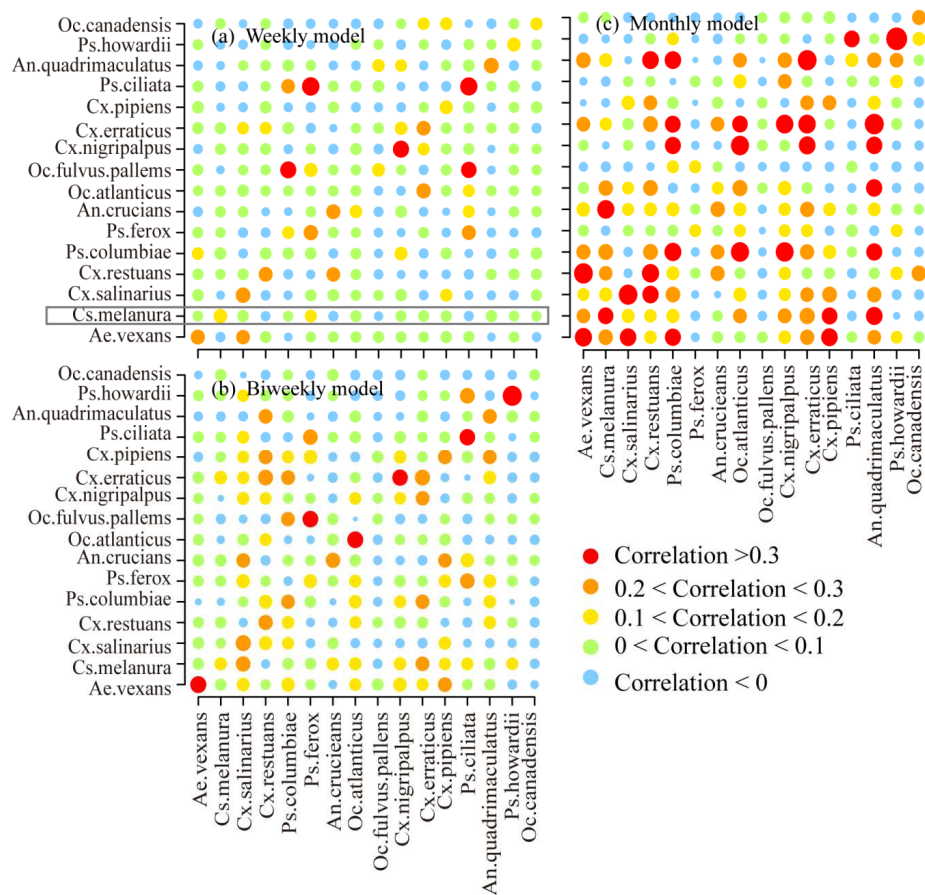


Figure 26: Results from co-prediction. Each point shows the correlation between the predicted and observed per capita growth rate. The size of the points is proportional to the values of the correlations. The plots should be read by row. For example: the row for *Cs.melanura* in the weekly model panel (in the grey box) shows the result of predicting the per capita growth rate of *Cs.melanura* by the lagged abundance of the 16 species.

I subsequently compared the results of the SP models with those from the reference random walk. Unlike results from Ward (2014), which showed that random walk models outperformed existing population models across a wide range of taxa, the SP models developed here resulted in higher correlations between predicted and observed values for both the per capita growth rate and the abundance, except for the abundance of *Cs.melanura* at weekly and monthly scales. In particular, correlations between predicted and observed per capita growth rates from the random walk model were low, indicating its inability to capture changes in the population size (Table 6). The high correlations for the predicted and the observed abundance in the random walk model were the result of positive autocorrelations in the time series of abundance.

Table 6: The correlations and RMSE for the random walk models at three time scales

Time scales	Correlation for N	Correlation for r	RMSE for N	RMSE for r
Week <i>Cs.melanura</i>	0.770	-0.026	27.749	0.683
Biweek <i>Cs.melanura</i>	0.747	0.186	26.284	0.766
Month <i>Cs.melanura</i>	0.725	0.095	24.594	1.122
Week <i>Ae.vexans</i>	0.751	-0.046	19.415	1.012
Biweek <i>Ae.vexans</i>	0.602	0.084	22.949	1.175
Month <i>Ae.vexans</i>	0.458	0.089	23.536	1.508

4.4 Discussion and conclusions

In environmental and ecological studies, nonlinearity and unobserved high dimensionality in a system can often impede the mechanistic understanding and model predictive abilities. The SSR method provides a tool for short-range prediction, especially when multiple time series (both the abundance and the environmental

forcings in the present study) are used to reconstruct the state space (Sugihara et al. 1990, Kantz and Schreiber 2004, Hsieh et al. 2005, Sugihara et al. 2012, Deyle et al. 2013, Liu et al. 2014). This dissertation developed the first application of the SSR approach to mosquito population dynamics and high correlations between the predicted and observed values were achieved. Similar to studies for other populations (Deyle et al. 2013), the predictability of the abundance is improved by including time series for environmental forcings (Deyle and Sugihara 2011). In theory, a SS can be reconstructed from a single time series that is adequately long and with small observational errors (Sugihara and May 1990, Kantz and Schreiber 2004). However, in realistic applications, time series are usually observed with limited length and non-negligible errors. Thus, additional information provided by multiple time series describing the same system can be useful for a more accurate reconstruction (Deyle and Sugihara 2011). Unlike the result from Ward et al (2014), the SSR model has greater predictive capability in the present application than the random walk model. Generally speaking, the SSR approach differs from linear models in that it searches the most similar points in the reconstructed state space rather than in the temporal domain, which may result in a more accurate prediction in the presence of nonlinearity (Perretti et al. 2013a).

Furthermore, the SSR models have additional advantages in predicting the change (in this case the per capita growth rate) of a system. Understanding the dynamics of a population and predicting its abundance are challenging problems in the general field ecology (Turchin 2003). This is especially true in mosquito populations, where fast, and apparently uncorrelated, fluctuations are the norm (Jian et al. 2014b). The evaluation

of predictive models for mosquito abundance is often performed as correlation between the predicted and observed abundance or variations in the abundance explained by models (Bomblies et al. 2008, Yang et al. 2008a, Yang et al. 2008b). I showed here that this method of evaluation artificially overestimates models' predictive abilities and that comparing per capita growth rates offers a far more realistic evaluation of model performance.

Knowing future abundance is of central interest for mosquito control programs. However, models with high correlations between the predicted and observed abundance may be of little use for mosquito control if the prediction cannot capture the change from the current abundance to the future abundance. Hence the comparison of predicted and observed the abundance is inadequate to evaluate mosquito population models. Although the per capita growth rate has been used in the field of ecology to understand density dependence and population development (Turchin 2003, Sibly et al. 2005, Clark 2007), its application in mosquito abundance modeling is rarely seen (Russell et al. 2011, Jian et al. 2014a). The present results suggest that a more robust evaluation of predictive models for mosquito abundance should include the investigation of both the predicted abundance and the per capita growth rate.

Previous studies have analyzed the choice of temporal intervals between two adjacent lags for SSR approaches using explorative analysis such as autocorrelation function and mutual information (Kantz and Schreiber 2004) for redundant dataset. However, these studies mostly focus on purely deterministic and data rich systems (Kantz and Schreiber 2004). In this study I focused on a long term mosquito abundance

sample captured under natural conditions, which as many dataset in ecological studies, was contaminated by observational errors. Uncertainties are here reduced by averaging the abundance over non-overlapping moving windows. Thus the fast fluctuations in the abundance likely caused by mosquito activity are partly removed, while the variability at longer time scales caused by true population changes is retained (Jian et al. 2014b). The predictability of abundance is here found to change as a function of modeling time scale, and the per capita growth rate can be reliably predicted only at the monthly scale. This result is corroborated by previous studies (Russell et al. 2011), and the low predictability at short time scales points to the possibility of missing important controlling mechanisms in the sampling and modeling of adult mosquito abundance.

A better prediction of 7-day-ahead mosquito growth rate can be obtained by daily mosquito observations compared to the once-per-week observations split from the same dataset. This improvement shows that daily mosquito observations contain important information for mosquito abundance and the extra effort in mosquito sampling can indeed result in improved prediction for the change of mosquito abundance. In our analysis, only the 7-day-ahead prediction is compared because this is what can be achieved by the once-per-week samples. This can be a conservative estimation of the benefit of the daily samples because predictions based on a shorter predictive horizon (such as 1-day-ahead prediction) can lead to more accurate results.

The results of co-prediction also show that the largest predictive capability are found at the monthly time scale. Although the method does not allow the identification of detailed causes of positive correlations, given the heterogeneity in mosquito habitats

and the diversity in their hosts, this predictability may most likely be attributed to the similarity of mosquito species' responses to the changing environment rather than to their direct biological interactions. This is further suggested by the lack of improvement in the single species models when related species are included, which is in contrast with existing studies on species interactions (Perretti et al. 2013b). The scale-dependent results from co-predictions are also interesting. The desynchronized fluctuations at short time scales are possibly linked with mosquito behavioral events, such as their ability to fly under unfavorable conditions (Clements 1992), while the more synchronized population changes at the monthly scale may be linked with their responses to accumulated external conditions which are more likely to influence the overall death and growth rates of populations (Jian et al. 2014b).

5. Dissertation conclusions

5.1 Overview of the results

This dissertation presents an integrated approach towards a better understanding of mosquito population dynamics in temperate regions and an improved predictability of mosquito abundance. Several related questions are addressed and they are summarized below:

1. Is mosquito population regulated by density dependence in the temperate regions, and if yes how does it operate?

Density dependence is detected and observed in all the studied mosquito species in this dissertation, as indicated by the fact that large mosquito abundance is linked with low per capita growth rate. The time scale at which density dependence operates is about one to several weeks, and it is related to the length of generation time for mosquito species. Density dependence interacts with environmental forcings and is influenced by habitat types. In the Po River delta area the carrying capacity of *Culex pipiens* is negatively related with distance to the nearest rice field, while the maximum population growth rate is positively related with the Normalized Difference Vegetation Index. Density dependence provides important information for the predictive models of mosquito abundance. It should be incorporated in mosquito abundance models simultaneously with environmental forcings. Under natural conditions the detection of density dependence in mosquito population can be influenced by (1) variations in the environmental factors, which can lead to uncertainties in the order of abundance lags

used in the model; (2) apparent fluctuations in the abundance linked with mosquito activity, especially when the sampling frequency is low. Thus the identification of density dependence needs careful considerations of the combined effect of exogenous controls and sampling frequency.

2. How do environmental forcings regulate fluctuations in mosquito abundance in temperate regions? Especially, what is the relative importance of soil moisture and rainfall in driving mosquito models?

In temperate regions mosquito abundance is governed simultaneously by multiple environmental forcings. The sophisticated interactions of these factors as well as intensive human modifications on the natural environment lead to a big challenge for revealing the controlling mechanisms for mosquito populations. Environmental forcings, as show in the case of rainfall in this dissertation, influence observed mosquito abundance not only through their current effects on mosquito activity and death rate, but also through the lagged impacts on mosquito development and survival rates of early stages. Thus, a robust prediction of mosquito abundance should be based on both current and historical weather conditions. Furthermore, nonlinearity is also found in the rainfall effect: heavy rainfalls are found to reduce the observed mosquito abundance by impeding mosquito activity while more evenly distributed rainfall can lead to an increase in mosquito abundance by increased water availability.

The comparison of modeled soil moisture and rainfall effects in regulating mosquito populations indicates that these two drivers lead to similar prediction for mosquito abundance in the studied area, which is different from the result found in

tropical regions (Patz et al. 1998). On one hand, surface runoff and artificial sources probably already provide sufficient water to sustain mosquito habitats in this humid study area, and thus mosquito abundance is not limited by water availability. On the other hand, the studied species *Cx. pipiens* is well adapted to human modified habitats and prefers eutrophic conditions for development. Thus, excessive water, either indicated by large rainfall amount or high soil moisture, does not lead to an abundance rise.

3. What are the temporal scales of variability in mosquito populations and what are the regulation mechanisms at different scales?

Individual based simulations and Fourier transform analysis of the mosquito populations in the Brunswick County provide clear indications of abundance fluctuations across a wide temporal spectrum. The range of time scales over which adult mosquito population variability takes place can be divided into three main parts: at small time scales (the microscale, indicatively <1month) apparent population fluctuations are driven by behavioral responses to rapid changes in weather conditions, at intermediate scales (1 to several months) endogenous dynamics dominate, fingerprinted by distinct peaks in the power spectrum, at longer scales (yearly) mosquito populations respond to seasonal and inter-annual environmental changes.

4. What sample resolution can fully resolve mosquito population dynamics?

Fast fluctuations are observed in the daily samples of mosquito abundance for all the studied species. Spectral analysis of the long term daily data indicates significant population fluctuations over characteristic periods between 2 days and several years.

Particularly, fluctuations in the abundance of *Cs.melanura* with periodicities shorter than 2 weeks are identified, suggesting that the commonly used once-per-week sample cannot capture the full population dynamics of this mosquito population. Considerable differences are found between the PACF of the daily data and the subsampled weekly data, and among the subsampled weekly data created on different dates. This suggests that time series analysis based on weekly samples can lead erroneous inference for mosquito populations due to inadequate sampling resolution. Furthermore, the investigation of models with the activity effect indicates that the fast observed fluctuations in the abundance, rather than to birth/death processes, are due to varying mosquito activity in response to rapid changes in meteorological conditions. Thus observations sampled once per a week or at longer time intervals can be seriously influenced by the changing fraction of active mosquitoes, and does not allow averaging out the effects of behavioral responses (e.g. by moving averages). Hence it can be concluded that observations of adult mosquito populations should be based on a sub-weekly sampling frequency to fully capture the fluctuations in mosquito population dynamics.

5. How does the predictability of mosquito abundance change as a function of aggregation time scales and the prediction horizon?

Mosquito abundance is auto-correlated at weekly and shorter time scales as indicated by the partial auto-correlation functions for the observed time series. Thus previous abundance can provide important information for further population size. However, model evaluations based on abundance can be misleading, because the

autocorrelation in the abundance can cause artificially high correlation between the predicted and the observed abundance, even if the model has a low predictive skill. Understanding and predicting the change in the abundance (represented by per capita growth rate) are much challenging, particularly at short time scales. The results from the state space model indicate that correlations between predicted and observed abundance decrease as the time scale of the models increases from one week to one month. However, correlations between the predicted and observed per capita growth rate increase together with the modeling time scale. The lack of predictability of the per capita growth rate at short time scales reveals limitations in our understanding, as well as in sampling practices and modelling approaches, of the driving mechanisms of the fast changes in mosquito populations.

5.2 Major contributions

A few, methodological conclusions can also be drawn from the work described in the present dissertation.

First, a hierarchical modeling structure provides an efficient way to fully exploit the information from a large network of observation sites. The model at the individual level (mosquitoes captured within a site) describes the response of mosquito abundance to environmental forcings, while the group –level (site difference) hierarchy shows the influence of land use and land cover on population dynamics.

Second, the inclusion of hydrological, GIS and remote sensing tools allows a comprehensive study of the environmental factors governing mosquito abundance and the influence of habitat type. The use of a detailed hydrological model offers the ability

to compare the relative merit of using rainfall or soil moisture information to drive mosquito abundance model. The application of this approach to a semi-humid environment suggests that, when water availability is not limiting mosquito dynamics, the use of rainfall or soil moisture lead to similar predictive skills.

Third, spectral analysis is shown to be a very useful tool to investigate potential cycles in mosquito populations, and to identify the related periodicities. This approach can be generalized to other species for the identification of population cycles and the evaluation of sampling frequency.

Fourth, the individual-based models developed in this dissertation synthesize the available information about mosquito dynamics available in the literature, and incorporates uncertainties from multiple sources in probabilistic distributions. It provides a convenient tool to inspect the influence of a single controlling factor and the related stochasticity by allowing the selective removal of the influence of other mechanisms.

Fifth, the state space reconstruction approach predicts future abundance and per capita growth rate by comparing current biological and environmental conditions with previous conditions and projecting their trajectories in the state space. It is a powerful tool to utilize observations accumulated over the years and is especially efficient for accounting for non-linear and delayed dependence relations.

Finally, this dissertation shows that mosquito activity is an important component of the observed fluctuations in adult mosquito abundance. Without it, the fast fluctuations in the observed abundance cannot be explained. To understand the actual

changes in mosquito population size, models should be designed to include the effects of mosquito activity or to reduce its influence through sampling/averaging strategies.

Appendix A

A1. Conditional plots for per capita growth rate, log of abundance and temperature

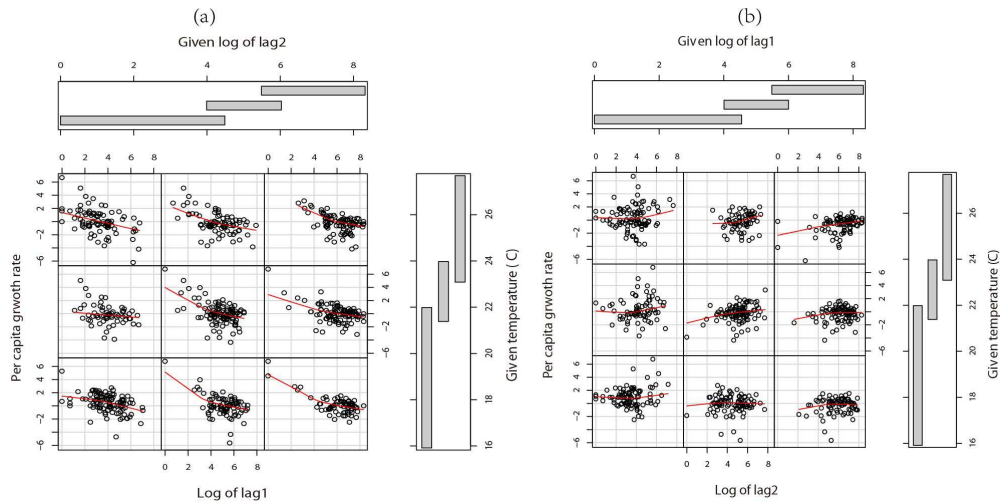


Figure 27: a) scatter plots between r and $\ln(x_{t-1})$, conditional on $\ln(x_{t-2})$, and temperature; b) scatter plots between r and $\ln(x_{t-2})$, conditional on $\ln(x_{t-1})$ and temperature. The red lines are the smoothing curves using locally-weighted polynomial regression.

A2. Relationship between rainfall and soil moisture

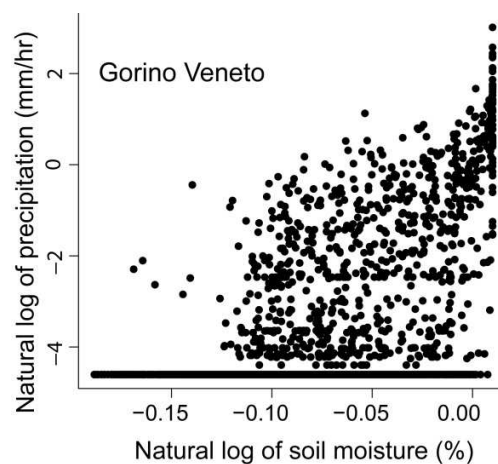


Figure 28: Nonlinear correlation between rainfall and soil moisture for site Gorino Veneto 2010 as an example.

A3. WinBUGS model script

```
## N is the observed abundance
## mu is the actual abundance
## MM is the modeled abundance

model=function() {
  logmu[I+1]<-0 # initial state
  for ( i in 1 : I){ # I is the total number of weeks
    N[i]~dpois(mu[i])
    mu[i]<-exp(logmu[i])
    logmu[i]~dnorm(logMM[i],tau.m)
    # process equation, week1[i] is the index for week t-1
    logMM[i]<-
a0[group[i]]+a1[group[i]]*logmu[week1[i]]+b2*temp[week1[i]]+b4*sw70[
week1[i]]+b5*rad[week1[i]]+b6*daylight[week1[i]]+b7*wind[week1[i]]
  }

  for ( j in 1 : J){ # J is the number of sites
    a0[j]~dnorm(mu.a0[j], tau.a0)
    mu.a0[j] <- theta.a0.0+ theta.a0.1*NDVI[j]
    a1[j]~dnorm(mu.a1[j], tau.a1)
    mu.a1[j] <- theta.a1.0+ theta.a1.1*rice[j]
  }
  # prior distributions, in WinBUGS normal distribution is defined by its
mean and #precision (1/variance)
  b2~dnorm(0, 0.01)
  b4~dnorm(0, 0.01)
  b5~dnorm(0, 0.01)
  b6~dnorm(0, 0.01)
  b7~dnorm(0, 0.01)
  theta.a0.0~dnorm(0,0.01)
  theta.a0.1~dnorm(0,0.01)
  theta.a1.0~dnorm(0,0.01)
  theta.a1.1~dnorm(0,0.01)
  tau.m <- pow(sigma.m,-2)
  sigma.m ~ dunif(0,10)
  tau.a0 <- pow(sigma.a0,-2)
  sigma.a0 ~ dunif(0,5)
  tau.a1 <- pow(sigma.a1,-2)
  sigma.a1 ~ dunif(0,5)
}
```

A4. Model evaluation

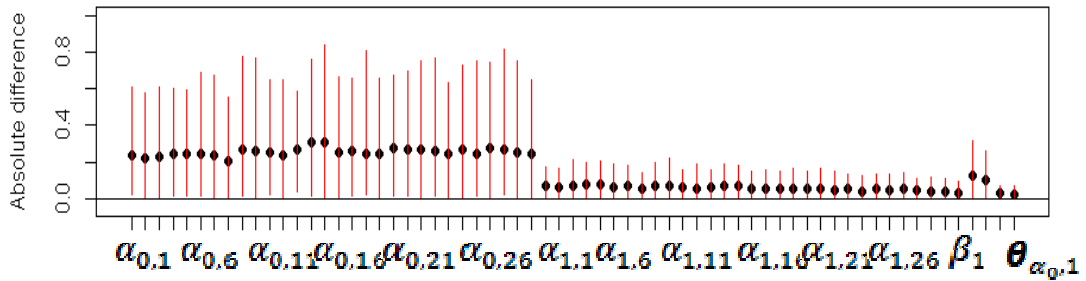


Figure 29: The hierarchical state space model was run 100 times using the synthetic data whose values represent those of the observed dataset. The plot shows the differences between the true parameters and modeled parameters. The dots are the mean of the absolute difference and the segments are the 95% credible intervals of the absolute difference. The difference is larger for $\alpha_{0,j}$ which has larger values.

Appendix B

B1. IBS model formulation, developmental stages, and processes.

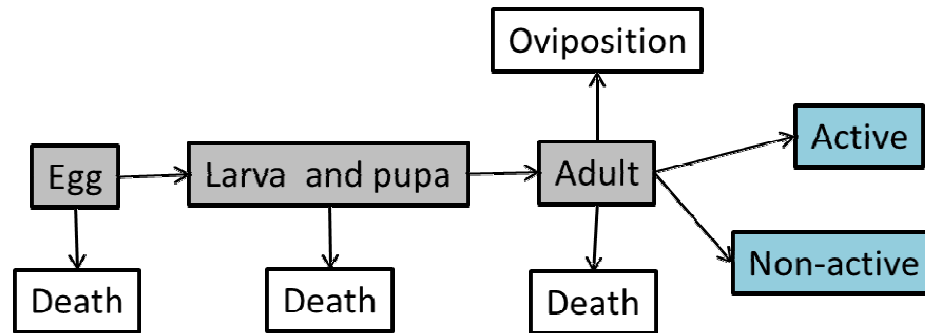


Figure 30: The IBS models explicitly describe three mosquito life stages: egg, larva/pupa, and adult. Each stage is characterized by a distribution of the time spent in that stage, dependent on physiology, environmental conditions, and population density. Each stage is characterized by a survival rate, also a function of environmental conditions. A proportion of the emerged female adults are successful in blood feeding and oviposition. I further assumed that the observed population is a varying fraction of the underlying actual adult population represented by an activity factor.

B2. Power spectrum of observed weather data

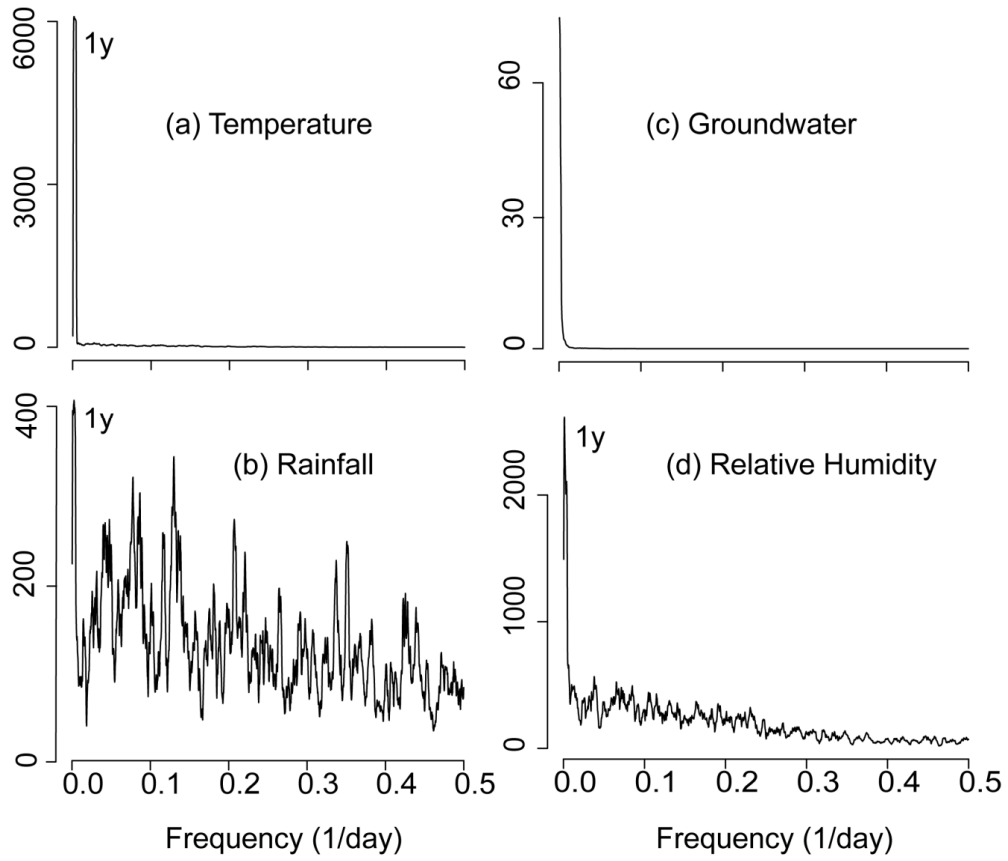


Figure 31: Spectral power for the weather observations

B3. Detailed functions and parameter values used in the IBS models

The IBS models explicitly describe three mosquito life stages: egg, larva/pupa, and adult (Becker et al. 2003). Each stage is characterized by a distribution of the time spent in that stage, dependent on physiology, environmental conditions, and population density. Each stage is characterized by a survival rate, also a function of environmental conditions. I based the description of the distributions of the time spent in each stage and of the survival rate for each stage on existing literature, to minimize the number of parameters which require ad hoc calibration (Figure 2).

For *Ae.vexans*, I assume the initial number of eggs equals to 10000. When the 10 days moving-average of daily temperature ($temp10$) is between 10-30°C, a proportion of these eggs hatch (Becker et al. 2003, Crans 2013a). The state of an egg is drawn from a Bernoulli distribution, where 1 represents a hatched egg while 0 represents unhatched one. Because rainfall can increase oviposition sites, I further assume that the hatching portion increases linearly with the 10 days moving-average of rainfall ($ppt10$, $p = 0.01 + ppt10 \times 0.015$ in the Bernoulli distribution). The expected number of days needed to develop from eggs to the 1st instar of larva is assumed to decrease with the temperature according to a power law ($\exp(7.5) \times temp10^{-1.90}$) (Horsfall 1973). The actual length of development is drawn from a normal distribution with the mean mentioned above and a standard deviation of 1 day. Because the eggs of *Ae.vexans* can live for years, I assume the daily survival rate for the eggs is high and decrease with the number of eggs ($1 - 0.00002 \times N_{egg}$) (Horsfall 1973, Becker et al. 2003). In the pupal/larval stage, the assumed mean development time is $\exp(8) \times temp10^{-1.86} + 4$ (Trpis and Shemanch.Ja 1970, Horsfall

1973, Becker et al. 2003). The actual length of development is drawn from a normal distribution with the this mean and a standard deviation of 1 day. The daily survival rate for the pupal/larval stage is assumed to be a quadratic function of temperature and decreases with the number of larvae because of potential competition for nutrients $0.9173 + 0.0060 \times temp10 - 0.00015 \times temp10^2 - 0.00002 \times Nlarva$ (Trpis and Shemanch.Ja 1970, Horsfall 1973). Furthermore, I assumed this rate decreases by 20% when ppt10 is smaller than 1mm/d due to drying out of the habitats, and decrease by 50% when temp10 is smaller than 10°C. After adult emergence, a proportion of the females are successful in finding blood meal (Bernoulli ($p = 0.8 + RH10/100$) for *Ae.vexans*, where RH10 is the 10 days moving-average of relative humidity;). The length of gonotrophic cycle is assumed to be drawn from a truncated normal distribution with the mean equals to 10 days, standard deviation equals to 1day, the minimum length equals to 7 days, and the maximum length equals to 13 days (Becker et al. 2003). The number of eggs laid by a female per batch is a random number from a normal distribution with the mean equals to $100 + ppt10$, the standard deviation equals to 10, and the lower bound equal to 0. The daily survival rate of adult females is assumed to be a quadratic function of temperature ($0.5 + 0.048 \times temp10 - 0.0012 \times temp10^2$). Furthermore, I assumed this rate decreases by 20% when ppt10 is smaller than 1mm/d, and decreases by 50% when temp10 is smaller than 10°C. Finally, the proportion of the active mosquitoes is calculated based on the observed data. I first calculated the ratio of the current abundance divided by the maximum abundance for moving window of 31 days, using the maximum abundance as an approximation of the true population. This ratio is then plotted against current day

rainfall, which I assumed to be the main driver of the activity factor. This plot suggested a nonlinear relationship between the ratio and the current day rainfall (Figure 22). The median of the ratio for each rainfall range is used as the activity factor.

The simulation for *Cs.melanura* is similar. Here I only mention the differences in the simulations for the two species. In addition to the initial number of eggs, I assumed a 5000 initial number of larvae, because *Cs.melanura* can over winter as larvae (Mahmood and Crans 1997, 1998a, b, Brunswick County Government 2011, Crans 2013c). The temperature limits for egg hatching is 5 to 32°C (Mahmood and Crans 1997, Becker et al. 2003). The expected number of days needed to develop from eggs to the 1st instar of larva is $\exp(8.35) \times \text{temp}10^{-2.30}$ (Mahmood and Crans 1998a, Brunswick County Government 2011, Buckner et al. 2012). In the pupal/larval stage, the assumed mean development time is $\exp(10.68) \times \text{temp}10^{-2.25}$ (Mahmood and Crans 1998a, Brunswick County Government 2011, Buckner et al. 2012). The daily survival rate for eggs is assumed to $1 - 0.000004 \times N_{\text{egg}}$. The daily survival rate for pupal/larval stage is assumed to $1 - 0.000004 \times N_{\text{larva}}$, and if ppt10 is smaller than 1 mm/d, the value decreases by 20%. The proportion of the females succeeding in finding blood meal and oviposition is $0.419 + 0.133 \times \text{temp}10 - 0.0035 \times \text{temp}10^2$ when $7.5 \leq \text{temp}10 \leq 28.5^\circ\text{C}$ (Mahmood and Crans 1997). The daily survival rate of adult females is assumed to be a quadratic function of temperature $(0.5 + 0.048 \times \text{temp}10 - 0.0012 \times \text{temp}10^2)$, and it decreases by 20% when ppt10 is smaller than 1mm/d. The expected length of the gonotrophic cycle is $95.87 / (\text{temp}10 - 6.4)$ (Mahmood and Crans 1997). The number of eggs laid per batch is from a normal

distribution with the mean equals to $93 + \text{ppt}10$, the standard deviation equals to 34, and the lower bound equal to 0 (Scott and Lorenz 1998, Buckner et al. 2012).

B4. Empirical relations between activity factor and rainfall

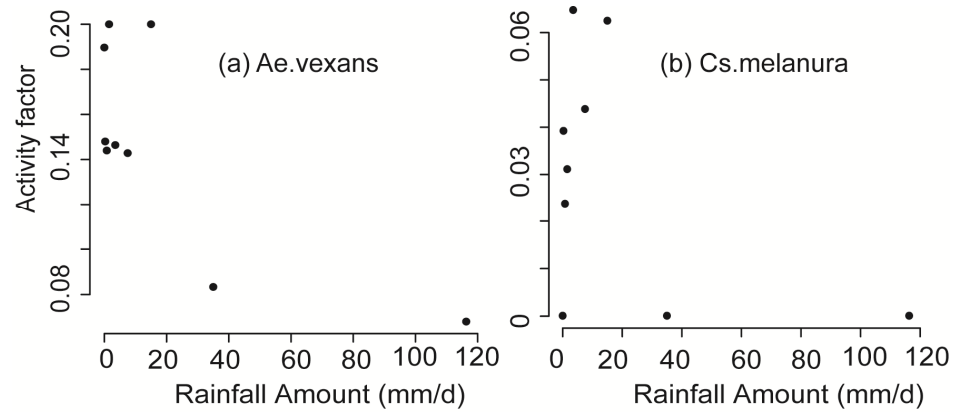


Figure 32: Relations between the activity factor and rainfall

B5 ACF and PACF of Gompertz models for *Ae.vexans* with different density dependence (results for the Ricker model, not shown, are analogous)

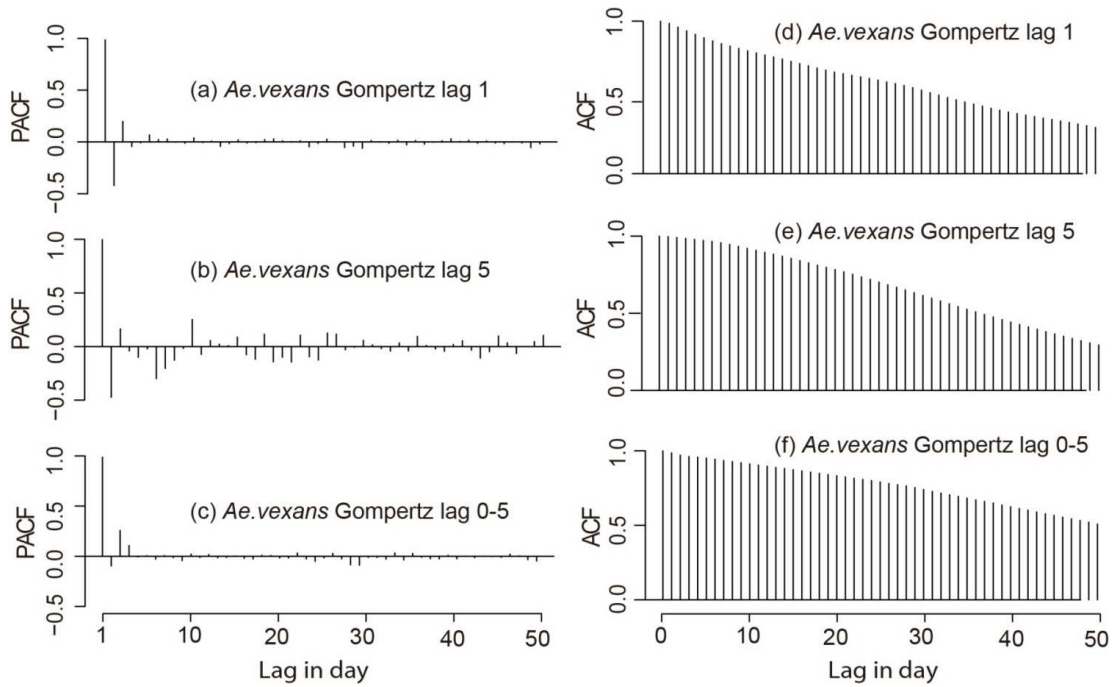


Figure 33: ACF and PACF of Gompertz models for *Ae.vexans* with different density dependence (results for the Ricker model, not shown, are analogous)

B6. ACF for observations and for models with different density dependence.

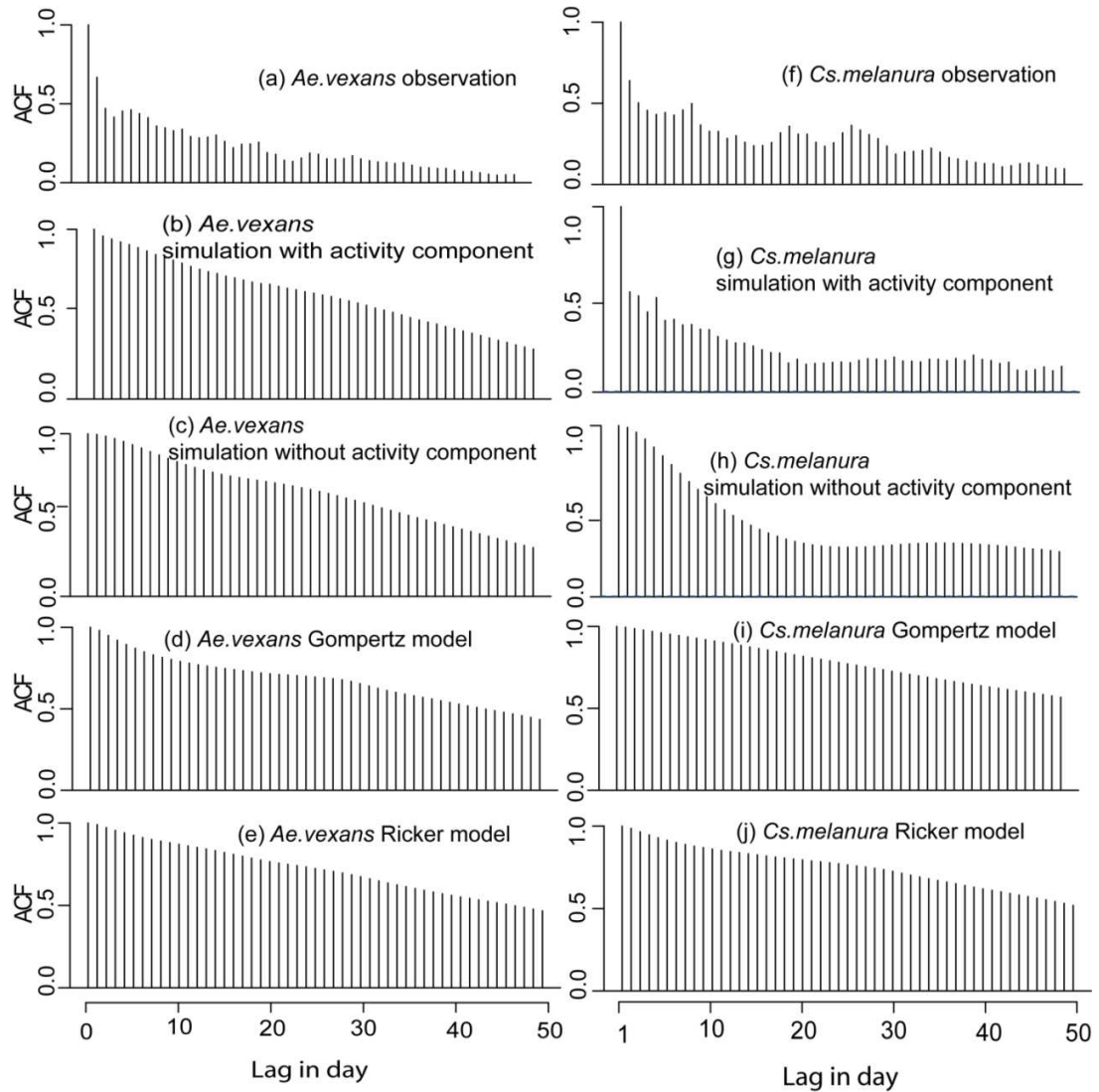


Figure 34: ACF of observed abundances for *Ae.vexans* and *Cs.melanura*, ((a) and (f)), for IBS model realizations including activity ((b) and (g)), IBS model realizations without activity ((c) and (h)); Gompertz model realizations with density dependence at lag=0 days ((d) and (i)), and Ricker model realizations with density dependence at lag=0 [57] and (j)).

B7. Estimated coefficients for density dependent models

Table 7: Estimated coefficients for density dependent models for mosquito abundance in the Brunswick County NC

<i>Cs.melanura</i>		<i>Ae.vexans</i>	
Gompertz lag0	Estimation	Gompertz lag0	Estimation
Intercept	0.145**	Intercept	0.294***
daily_logN	-0.166***	daily_logN	-0.165***
daily_temp	0.005	daily_temp	0.022**
daily_temp2	0.000	daily_temp2	0.000*
daily_ppt	0.001	daily_ppt	-0.001
daily_RH	-0.002**	daily_RH	-0.005***
Gompertz lag1	Estimate	Gompertz lag1	Estimate
Intercept	0.179**	Intercept	0.318***
daily_logN1	-0.061***	daily_logN1	-0.073***
daily_temp	-0.002	daily_temp	0.010
daily_temp2	0.000	daily_temp2	0.000
daily_ppt	0.001	daily_ppt	-0.001
daily_RH	-0.002**	daily_RH	-0.004***
Gompertz lag5	Estimate	Gompertz lag5	Estimate
Intercept	0.205***	Intercept	0.373***
daily_logN5	-0.007	daily_logN5	-0.005
daily_temp	-0.005	daily_temp	0.002
daily_temp2	0.000	daily_temp2	0.000
daily_ppt	0.001	daily_ppt	-0.001
daily_RH	-0.002**	daily_RH	-0.005***
Gompertz lag0 to lag5	Estimate	Gompertz lag0 to lag5	Estimate
Intercept	0.104*	Intercept	0.280***
daily_logN	-0.500***	daily_logN	-0.405
daily_logN1	0.051**	daily_logN1	0.033
daily_logN2	0.107***	daily_logN2	0.065**
daily_logN3	0.086***	daily_logN3	0.109***
daily_logN4	0.108***	daily_logN4	0.053**

daily_logN5	0.085***	daily_logN5	0.063***
daily_temp	0.008	daily_temp	0.021**
daily_temp2	0.000	daily_temp2	0.000*
daily_ppt	0.000	daily_ppt	-0.002*
daily_RH	-0.002**	daily_RH	-0.005***
Ricker lag0	Estimate	Ricker lag0	Estimate
Intercept	0.171**	Intercept	0.359***
daily_N	-0.006***	daily_N	-0.004***
daily_temp	-0.002	daily_temp	0.008
daily_temp2	0.000	daily_temp2	0.000
daily_ppt	0.001	daily_ppt	-0.001
daily_RH	-0.002**	daily_RH	-0.005***
Ricker lag1	Estimate	Ricker lag1	Estimate
Intercept	0.184**	Intercept	0.343***
daily_N1	-0.004***	daily_N1	-0.003***
daily_temp	-0.003	daily_temp	0.006
daily_temp2	0.000	daily_temp2	0.000
daily_ppt	0.001	daily_ppt	-0.001
daily_RH	-0.002**	daily_RH	-0.004***
Ricker lag5	Estimate	Ricker lag5	Estimate
Intercept	0.205***	Intercept	0.373***
daily_N5	0.000	daily_N5	0.000
daily_temp	-0.006	daily_temp	0.002
daily_temp2	0.000	daily_temp2	0.000
daily_ppt	0.001	daily_ppt	-0.001
daily_RH	-0.002**	daily_RH	-0.005***
Ricker lag0 to lag5	Estimate	Ricker lag0 to lag5	Estimate
Intercept	0.151**	Intercept	0.365***
daily_N	-0.008***	daily_N	-0.004***
daily_N1	-0.003**	daily_N1	-0.002**
daily_N2	0.002*	daily_N2	0.000
daily_N3	0.002.	daily_N3	0.003***
daily_N4	0.002	daily_N4	-0.001
daily_N5	0.001	daily_N5	0.002**

daily_temp	-0.003	daily_temp	0.004
daily_temp2	0.000	daily_temp2	0.000
daily_ppt	0.000	daily_ppt	-0.001
daily_RH	-0.002*	daily_RH	-0.005***

levels of significance are: * $p < 0.1$, ** $p < 0.05$, and *** $p < 0.01$

Appendix C

C1. Change of correlation between the predicted and observed values for prediction horizon

Table 8: Correlation between the predicted and observed per capital growth rate changes for prediction horizon

Weekly	1	2	3	4	5	6	7	8	9	10	11	12	13	14	15
Cs.melanura	0.25	0.17	0.14	0.15	0.16	0.00	0.09	0.09	0.04	0.10	0.00	0.02	-0.05	0.02	0.06
Ae.vexans	0.33	0.29	0.19	0.15	0.14	0.11	0.13	0.09	0.11	0.16	0.05	0.08	0.09	0.14	0.10
	16	17	18	19	20	21	22	23	24	25	26	27	28	29	30
	-0.02	0.07	0.10	0.08	0.13	0.15	0.13	0.06	0.06	0.12	0.11	0.09	0.13	0.06	0.05
	0.08	0.07	0.10	0.08	0.08	0.09	0.08	0.05	0.04	0.03	0.05	0.09	0.17	0.19	0.18
Biweekly	1	2	3	4	5	6	7	8	9	10	11	12	13	14	15
Cs.melanura	0.50	0.42	0.09	0.12	0.11	0.19	0.07	0.13	0.20	0.22	0.25	0.14	0.16	0.26	0.19
Ae.vexans	0.51	0.38	0.24	0.23	0.19	0.09	0.26	0.27	0.17	0.26	0.20	0.17	0.09	0.20	0.27
	16	17	18	19	20	21	22	23	24	25	26	27	28	29	30
	0.16	0.17	0.15	0.10	-0.04	0.02	0.00	0.12	0.15	0.06	-0.02	0.05	0.09	0.14	0.14
	0.30	0.25	0.22	0.20	0.10	0.23	0.20	0.15	0.03	0.15	0.21	0.21	0.23	0.19	0.14
Monthly	1	2	3	4	5	6	7	8	9	10	11	12	13	14	15
Cs.melanura	0.64	0.28	0.27	0.22	0.33	0.31	0.31	0.31	0.14	0.15	0.14	0.13	0.04	0.16	0.19
Ae.vexans	0.68	0.48	0.40	0.36	0.37	0.35	0.20	0.35	0.39	0.37	0.45	0.33	0.39	0.48	0.46
	16	17	18	19	20	21	22	23	24	25	26	27	28	29	30
	0.12	0.35	0.14	0.24	0.23	0.41	0.24	0.36	0.09	0.15	0.00	0.12	-0.15	0.15	0.18
	0.23	0.26	0.30	0.10	0.26	0.38	0.37	0.48	0.33	0.33	0.42	0.38	0.18	0.35	0.33

Table 9: Correlation between the predicted and observed abundance changes for prediction horizon

Weekly	1	2	3	4	5	6	7	8	9	10	11	12	13	14	15
Cs.melanura	0.75	0.58	0.55	0.47	0.42	0.33	0.32	0.31	0.27	0.34	0.39	0.41	0.34	0.26	0.13
Ae.vexans	0.77	0.59	0.43	0.34	0.27	0.16	0.15	0.19	0.23	0.21	0.16	0.13	0.09	0.08	0.06
	16	17	18	19	20	21	22	23	24	25	26	27	28	29	30
	0.08	0.04	0.04	0.04	0.05	0.04	0.04	0.05	0.02	-0.02	-0.03	-0.01	-0.01	0.03	0.03
	0.04	0.06	0.05	0.05	0.09	0.10	0.11	0.14	0.17	0.19	0.16	0.15	0.13	0.13	0.14
Biweekly	1	2	3	4	5	6	7	8	9	10	11	12	13	14	15
Cs.melanura	0.77	0.55	0.45	0.53	0.52	0.46	0.19	0.07	0.05	0.07	0.08	0.00	-0.08	-0.05	-0.03
Ae.vexans	0.67	0.46	0.33	0.23	0.25	0.15	0.15	0.18	0.10	0.09	0.25	0.21	0.19	0.17	0.11
	16	17	18	19	20	21	22	23	24	25	26	27	28	29	30
	-0.05	-0.09	-0.09	-0.10	-0.09	-0.06	-0.02	-0.04	-0.04	-0.05	-0.04	-0.01	-0.01	0.02	-0.04
	0.06	0.13	0.25	0.22	0.08	0.08	0.35	0.22	0.00	0.02	0.07	0.16	0.13	0.03	0.02
Monthly	1	2	3	4	5	6	7	8	9	10	11	12	13	14	15
Cs.melanura	0.71	0.48	0.45	0.27	0.15	0.02	-0.04	-0.06	-0.10	-0.10	-0.07	-0.11	-0.11	-0.10	-0.11
Ae.vexans	0.58	0.26	0.19	0.16	0.17	0.26	0.21	0.21	0.08	0.14	0.29	0.29	0.22	0.05	0.06
	16	17	18	19	20	21	22	23	24	25	26	27	28	29	30
	-0.09	-0.09	-0.09	-0.10	-0.08	-0.03	-0.01	0.00	-0.03	-0.03	-0.01	-0.10	-0.12	-0.13	-0.13
	0.26	0.21	0.10	0.12	-0.05	-0.10	0.08	0.02	0.16	0.10	0.19	0.20	0.13	0.04	0.06

C2. Correlation between the predicted and observed values for co-prediction

Table 10: Correlation for co-prediction at weekly scale. Index for species: 1, Ae.vexans; 2, Cs.melanura; 3, Cx.salinaris; 4, Cx.restuans; 5, Ps.columbiae; 6, Ps.ferox; 7, An.crucians; 8, Oc.atlanticus; 9, Oc.fulvus,pallens; 10, Cx.nigripalpus; 11, Cx.erraticus; 12, Cx.pipiens; 13, Ps.ciliata; 14, An.quadrimalculatus; 15, Ps.howardii; 16, Oc.canadensis

Species	1	2	3	4	5	6	7	8	9	10	11	12	13	14	15	16
1	0.23	-0.01	0.21	0.07	-0.09	0.02	0.03	0.04	0.07	0.06	0.03	0.08	0.06	-0.09	0.02	-0.04
2	0.01	0.20	0.08	-0.02	0.01	0.11	0.00	0.06	-0.05	0.05	0.06	0.06	-0.01	0.08	0.01	0.00
3	0.09	-0.08	0.26	-0.01	-0.05	0.08	0.09	0.02	0.02	0.10	-0.02	0.12	-0.06	-0.05	-0.03	0.06
4	0.06	0.01	0.06	0.23	-0.02	-0.05	0.21	0.03	-0.02	-0.08	-0.07	-0.05	-0.01	0.04	0.05	0.04
5	0.11	0.10	-0.03	0.08	0.07	0.09	-0.02	0.05	-0.06	0.17	-0.02	0.07	-0.08	-0.01	0.00	0.08
6	0.05	0.01	0.00	-0.01	0.11	0.25	0.03	0.00	-0.04	-0.08	0.04	-0.05	0.22	-0.04	-0.06	0.00
7	0.00	0.04	0.02	-0.09	-0.10	0.02	0.24	0.14	-0.01	0.09	-0.04	-0.13	0.11	-0.10	0.02	0.02
8	0.01	0.04	0.09	0.02	0.02	0.02	0.03	0.03	-0.05	-0.04	0.25	0.04	0.11	0.02	0.00	0.00
9	0.05	-0.10	0.00	0.02	0.34	0.19	0.01	0.03	0.16	0.00	-0.02	0.04	0.31	-0.09	0.00	0.00
10	-0.03	0.05	0.06	0.07	-0.04	0.01	0.00	0.08	0.00	0.35	0.11	0.04	0.07	-0.12	0.00	0.00
11	0.08	0.07	0.10	0.11	0.08	0.00	-0.12	0.00	0.04	0.15	0.22	0.05	0.02	0.01	0.03	0.00
12	0.10	-0.08	-0.03	0.10	-0.05	0.00	0.05	-0.02	-0.05	-0.02	0.01	0.18	0.08	-0.07	0.03	0.08
13	0.06	-0.01	-0.02	0.00	0.21	0.42	0.03	0.06	0.09	-0.07	-0.03	0.00	0.41	0.01	0.08	-0.03
14	-0.02	-0.08	0.00	0.03	0.08	0.01	-0.05	-0.03	0.13	0.10	-0.05	0.02	0.09	0.27	0.00	0.02
15	0.02	-0.03	-0.03	0.02	0.00	-0.08	-0.01	0.01	0.00	-0.01	0.01	0.00	0.03	0.00	0.19	0.01
16	-0.05	0.02	-0.10	0.02	0.00	-0.02	-0.04	0.00	0.00	0.00	0.10	0.12	-0.11	0.00	0.03	0.12

Table 11: Correlation for co-prediction at biweekly scale. Index for species: 1, Ae.vexans; 2, Cs.melanura; 3, Cx.salinarius; 4, Cx.restuans; 5, Ps.columbiae; 6, Ps.ferox; 7, An.crucians; 8, Oc.atlanticus; 9, Oc.fulvus.pallens; 10, Cx.nigripalpus; 11, Cx.erraticus; 12, Cx.piptens; 13, Ps.ciliata; 14, An.quadrinaculatus; 15, Ps.howardii; 16, Oc.canadensis

Species	1	2	3	4	5	6	7	8	9	10	11	12	13	14	15	16
1	0.35	0.08	0.16	0.01	0.19	0.02	-0.08	0.12	0.10	0.19	0.12	0.23	0.03	0.06	-0.02	-0.09
2	0.08	0.14	0.26	-0.06	0.07	0.07	0.15	0.14	-0.01	0.14	0.22	0.11	0.12	0.09	0.11	-0.01
3	0.09	0.01	0.30	0.19	0.11	-0.04	0.08	-0.03	-0.06	-0.04	0.00	0.14	-0.08	-0.04	-0.05	-0.02
4	0.05	0.07	-0.05	0.25	0.14	-0.07	-0.05	0.11	0.02	0.09	0.06	-0.07	-0.02	0.14	0.01	-0.01
5	-0.19	-0.12	0.01	0.19	0.21	0.09	-0.19	0.16	-0.04	0.12	0.22	0.05	-0.10	0.14	-0.26	-0.02
6	0.04	0.05	0.19	0.03	-0.05	0.18	0.04	0.12	-0.05	0.08	0.03	0.14	0.26	0.16	0.04	-0.05
7	0.09	0.09	0.22	-0.01	0.04	0.03	0.25	0.08	-0.06	-0.05	-0.01	0.20	0.20	0.01	0.05	0.01
8	0.06	-0.10	0.09	0.12	-0.10	-0.10	0.09	0.34	-0.01	0.01	0.00	0.09	-0.02	-0.06	-0.04	-0.01
9	0.00	0.00	-0.08	-0.01	0.21	0.33	0.06	-0.32	0.03	0.00	-0.04	0.01	-0.01	0.00	0.00	0.00
10	0.02	-0.21	0.14	0.11	0.02	0.02	-0.05	0.11	0.01	0.10	0.21	-0.03	0.04	0.04	-0.02	0.00
11	0.08	0.16	0.12	0.28	0.23	-0.16	0.00	0.04	-0.01	0.31	0.29	-0.07	-0.22	0.16	-0.01	-0.01
12	-0.02	0.02	0.11	0.22	0.12	0.20	-0.05	-0.01	0.09	0.15	0.04	0.22	0.08	0.21	-0.02	0.00
13	0.06	0.03	0.13	-0.01	-0.02	0.27	0.02	0.08	-0.02	0.10	0.01	0.06	0.32	0.04	-0.12	0.02
14	-0.04	-0.02	-0.02	0.23	0.10	-0.13	0.00	0.09	-0.08	-0.10	0.07	-0.02	0.02	0.23	0.08	0.03
15	0.03	0.01	0.11	0.04	0.03	-0.02	0.01	0.00	0.00	0.00	0.00	0.01	0.28	0.00	0.52	-0.11
16	-0.10	0.08	-0.21	-0.01	0.00	-0.04	0.08	0.00	0.00	0.00	0.00	0.00	-0.02	0.00	-0.05	0.05

Table 12: Correlation for co-prediction at monthly scale. Index for species: 1, *Ae.vexans*; 2, *Cs.melanura*; 3, *Cx.salinaris*; 4, *Cx.restuans*; 5, *Ps.columbiae*; 6, *Ps.ferox*; 7, *An.crucians*; 8, *Oc.atlanticus*; 9, *Oc.fulvus*; 10, *Cx.nigripalpus*; 11, *Cx.erraticus*; 12, *Cx.piptiens*; 13, *Ps.ciliata*; 14, *An.quadrimaculatus*; 15, *Ps.howardii*; 16, *Oc.canadensis*

Species	1	2	3	4	5	6	7	8	9	10	11	12	13	14	15	16
1	0.41	0.26	0.37	0.14	0.35	-0.07	0.07	0.06	0.04	0.15	0.24	0.38	0.03	0.21	0.10	0.05
2	0.21	0.32	0.17	0.14	0.19	-0.02	0.03	0.21	-0.03	0.22	0.30	0.33	-0.02	0.38	-0.16	-0.03
3	0.11	0.17	0.50	0.37	0.27	-0.12	-0.17	0.18	-0.04	0.12	0.20	0.27	-0.08	0.25	-0.01	-0.01
4	0.51	0.20	-0.06	0.41	0.17	0.02	0.24	0.04	-0.02	0.13	0.04	0.05	-0.02	0.05	0.14	0.27
5	0.24	0.28	-0.04	0.28	0.40	-0.07	0.22	0.47	-0.08	0.46	0.25	0.18	0.01	0.35	-0.05	-0.03
6	0.05	-0.03	0.03	0.01	0.05	0.11	0.03	0.11	-0.17	0.11	0.11	-0.04	0.10	0.00	0.11	-0.07
7	0.20	0.42	0.11	0.16	0.17	0.02	0.26	0.16	-0.07	0.14	0.24	0.15	0.04	0.16	0.06	0.00
8	0.06	0.25	0.11	0.27	-0.01	-0.07	0.11	0.29	0.02	0.19	0.05	-0.05	-0.06	0.36	-0.03	-0.01
9	-0.06	0.00	-0.02	-0.10	0.12	0.12	0.01	-0.03	-0.07	0.00	-0.04	-0.03	0.07	-0.08	0.00	-0.04
10	0.02	-0.14	0.01	-0.03	0.34	-0.09	-0.10	0.47	0.03	0.05	0.39	-0.04	-0.04	0.36	-0.06	-0.04
11	0.21	0.13	0.08	0.27	0.33	-0.05	0.21	0.32	0.00	0.43	0.43	0.00	-0.06	0.52	0.06	-0.05
12	-0.18	-0.07	0.18	0.21	0.09	-0.23	0.07	-0.09	0.02	-0.06	0.21	0.22	-0.06	0.17	0.03	-0.02
13	-0.12	-0.02	0.01	0.00	-0.18	0.04	0.01	0.18	-0.07	0.21	0.06	-0.09	0.03	0.03	0.16	-0.01
14	0.27	0.17	-0.14	0.38	0.38	-0.24	-0.08	0.21	-0.24	0.25	0.51	-0.03	0.16	0.25	0.21	0.03
15	-0.03	-0.10	-0.06	0.03	0.11	-0.13	-0.01	0.00	0.00	0.00	-0.07	0.01	0.32	0.00	0.63	0.16
16	0.03	0.03	-0.01	-0.02	-0.05	-0.01	-0.07	0.00	0.00	0.06	0.03	0.10	-0.05	-0.03	-0.03	0.23

C3. SP results of 7-day-ahead prediction using the once-per-week samples

Table 13: SP results of 7-day-ahead prediction using the once-per-week samples for *Cs.melanura*

	Correlation for N	Correlation for r	RMSE for N	RMSE for r	Variables
Day1	0.40	0.41	0.71	39.36	logN lag 0-3 and rainfall lag 0
Day2	0.31	0.38	0.73	48.64	logN lag 0-3 and rainfall lag 0-3
Day3	0.32	0.61	0.72	44.69	logN lag 0-7 and rainfall lag 0
Day4	0.42	0.73	0.75	28.02	logN lag 0-2 and rainfall lag 0-1
Day5	0.17	0.45	0.77	54.54	logN lag 0-2 and rainfall lag 0-3
Day6	0.32	0.71	0.70	30.03	logN lag 0-3 and rainfall lag 0-1
Day7	0.40	0.42	0.78	45.15	logN lag 0-3 and rainfall lag 0

Table 14: SP results of 7-day-ahead prediction using the once-per-week samples for *Ae.vexans*

	Correlation for N	Correlation for r	RMSE for N	RMSE for r	Variables
Day1	0.41	0.32	1.02	44.20	logN lag 0-3 and rainfall lag 0
Day2	0.42	0.51	1.00	27.38	logN lag 0-4 and rainfall lag 2
Day3	0.41	0.40	1.10	38.23	logN lag 0-7 and rainfall lag 3
Day4	0.44	0.42	1.01	30.35	logN lag 0 and rainfall lag 0-1
Day5	0.36	0.58	0.97	24.05	logN lag 0-1 and rainfall lag 0-1
Day6	0.31	0.43	1.01	32.56	logN lag 0-7 and rainfall lag 0
Day7	0.47	0.47	1.01	36.22	logN lag 0-3 and rainfall lag 0-3

C4. SP results of 7-day-ahead prediction using the daily samples

Table 15: SP results of 7-day-ahead prediction using the daily samples for *Cs.melanura*

	Correlation for N	Correlation for r	RMSE for N	RMSE for r	Variables
Day1	0.39	0.41	0.73	39.33	logN lag 0 and rainfall lag 0
Day2	0.39	0.37	0.71	49.85	logN lag 0-6 and rainfall lag 0-1
Day3	0.44	0.74	0.68	38.87	logN lag 0-4 and rainfall lag 0-3
Day4	0.48	0.70	0.72	27.84	logN lag 0-1 and rainfall lag 0
Day5	0.42	0.47	0.70	55.12	logN lag 0-5 and rainfall lag 0-2
Day7	0.45	0.45	0.76	43.94	logN lag 0-2 and rainfall lag 0

Table 16: SP results of 7-day-ahead prediction using the daily samples for *Ae.vexans*

	Correlation for N	Correlation for r	RMSE for N	RMSE for r	Variables
Day1	0.48	0.40	0.97	42.89	logN lag 0-2 and rainfall lag 0-2
Day2	0.50	0.39	0.97	29.44	logN lag 0 and rainfall lag 0-1
Day3	0.52	0.40	1.03	38.28	logN lag 0-2 and rainfall lag 0-2
Day4	0.51	0.38	0.97	32.01	logN lag 0-1 and rainfall lag 0-2
Day5	0.45	0.59	0.92	23.82	logN lag 0-5 and rainfall lag 0-2
Day6	0.43	0.50	0.97	31.16	logN lag 0-1 and rainfall lag 0-3
Day7	0.50	0.54	0.99	35.05	logN lag 0-1 and rainfall lag 0-2

References

- Allen, R. G., L. S. Pereira, D. Raes, and M. Smith. 1998. Crop evapotranspiration - Guidelines for computing crop water requirements - FAO Irrigation and drainage paper 56. M-56, ISBN 92-5-104219-5 Food and Agriculture Organization of the United Nations. <http://www.fao.org/docrep/X0490E/X0490E00.htm>.
- Alonso, D., M. J. Bouma, and M. Pascual. 2011. Epidemic malaria and warmer temperatures in recent decades in an East African highland. *Proceedings of the Royal Society B-Biological Sciences* **278**:1661-1669.
- Azil, A. H., D. Bruce, and C. R. Williams. 2014. Determining the spatial autocorrelation of dengue vector populations: influences of mosquito sampling method, covariables, and vector control. *Journal of Vector Ecology* **39**:153-163.
- Becker, N., D. Petric, M. Zgnomba, C. Boase, C. Dahl, J. Lane, and A. Kaiser. 2003. Mosquitoes and their control. Kluwer Academic / Plenum Publisher, New York.
- Berryman, A. and P. Turchin. 2001. Identifying the density-dependent structure underlying ecological time series. *Oikos* **92**:265-270.
- Bidlingmayer, W. L. 1971. Mosquito Flight Paths in Relation to the Environment. 1. Illumination Levels, Orientation, and Resting Areas. *Annals of the Entomological Society of America* **64**:1121-1131.
- Bombliès, A., J. B. Duchemin, and E. A. B. Eltahir. 2008. Hydrology of malaria: Model development and application to a Sahelian village. *Water Resources Research* **44**.
- Box, G. E. P., G. M. Jenkins, and G. C. Reinsel. 2008. Time series analysis : forecasting and control. 4th edition. John Wiley, Hoboken, N.J.
- Brunswick County Government. 2011. Mosquito Control. <http://www.brunsko.net/Departments/OperationServices/MosquitoControl.aspx>.
- Buckner, E., A. Showman, and C. R. Connelly. 2012. Featured Creatures. http://entnemdept.ifas.ufl.edu/creatures/aquatic/Culiseta_melanura.htm.
- Cailly, P., A. Tran, T. Balenghien, G. L'Ambert, C. Toty, and P. Ezanno. 2012. A climate-driven abundance model to assess mosquito control strategies. *Ecological Modelling* **227**:7-17.

- Camporese, M., C. Paniconi, M. Putti, and S. Orlandini. 2010. Surface-subsurface flow modeling with path-based runoff routing, boundary condition-based coupling, and assimilation of multisource observation data. *Water Resources Research* **46**.
- Carpenter, S. R. and W. A. Brock. 2010. Early warnings of regime shifts in spatial dynamics using the discrete Fourier transform. *Ecosphere* **1**.
- Chadee, D. D., J. M. Sutherland, and J. R. L. Gilles. 2014. Diel sugar feeding and reproductive behaviours of *Aedes aegypti* mosquitoes in Trinidad: With implications for mass release of sterile mosquitoes. *Acta Tropica* **132**, **Supplement**:S86-S90.
- Chaves, L. F., Y. Higa, S. H. Lee, J. Y. Jeong, S. T. Heo, M. Kim, N. Minakawa, and K. H. Lee. 2013. Environmental Forcing Shapes Regional House Mosquito Synchrony in a Warming Temperate Island. *Environmental Entomology* **42**:605-613.
- Chaves, L. F. and U. D. Kitron. 2011. Weather variability impacts on oviposition dynamics of the southern house mosquito at intermediate time scales. *Bulletin of Entomological Research* **101**:633-641.
- Chaves, L. F., A. C. Morrison, U. D. Kitron, and T. W. Scott. 2012. Nonlinear impacts of climatic variability on the density-dependent regulation of an insect vector of disease. *Global Change Biology* **18**:457-468.
- Chuang, T. W., G. M. Henebry, J. S. Kimball, D. L. VanRoekel-Patton, M. B. Hildreth, and M. C. Wimberly. 2012. Satellite microwave remote sensing for environmental modeling of mosquito population dynamics. *Remote Sensing of Environment* **125**:147-156.
- Church, S. C. and T. N. Sherratt. 1996. The selective advantages of cannibalism in a Neotropical mosquito. *Behavioral Ecology and Sociobiology* **39**:117-123.
- Clark, J. S. 2007. *Models for ecological data : an introduction*. Princeton University Press, Princeton, N.J.
- Clark, J. S. and O. N. Bjornstad. 2004. Population time series: Process variability, observation errors, missing values, lags, and hidden states. *Ecology* **85**:3140-3150.
- Clements, A. N. 1992. *The biology of mosquitoes*. 1st edition. Chapman & Hall, London ; New York.

- Crans, W. J. 2013a. *Aedes vexans* (Meigen). <http://www.rci.rutgers.edu/~insects/sp13.htm>.
- Crans, W. J. 2013b. *Culex pipiens* Linnaeus <http://www-rci.rutgers.edu/~insects/pip2.htm>.
- Crans, W. J. 2013c. *Culiseta Melanura* (Coquillett). <http://www.rci.rutgers.edu/~insects/sp25.htm>.
- Day, J. F. and J. Shaman. 2008. Using hydrologic conditions to forecast the risk of focal and epidemic arboviral transmission in peninsular Florida. *Journal of Medical Entomology* **45**:458-465.
- Day, J. F. and J. Shaman. 2009. Severe Winter Freezes Enhance St. Louis Encephalitis Virus Amplification and Epidemic Transmission in Peninsular Florida. *Journal of Medical Entomology* **46**:1498-1506.
- de Meillon, B., A. Sebastian, and Z. H. Khan. 1967. Time of arrival of gravid *Culex pipiens fatigans* at an oviposition site, the oviposition cycle and the relationship between time of feeding and time of oviposition. *Bull World Health Organ* **36**:39-46.
- DeGroot, J. P. and R. Sugumaran. 2012. National and Regional Associations Between Human West Nile Virus Incidence and Demographic, Landscape, and Land Use Conditions in the Conterminous United States. *Vector-Borne and Zoonotic Diseases* **12**.
- Dennis, B., J. M. Ponciano, S. R. Lele, M. L. Taper, and D. F. Staples. 2006. Estimating density dependence, process noise, and observation error. *Ecological Monographs* **76**:323-341.
- Deyle, E. R., M. Fogarty, C. H. Hsieh, L. Kaufman, A. D. MacCall, S. B. Munch, C. T. Perretti, H. Ye, and G. Sugihara. 2013. Predicting climate effects on Pacific sardine. *Proceedings of the National Academy of Sciences of the United States of America* **110**:6430-6435.
- Deyle, E. R. and G. Sugihara. 2011. Generalized Theorems for Nonlinear State Space Reconstruction. *Plos One* **6**.

- Dohm, D. J., M. L. O'Guinn, and M. J. Turell. 2002. Effect of environmental temperature on the ability of *Culex pipiens* (Diptera : Culicidae) to transmit West Nile virus. *Journal of Medical Entomology* **39**:221-225.
- Enserink, M. 2008. A mosquito goes global. *Science* **320**:864-866.
- Ermert, V., A. H. Fink, A. E. Jones, and A. P. Morse. 2011a. Development of a new version of the Liverpool Malaria Model. I. Refining the parameter settings and mathematical formulation of basic processes based on a literature review. *Malaria Journal* **10**.
- Ermert, V., A. H. Fink, A. E. Jones, and A. P. Morse. 2011b. Development of a new version of the Liverpool Malaria Model. II. Calibration and validation for West Africa. *Malaria Journal* **10**.
- Fowler, C. W. 1981. Density Dependence as Related to Life-History Strategy. *Ecology* **62**:602-610.
- Gao, H. W., L. P. Wang, S. Liang, Y. X. Liu, S. L. Tong, J. J. Wang, Y. P. Li, X. F. Wang, H. Yang, J. Q. Ma, L. Q. Fang, and W. C. Cao. 2012. Change in Rainfall Drives Malaria Re-Emergence in Anhui Province, China. *Plos One* **7**.
- Gelman, A. and J. Hill. 2007. Data analysis using regression and multilevel/hierarchical models. Cambridge University Press, Cambridge ; New York.
- Gu, W. D., J. L. Regens, J. C. Beier, and R. J. Novak. 2006. Source reduction of mosquito larval habitats has unexpected consequences on malaria transmission. *Proceedings of the National Academy of Sciences of the United States of America* **103**:17560-17563.
- Hamer, G. L., U. D. Kitron, J. D. Brawn, S. R. Loss, M. O. Ruiz, T. L. Goldberg, and E. D. Walker. 2008. *Culex pipiens* (Diptera : Culicidae): A bridge vector of West Nile virus to humans. *Journal of Medical Entomology* **45**:125-128.
- Hart, E. M. and N. J. Gotelli. 2011. The effects of climate change on density-dependent population dynamics of aquatic invertebrates. *Oikos* **120**:1227-1234.
- Hayes, E. B., N. Komar, R. S. Nasci, S. P. Montgomery, D. R. O'Leary, and G. L. Campbell. 2005. Epidemiology and transmission dynamics of West Nile Virus disease. *Emerging Infectious Diseases* **11**:1167-1173.

- Heptonstall (England : Parish) and E. Horsfall. 1925. The parish registers of Heptonstall, in the County of York. Priv. print. for the Yorkshire Parish Register Society, Wakefield, Eng.
- Horsfall, W. R. 1973. Bionomics and embryology of the inland floodwater mosquito *Aedes vexans*. University of Illinois Press, Urbana,.
- Hsieh, C. H., S. M. Glaser, A. J. Lucas, and G. Sugihara. 2005. Distinguishing random environmental fluctuations from ecological catastrophes for the North Pacific Ocean. *Nature* **435**:336-340.
- IPCC. 2007. Climate Change 2007: Synthesis Report Intergovernmental Panel on Climate Change, Cambridge, UK.
- Ives, A. R. and J. Zhu. 2006. Statistics for correlated data: Phylogenies, space, and time. *Ecological Applications* **16**:20-32.
- Jian, Y., S. Silvestri, E. Belluco, A. Saltarin, G. Chillemi, and M. Marani. 2014a. Environmental forcing and density-dependent controls of *Culex pipiens* abundance in a temperate climate (Northeastern Italy). *Ecological Modelling* **272**:301-310.
- Jian, Y., S. Silvestri, J. Brown, R. Hickman, and M. Marani. 2014b. The temporal spectrum of adult mosquito population fluctuations: conceptual and modeling implications *Plos One*.
- Johnston, E., P. Weinstein, D. Slaney, A. S. Flies, S. Fricker, and C. Williams. 2014. Mosquito communities with trap height and urban-rural gradient in Adelaide, South Australia: implications for disease vector surveillance. *Journal of Vector Ecology* **39**:48-55.
- Jones, K. E., N. G. Patel, M. A. Levy, A. Storeygard, D. Balk, J. L. Gittleman, and P. Daszak. 2008. Global trends in emerging infectious diseases. *Nature* **451**:990-U994.
- Juliano, S. A. 2007. Population dynamics. *J Am Mosq Control Assoc* **23**:265-275.
- Kantz, H. and T. Schreiber. 2004. Nonlinear time series analysis. 2nd edition. Cambridge University Press, Cambridge, UK ; New York.

- Kilpatrick, A. M. 2011. Globalization, Land Use, and the Invasion of West Nile Virus. *Science* **334**:323-327.
- Koenraadt, C. J. M. and W. Takken. 2003. Cannibalism and predation among larvae of the *Anopheles gambiae* complex. *Medical and Veterinary Entomology* **17**:61-66.
- Lacaux, J. P., Y. M. Tourre, C. Vignolles, J. A. Ndione, and M. Lafaye. 2007. Classification of ponds from high-spatial resolution remote sensing: Application to Rift Valley Fever epidemics in Senegal. *Remote Sensing of Environment* **106**:66-74.
- LaDeau, S. L., G. E. Glass, N. T. Hobbs, A. Latimer, and R. S. Ostfeld. 2011. Data-model fusion to better understand emerging pathogens and improve infectious disease forecasting. *Ecological Applications* **21**:1443-1460.
- LaDeau, S. L., A. M. Kilpatrick, and P. P. Marra. 2007. West Nile virus emergence and large-scale declines of North American bird populations. *Nature* **447**:710-U713.
- Lafferty, K. D. 2009. The ecology of climate change and infectious diseases. *Ecology* **90**:888-900.
- Linard, C., N. Ponçon, D. Fontenille, and E. F. Lambin. 2009. A multi-agent simulation to assess the risk of malaria re-emergence in southern France. *Ecological Modelling* **220**:160-174.
- Lindquist, A. W., T. Ikeshoji, B. Grab, B. de Meillon, and Z. H. Khan. 1967. Dispersion studies of *Culex pipiens fatigans* tagged with ³²P in the Kemmendine area of Rangoon, Burma. *Bull World Health Organ* **36**:21-37.
- Liu, H., M. J. Fogarty, S. M. Glaser, I. Altman, C. H. Hsieh, L. Kaufman, A. A. Rosenberg, and G. Sugihara. 2012. Nonlinear dynamic features and co-predictability of the Georges Bank fish community. *Marine Ecology Progress Series* **464**:195-U228.
- Liu, H., M. J. Fogarty, J. A. Hare, C. H. Hsieh, S. M. Glaser, H. Ye, E. Deyle, and G. Sugihara. 2014. Modeling dynamic interactions and coherence between marine zooplankton and fishes linked to environmental variability. *Journal of Marine Systems* **131**:120-129.
- Loetti, M. V., N. E. Burrioni, N. Schweigmann, and A. de Garin. 2007. Effect of different thermal conditions on the pre-imaginal biology of *Culex apicinus* (Philippi, 1865) (Diptera : Culicidae). *Journal of Vector Ecology* **32**:106-111.

- Loetti, V., N. Schweigmann, and N. Burroni. 2011. Development Rates, Larval Survivorship and Wing Length of *Culex pipiens* (Diptera: Culicidae) at constant temperatures. *Journal of Natural history* **45**:2207-2217.
- Lunn, D. J., A. Thomas, N. Best, and D. Spiegelhalter. 2000. WinBUGS - A Bayesian modelling framework: Concepts, structure, and extensibility. *Statistics and Computing* **10**:325-337.
- MacKenzie, D. I. 2006. *Occupancy estimation and modeling : inferring patterns and dynamics of species occurrence*. Elsevier/Academic Press, Burlington, MA.
- MacKenzie, D. I., J. D. Nichols, G. B. Lachman, S. Droege, J. A. Royle, and C. A. Langtimm. 2002. Estimating site occupancy rates when detection probabilities are less than one. *Ecology* **83**:2248-2255.
- MacKenzie, D. I., J. D. Nichols, K. H. Pollock, J. A. Royle, L. L. Bailey, and J. E. Hines. 2005. *Occupancy Estimation and Modeling Inferring Patterns and Dynamics of Species Occurrence*. Academic Press Imprint
Elsevier Science & Technology Books, San Diego.
- Madder, D. J., G. A. Surgeoner, and B. V. Helson. 1983. Number of Generations, Egg-Production, and Developmental Time of *Culex-Pipiens* and *Culex-Restuans* (Diptera, Culicidae) in Southern Ontario. *Journal of Medical Entomology* **20**:275-287.
- Mahmood, F. and W. J. Crans. 1997. A thermal heat summation model to predict the duration of the gonotrophic cycle of *Culiseta melanura* in nature. *Journal of the American Mosquito Control Association* **13**:92-94.
- Mahmood, F. and W. J. Crans. 1998a. Effect of temperature on the development of *Culiseta melanura* (Diptera : Culicidae) and its impact on the amplification of eastern equine encephalomyelitis virus in birds. *Journal of Medical Entomology* **35**:1007-1012.
- Mahmood, F. and W. J. Crans. 1998b. Ovarian development and parity determination in *Culiseta melanura* (Diptera : Culicidae). *Journal of Medical Entomology* **35**:980-988.

- Maloney, J. M. and R. C. Wallis. 1976. Response of Colonized *Culiseta-Melanura* to Photoperiod and Temperature. *Mosquito News* **36**:190-196.
- McCarthy, M. A., J. L. Moore, W. K. Morris, K. M. Parris, G. E. Garrard, P. A. Vesk, L. Rumpff, K. M. Giljohann, J. S. Camac, S. S. Bau, T. Friend, B. Harrison, and B. Yue. 2013. The influence of abundance on detectability. *Oikos* **122**:717-726.
- Midekisa, A., G. Senay, G. M. Henebry, P. Semuniguse, and M. C. Wimberly. 2012. Remote sensing-based time series models for malaria early warning in the highlands of Ethiopia. *Malaria Journal* **11**.
- Montosi, E., S. Manzoni, A. Porporato, and A. Montanari. 2012. An ecohydrological model of malaria outbreaks. *Hydrology and Earth System Sciences* **16**:2759-2769.
- Munga, S., N. Minakawa, G. F. Zhou, E. Mushinzimana, O. O. J. Barrack, A. K. Githeko, and G. Y. Yan. 2006. Association between land cover and habitat productivity of malaria vectors in western Kenyan highlands. *American Journal of Tropical Medicine and Hygiene* **74**:69-75.
- Munkres, J. R. 1984. *Elements of algebraic topology*. Addison-Wesley, Menlo Park, Calif.
- Nadeem, K. and S. R. Lele. 2012. Likelihood based population viability analysis in the presence of observation error. *Oikos* **121**:1656-1664.
- Nayar, J. K. and E. Van Handel. 1971. The fuel for sustained mosquito flight. *Journal of Insect Physiology* **17**:471-481.
- Oda, T., Y. Eshita, K. Uchida, M. Mine, K. Kurokawa, Y. Ogawa, K. Kato, and H. Tahara. 2002. Reproductive activity and survival of *Culex pipiens pallens* and *Culex quinquefasciatus* (Diptera: Culicidae) in Japan at high temperature. *Journal of Medical Entomology* **39**:185-190.
- Overgaard, H. J., B. Ekbom, W. Suwonkerd, and M. Takagi. 2003. Effect of landscape structure on anopheline mosquito density and diversity in northern Thailand: Implications for malaria transmission and control. *Landscape Ecology* **18**:605-619.
- Paniconi, C. and M. Putti. 1994. A Comparison of Picard and Newton Iteration in the Numerical-Solution of Multidimensional Variably Saturated Flow Problems. *Water Resources Research* **30**:3357-3374.

- Pascual, M., J. A. Ahumada, L. F. Chaves, X. Rodo, and M. Bouma. 2006. Malaria resurgence in the East African highlands: Temperature trends revisited. *Proceedings of the National Academy of Sciences of the United States of America* **103**:5829-5834.
- Patz, J. A., K. Strzepek, S. Lele, M. Hedden, S. Greene, B. Noden, S. I. Hay, L. Kalkstein, and J. C. Beier. 1998. Predicting key malaria transmission factors, biting and entomological inoculation rates, using modelled soil moisture in Kenya. *Tropical Medicine & International Health* **3**:818-827.
- Pebesma, E. 2012. Spatial and spatio-temporal geostatistical modelling, prediction and simulation.
- Pebesma, E. J. 2004. Multivariable geostatistics in S: the gstat package. *Computers & Geosciences* **30**:683-691.
- Perretti, C. T., S. B. Munch, and G. Sugihara. 2013a. Model-free forecasting outperforms the correct mechanistic model for simulated and experimental data. *Proceedings of the National Academy of Sciences of the United States of America* **110**:5253-5257.
- Perretti, C. T., G. Sugihara, and S. B. Munch. 2013b. Nonparametric forecasting outperforms parametric methods for a simulated multispecies system. *Ecology* **94**:794-800.
- Petersen, L. R., P. J. Carson, B. J. Biggerstaff, B. Custer, S. M. Borchardt, and M. P. Busch. 2013. Estimated cumulative incidence of West Nile virus infection in US adults, 1999-2010. *Epidemiology and Infection* **141**:591-595.
- Polansky, L., G. Wittemyer, P. C. Cross, C. J. Tambling, and W. M. Getz. 2010. From moonlight to movement and synchronized randomness: Fourier and wavelet analyses of animal location time series data. *Ecology* **91**:1506-1518.
- Press, W. H. 2007. *Numerical recipes : the art of scientific computing*. 3rd edition. Cambridge University Press, Cambridge, UK ; New York.
- R Core Team. 2012. *R: A language and environment for statistical computing*. R Foundation for Statistical Computing, Vienna, Austria.

- Rahman, A., F. Kogan, L. Roytman, M. Goldberg, and W. Guo. 2011. Modelling and prediction of malaria vector distribution in Bangladesh from remote-sensing data. *International Journal of Remote Sensing* **32**:1233-1251.
- Randolph, S. E. and D. J. Rogers. 2010. The arrival, establishment and spread of exotic diseases: patterns and predictions. *Nature Reviews Microbiology* **8**:361-371.
- Reisen, W. K., K. Boyce, R. C. Cummings, O. Delgado, A. Gutierrez, R. P. Meyer, and T. W. Scott. 1999. Comparative effectiveness of three adult mosquito sampling methods in habitats representative of four different biomes of California. *Journal of the American Mosquito Control Association* **15**:24-31.
- Reisen, W. K. and H. D. Lothrop. 1999. Effects of sampling design on the estimation of adult mosquito abundance. *Journal of the American Mosquito Control Association* **15**:105-114.
- Reisen, W. K., R. P. Meyer, R. F. Cummings, and O. Delgado. 2000. Effects of trap design and CO₂ presentation on the measurement of adult mosquito abundance using centers for disease control-style miniature light traps. *Journal of the American Mosquito Control Association* **16**:13-18.
- Reisen, W. K. and A. R. Pfuntner. 1987. Effectiveness of Five Methods for Sampling Adult Culex Mosquitos in Rural and Urban Habitats in San-Bernardino County, California. *Journal of the American Mosquito Control Association* **3**:601-606.
- Ricker, W. E. 1954. Stock and Recruitment. *Journal of the Fisheries Research Board of Canada* **11**:559-623.
- Rogers, D. J., S. E. Randolph, R. W. Snow, and S. I. Hay. 2002. Satellite imagery in the study and forecast of malaria. *Nature* **415**:710-715.
- Royle, J. A. and R. M. Dorazio. 2008. Hierarchical modeling and inference in ecology : the analysis of data from populations, metapopulations and communities. 1st edition. Academic, Amsterdam ; Boston.
- Russell, T. L., D. W. Lwetoijera, B. G. J. Knols, W. Takken, G. F. Killeen, and H. M. Ferguson. 2011. Linking individual phenotype to density-dependent population growth: the influence of body size on the population dynamics of malaria vectors. *Proceedings of the Royal Society B-Biological Sciences* **278**:3142-3151.

- Sanford, M. R. and J. K. Tomberlin. 2011. Conditioning Individual Mosquitoes to an Odor: Sex, Source, and Time. *Plos One* **6**.
- Schaffner, F. 2009. Development of *aedes albopictus* risk map. European Center for Disease Prevention and Control, Stockholm.
- Scott, T. W. and L. H. Lorenz. 1998. Reduction of *Culiseta melanura* fitness by eastern equine encephalomyelitis virus. *American Journal of Tropical Medicine and Hygiene* **59**:341-346.
- Shaman, J. and J. F. Day. 2005. Achieving operational hydrologic monitoring of mosquitoborne disease. *Emerging Infectious Diseases* **11**:1343-1350.
- Shaman, J. and J. F. Day. 2007. Reproductive Phase Locking of Mosquito Populations in Response to Rainfall Frequency. *Plos One* **2**.
- Shaman, J., J. F. Day, and M. Stieglitz. 2004. The spatial-temporal distribution of drought, wetting, and human cases of St. Louis encephalitis in southcentral Florida. *American Journal of Tropical Medicine and Hygiene* **71**:251-261.
- Shaman, J., J. F. Day, and M. Stieglitz. 2005. Drought-induced amplification and epidemic transmission of West Nile Virus in southern Florida. *Journal of Medical Entomology* **42**:134-141.
- Shaman, J., K. Harding, and S. R. Campbell. 2011. Meteorological and Hydrological Influences on the Spatial and Temporal Prevalence of West Nile Virus in *Culex* Mosquitoes, Suffolk County, New York. *Journal of Medical Entomology* **48**:867-875.
- Shaman, J., M. Spiegelman, M. Cane, and M. Stieglitz. 2006. A hydrologically driven model of swamp water mosquito population dynamics. *Ecological Modelling* **194**:395-404.
- Shaman, J., M. Stieglitz, C. Stark, S. Le Blancq, and M. Cane. 2002. Using a dynamic hydrology model to predict mosquito abundances in flood and swamp water. *Emerging Infectious Diseases* **8**:6-13.
- Shumway, R. H. and D. S. Stoffer. 2006. Time series analysis and its applications : with R examples. 2nd [updated] edition. Springer, New York.

- Shumway, R. H. and D. S. Stoffer. 2011. Time series analysis and its applications with R examples. Page 1 online resource. Springer texts in statistics. Springer, New York.
- Sibly, R. M., D. Barker, M. C. Denham, J. Hone, and M. Pagel. 2005. On the regulation of populations of mammals, birds, fish, and insects. *Science* **309**:607-610.
- Snow, K. and C. Ramsdale. 1999. Distribution chart for European mosquitoes. *European Mosquito Bulletin*:14 - 31.
- Spielman, A. and M. D'Antonio. 2001. Mosquito : a natural history of our most persistent and deadly foe. 1st edition. Hyperion, New York.
- Spitzen, J., C. W. Spoor, F. Grieco, C. ter Braak, J. Beeuwkes, S. P. van Brugge, S. Kranenbarg, L. P. J. J. Noldus, J. L. van Leeuwen, and W. Takken. 2013. A 3D Analysis of Flight Behavior of *Anopheles gambiae* sensu stricto Malaria Mosquitoes in Response to Human Odor and Heat. *Plos One* **8**.
- Stenseth, N. C., A. Mysterud, G. Ottersen, J. W. Hurrell, K. S. Chan, and M. Lima. 2002. Ecological effects of climate fluctuations. *Science* **297**:1292-1296.
- Sugihara, G., B. Grenfell, and R. M. May. 1990. Distinguishing Error from Chaos in Ecological Time-Series. *Philosophical Transactions of the Royal Society of London Series B-Biological Sciences* **330**:235-251.
- Sugihara, G., R. May, H. Ye, C. H. Hsieh, E. Deyle, M. Fogarty, and S. Munch. 2012. Detecting Causality in Complex Ecosystems. *Science* **338**:496-500.
- Sugihara, G. and R. M. May. 1990. Nonlinear Forecasting as a Way of Distinguishing Chaos from Measurement Error in Time-Series. *Nature* **344**:734-741.
- Trawinski, P. R. and D. S. Mackay. 2008. Meteorologically conditioned time-series predictions of West Nile virus vector mosquitoes. *Vector-Borne and Zoonotic Diseases* **8**:505-521.
- Trpis, M. and Shemanch.Ja. 1970. Effect of Constant Temperature on Larval Development of *Aedes-Vexans* (Dipter-Culicidae). *Canadian Entomologist* **102**:1048-&.

- Turchin, P. 1990. Rarity of Density Dependence or Population Regulation with Lags. *Nature* **344**:660-663.
- Turchin, P. 2001. Does population ecology have general laws? *Oikos* **94**:17-26.
- Turchin, P. 2003. *Complex population dynamics : a theoretical/empirical synthesis*. Princeton University Press, Princeton, N.J.
- Turchin, P. and A. D. Taylor. 1992. Complex Dynamics in Ecological Time-Series. *Ecology* **73**:289-305.
- Tzeng, W. N., Y. H. Tseng, Y. S. Han, C. C. Hsu, C. W. Chang, E. Di Lorenzo, and C. H. Hsieh. 2012. Evaluation of Multi-Scale Climate Effects on Annual Recruitment Levels of the Japanese Eel, *Anguilla japonica*, to Taiwan. *Plos One* **7**.
- U.S. Centers for Disease Control and Prevention. 2007. Mosquito-Borne Diseases. http://www.cdc.gov/ncidod/diseases/list_mosquitoborne.htm.
- U.S. Centers for Disease Control and Prevention. 2014a. Dengue.
- U.S. Centers for Disease Control and Prevention. 2014b. Impact of Malaria. http://www.cdc.gov/malaria/malaria_worldwide/impact.html.
- U.S. Centers for Disease Control and Prevention. 2014c. West Nile Virus. <http://www.cdc.gov/westnile/index.html>.
- Vinogradova, E. B. 2000. *Culex pipiens pipiens* mosquitoes : taxonomy, distribution, ecology, physiology, genetic, applied importance and control. Pensoft, Sofia.
- Ward, E. J., E. E. Holmes, J. T. Thorson, and B. Collen. 2014. Complexity is costly: a meta-analysis of parametric and non-parametric methods for short-term population forecasting. *Oikos* **123**:652-661.
- Weill, S., M. Altissimo, G. Cassiani, R. Deiana, M. Marani, and M. Putti. 2013. Saturated area dynamics and streamflow generation from coupled surface–subsurface simulations and field observations. *Advances in Water Resources*.
- Yamana, T. K. and E. A. B. Eltahir. 2011. On the use of satellite-based estimates of rainfall temporal distribution to simulate the potential for malaria transmission in rural Africa. *Water Resources Research* **47**.

- Yang, G. J., C. J. A. Bradshaw, P. I. Whelan, and B. W. Brook. 2008a. Importance of endogenous feedback controlling the long-term abundance of tropical mosquito species. *Population Ecology* **50**:293-305.
- Yang, G. J., B. W. Brook, P. I. Whelan, S. Cleland, and C. J. A. Bradshaw. 2008b. Endogenous and Exogenous Factors Controlling Temporal Abundance Patterns of Tropical Mosquitoes. *Ecological Applications* **18**:2028-2040.
- Zhang, H. L., Y. Z. Zhang, W. H. Yang, Y. Feng, R. S. Nasci, J. Yang, Y. H. Liu, C. L. Dong, S. Li, B. S. Zhang, Z. L. Yin, P. Y. Wang, S. H. Fu, M. H. Li, F. Liu, J. Zhang, J. Sun, C. W. Li, X. Y. Gao, H. Liu, H. Y. Wang, L. R. Petersen, and G. D. Liang. 2013. Mosquitoes of Western Yunnan Province, China: Seasonal Abundance, Diversity, and Arbovirus Associations. *Plos One* **8**.

Biography

Yun Jian was born in Chengdu, China in September 25, 1985. She has received a Bachelor of Environmental Sciences from East China Normal University (ECNU), Shanghai, China, in June 2008. She joined the Nicholas School of the Environment to pursue her doctoral studies in environmental sciences in 2009. Her doctoral research is focused on understanding and predicting the fluctuations in mosquito abundance in temperate regions.

During her doctoral studies, she was also involved in several research projects that included (1) a hierarchical model for estimating long-term trend of atrazine concentration in the surface water of the contiguous United States (2) environmental impacts of swine Confined Animal Feeding Operations (CAFOs) on atmospheric and aquatic resources within North Carolina's Neuse River Basin, and (3) a Bayesian Hierarchical model to predict chlorophyll a in the New River Estuary, North Carolina.

Yun Jian was awarded the State Scholar Fund Scholarship from Chinese Scholarship Council in 2009. She has received several scholarships and awards from Shanghai Municipal Education Commission and ECNU. She also received several Conference Scholarships from Duke University graduate school, and Nicholas School of

the Environment. She has presented her work at many national and international conferences.

Her publications include:

Jian Y., Silvestri S, Belluco E, Saltarin A, Chillemi G, and Marani M. 2014.

Environmental forcing and density-dependent controls of *Culex pipiens* abundance in a temperate climate (Northeastern Italy). *Ecological Modelling* 272:301-310.

Jian Y., Silvestri S, Brown J, Hickman R, Marani M. 2014. The Temporal Spectrum of Adult Mosquito Population Fluctuations: Conceptual and Modeling Implications.

PLoS ONE 9(12): e114301. doi:10.1371/journal.pone.0114301

Jian Y., Qian S. A Hierarchical Model for Long-Term Trend of Atrazine

Concentration in the Surface Water of the Continental United States. *JAWRA*

(accepted)

Jian Y., Shi L, Li D, Zhang C, Wang R and Chen X. Effects of Deforestation on the Genetic Structure of *Castanopsis Sclerophylla*, *Acta Ecologica Sinica* 2008 (28):11.

Yang K, Che Y, Shang Y, Tai J and **Jian Y.** Industrial solid waste flow analysis of eco-industrial parks: implications for sustainable waste management in China. *Frontiers of Environmental Science & Engineering in China*. DOI: 10.1007/s11783-011-0344-0